Democratic and People's Republic of Algeria
Ministry of Higher Education and Scientific Research
Abbes Laghrour University of Khenchela
Faculty of Science and Technology
Department of Science of Matter

Thesis

Presented to Obtain a Doctoral Degree in Chemistry

Specialty: Physical Chemistry

By:

Bouchareb Nabila

Entitled:

Synthesis, structural, electrochemical and tribological characterization of nanostructured compound based on titanium (Ti-Ni) for biomedical applications

Graduation Committee

Chermim Ibrahim	**Dr**	**Abbes Laghrour Khenchela University**	**President**
Hezil Naouel	**Prof**	**Abbes Laghrour Khenchela University**	**Superviser**
Fellah Mamoun	**Prof**	**Abbes Laghrour Khenchela University**	**Co-superviser**
Allaoui Abdelhalim	**Dr**	**Abbes Laghrour Khenchela University**	**Reviewer**
Touhami Mohammed Zine	**Prof**	**Badji Mokhtar Annaba University**	**Reviewer**
Mechachti Said	**Prof**	**Badji Mokhtar Annaba University**	**Reviewer**
Hamadi Fouzia	**Dr**	**Abbes Laghrour Khenchela University**	**Invited Membre**

2024/2025

DEDICATE

I dedicate this work to:

My grandparents

My parents

My sisters

All my family

And to all my friends without exception

For their love and constant support

ACKNOWLEDGMENTS

*First and foremost, I thank **ALLAH** Almighty, for giving me the strength, knowledge, and courage to understand, learn, and complete this thesis.*

*My profound gratitude goes out to my supervisor **Professor HEZIL Naouel,** for her great assistance, wise counsel, and unwavering support during my research journey. Her guidance helped me in all the time of research and writing of this thesis.*

*I want to express my gratitude to my co-supervisor **Professor FELLAH Mamoun,** for his invaluable guidance, patience, and constant support during this research journey. His expertise and astute advice have substantially advanced my understanding of this field. I truly value the time and effort he invested in mentoring me, sharing his knowledge, and helping me get beyond challenges. His encouragement and insightful critique have been invaluable to the creation and completion of this work.*

*I would also like to thank the Members of the Jury, **Doctor CHERMIM Ibrahim, Doctor ALLAOUI Abdelhalim, Doctor HAMADI Fouzia, Professor TOUHAMI Mohammed Zine**, and **Professor MECHACHTI Said** for giving me the honor of accepting to be a member of the Jury and for having evaluated my work with attention and kindness. Their expertise and valuable input have contributed to this research.*

*I would like to express my deep gratitude to **Mr. OBROSOV Aleksei** and **Professor WEISS Sabine** of the Brandenburg University of Technology in Germany for welcoming me into their research group. Thank you very much for your valuable help and vital contribution, which allowed me to conduct experimental trials in their laboratory.*

*My sincere thanks go to all the professors of the **Matter Sciences department** who have contributed to my training.*

Nabila

ABSTRACT

Medical implants are essential for improving the quality of life of people who suffer, especially in the orthopedic field. Therefore, the need for biomaterials has increased exponentially as a result of the necessity for replacing or repairing damaged parts of the human body to regain the missing shape or functionality of biological tissue. To achieve the long-term performance of these implants, they must have distinct mechanical, tribological, and electrochemical properties.

In this context, this study aims to examine the effect of milling times on the mechanical, tribological, and electrochemical properties of Ti_{50}-Ni_{50} (or Nitinol), which is one of the most attractive materials in the medical field for orthopedic implants due to its unique properties.

Ti_{50}-Ni_{50} alloys were synthesized using high-energy ball milling under different milling times (2, 6, 12, and 18 h). The size, shape, and uniform chemical composition of the powder particles were examined using scanning electron microscopy (SEM) and energy dispersive spectroscopy (EDS). The alloyed particles' structural characteristics were determined through the use of X-ray diffraction (XRD). Mechanical properties were assessed using hardness tests, while tribological behavior was examined using a ball-on-plate tribometer operating in Ringer's Solution under various applied load of 2, 10, and 20 N. The electrochemical properties were characterized by open-circuit potential (OCP) measurement, potentiodynamic polarization (PD), and the Electrochemical Impedance Spectroscopy (EIS) technique. To simulate typical biological conditions, Hank's solution at pH = 7.4 and T = 37 °C were used as the electrolyte.

The results revealed that the milling process influences the particle size and shape of powders, where the proportion of fine particles increased with increasing grinding times from 2 h to 18 h due to severe deformation and fracturing. This improvement in particle refinement contributed to enhanced mechanical attributes, wear resistance, and corrosion resistance, making the material useful for bone implants.

Keywords: *Biomaterials; Titanium; Nickel; Corrosion; Friction; wear; Total hip replacement.*

RESUME

Les implants médicaux sont essentiels pour améliorer la qualité de vie des personnes qui souffrent, notamment dans le domaine orthopédique. Par conséquent, le besoin de biomatériaux a augmenté de façon exponentielle en raison de la nécessité de remplacer ou de réparer les parties endommagées du corps humain pour retrouver la forme ou la fonctionnalité manquantes des tissus biologiques. Pour obtenir des performances à long terme, ces implants doivent posséder des propriétés mécaniques, tribologiques et électrochimiques distinctes.

Dans ce contexte, cette étude vise à examiner l'effet des temps de broyage sur les propriétés mécaniques, tribologiques et électrochimiques du Ti_{50}-Ni_{50} (ou Nitinol), qui est l'un des matériaux les plus attrayants dans le domaine médical pour les implants orthopédiques en raison de ses propriétés uniques.

Les alliages Ti_{50}-Ni_{50} ont été synthétisés en utilisant le fraisage à billes de haute énergie sous différents temps de fraisage (2, 6, 12 et 18 h). La taille, la forme et la composition chimique uniforme des particules de poudre ont été examinées à l'aide de microscopie électronique à balayage (SEM) et de spectroscopie à dispersion d'énergie (EDS). Les caractéristiques structurelles des particules alliées ont été déterminées par diffraction de rayons X (XRD). Les propriétés mécaniques ont été évaluées à l'aide d'essais de dureté, tandis que le comportement tribologique a été examiné à l'aide d'un tribomètre à billes fonctionnant en solution de Ringer sous diverses contraintes appliquées de 2, 10 et 20 N. Les propriétés électrochimiques ont été caractérisées par des mesure du potentiel de circuit (OCP), polarisation potentiodynamiques (PD) et la technique de spectroscopie d'impédance électrochimique (EIS). Pour simuler des conditions biologiques typiques, on a utilisé comme électrolyte la solution de Hank à pH = 7,4 et T = 37 °C.

Les résultats ont révélé que le processus de fraisage influence la taille et la forme des particules des poudres, où la proportion de particules fines augmente avec l'augmentation des temps de broyage de 2 h à 18 h en raison de déformations et de fracturations sévères. Cette amélioration du raffinement des particules a contribué à améliorer les attributs mécaniques, la résistance à l'usure et la résistance à la corrosion, ce qui rend le matériau utile pour les implants osseux.

Mots-clés : *Biomatériaux; Titane; Nickel; Corrosion; Friction; Usure; Prothèse total de la hanche.*

ملخص

الغرسات الطبية ضرورية لتحسين جودة حياة الأشخاص الذين يعانون، خاصة في مجال جراحة العظام. لذلك، زادت الحاجة إلى المواد الحيوية بشكل كبير نتيجة لضرورة استبدال أو إصلاح الأجزاء التالفة من جسم الإنسان لاستعادة الشكل أو الوظيفة المفقودة للأنسجة البيولوجية. لتحقيق الأداء طويل المدى لهذه الغرسات، يجب أن يكون لها خصائص ميكانيكية وقبلية وكهروكيميائية مميزة.

في هذا السياق، تهدف هذه الدراسة إلى فحص تأثير أوقات الطحن على الخصائص الميكانيكية والقبلية والكهروكيميائية لسبائك Ti_{50}-Ni_{50}، وهي واحدة من أكثر المواد جاذبية في المجال الطبي لزراعة العظام بسبب خصائصها الفريدة.

تم تصنيع سبائك Ti_{50}-Ni_{50} باستخدام طحن الكرة عالي الطاقة في أوقات طحن مختلفة (2 و 6 و 12 و 18 ساعة). تم فحص الحجم والشكل والتركيب الكيميائي الموحد لجزيئات المسحوق باستخدام الفحص المجهري الإلكتروني (SEM) والتحليل الطيفي المشتت للطاقة (EDS). تم تحديد الخصائص الهيكلية للجسيمات المطحونة من خلال استخدام حيود الأشعة السينية (XRD). تم تقييم الخصائص الميكانيكية باستخدام اختبارات الصلابة، بينما تم فحص السلوك القبلي باستخدام مقياس ترايبومتر للكرة على اللوحة يعمل في محلول Ringer تحت ضغوط تطبيقية مختلفة من 2 و 10 و 20 نيوتن. لمحاكاة الظروف البيولوجية النموذجية، تم استخدام محلول Hank عند درجة الحموضة 7.4 و حرارة الوسط 37 درجة مئوية.

كشفت النتائج أن عملية الطحن تؤثر على حجم الجسيمات وشكل المساحيق، حيث زادت نسبة الجسيمات الدقيقة مع زيادة أوقات الطحن من 2 ساعة إلى 18 ساعة بسبب التشوه الشديد والكسر. ساهم هذا التحسن في صقل الجسيمات في تعزيز السمات الميكانيكية ومقاومة الكشط ومقاومة التآكل، مما جعل المادة مفيدة لزراعة العظام.

الكلمات المفتاحية: المواد الحيوية, التيتان, النيكال, التأكل, الكشط, الاحتكاك, مفصل الورك.

TABLE OF CONTENT

LIST OF FIGURES

CHAPTER I

CHAPTER II

CHAPTER V

LIST OF TABLES

CHAPTER I

CHAPTER II

CHAPTER III

CHAPTER IV

CHAPTER V

LIST OF ABBREVIATIONS AND ACRONYMS

Ti:	Titanium
Ni:	Nickel
Co:	Cobalt
Cr:	Chromium
BC:	Before Christ
AC:	After Christ
DNA:	Deoxyribonucleic acid
RNA:	Ribonucleic acid
THR:	Total hip replacement
THA:	Total hip arthroplasty
ASTM:	American Society for Testing and Materials
Wt. %:	Weight percentage
Cp:	Commercial pure
PMMA:	Polymethylmethacrylate
UHMWPE:	Ultra high molecular weight polyethylene
PTFE:	Polytetrafluoroethylene
CoC:	Ceramic-on-Ceramic
MoM:	Metal-on-Metal
MoP:	Metal-on-Polymer
CoP:	Ceramic-on-Polymer
COF:	Coefficient of friction
SMAs:	Shape memory alloys
SME:	Shape memory effect
SE:	Superelasticity
NOL:	Naval Ordnance Lab
CVD:	Chemical vapour deposition

HIP:	Hot isostatic pressing
XRD:	X-ray diffraction
SEM:	Scanning electron microscopy
EDS:	Energy dispersive spectroscopy
N:	Newton
at. %:	Atomic percentage
rpm:	Revolutions per minute
BPR:	Ball-to-powder ratio
λ:	The wavelength of the X-rays
d_{hkl}:	The interplanar spacing generating the diffraction
θ:	The diffraction angle
Cu-K:	Copper radiation
W-H:	William-son-Hall
β:	The peak width at half the maximum intensity
ε:	Internal strain (microstrain)
D:	Crystallite size
h, k, l:	Miller indices of the diffraction planes
ρ_w:	Density of distilled water
w_a:	Weight of sample in air
w_w:	Weight of sample in water
ρ_{sint}:	Density of the sintered samples
ρ_{th}:	Theoretical density
Ra:	Roughness average
ISO:	International Organization for Standardization
HV:	Hardness Vickers
OCP:	Open Circuit Potential

PD:	Potentiodynamic Polarization
EIS:	Electrochemical Impedance Spectroscopy
SCE:	Saturated calomel electrode
CR:	Corrosion rate
i_{corr}:	Corrosion current density
E_{corr}:	Corrosion potential
Hz:	Hertz
ICCD:	International Centre for Diffraction Data
fcc:	Face-centered cubic
Å:	ångström
PSD:	Pore size distribution
Sec:	Seconds
MA:	Mechanical alloying
I_{pass}:	Passive current density
βa:	Anodic Tafel slope values
βc:	Cathodic Tafel slope values
R_p:	Polarization resistance
Z″:	Imaginary impedance component
Z′:	Real impedance component
R1:	Resistance of the porous layer
R2:	Barrier layer's charge transfer resistance
CPE:	Constant phase element
C:	Capacitance

GENERAL INTRODUCTION

GENERAL INTRODUCTION

Millions of people worldwide suffer from inflammation of the bones and joints these days. Surgical intervention is often necessary to repair these problems, and in very extreme situations, whole joint replacements are necessary [1]. The most typically replaced joints are the knee and hip [1-3]. Severe bone defects and fractures present major treatment challenges, especially when they involve large or complex injuries. To address these challenges, commercially available bone implants, crafted from advanced biomedical material, have become a crucial solution.

Any implantable biomedical material having therapeutic value must be biocompatible with the human body, meaning that it must not have any negative effects [4, 5], as well as possess mechanical qualities suitable for bone structure [6]. In recent years, the field of bone implant research has expanded rapidly. However, most implants have not shown a long working life due to lack of compatibility of the implant material with the human body [7]. In addition, the performance of these implants reduces in certain working conditions such as jumping, running, loaded for long duration, etc [7]. As a result, creating an implant material with better properties that can solve the aforementioned issues is essential.

It is estimated that 70-80 % of biomedical implants are made of metallic materials [8-10]. They should have sufficient fatigue strength because they are typically used in load-bearing applications [11]. The usage of metals as biomaterials and related technologies is constantly improving in comparison to ceramics and polymeric materials because their properties can be altered to suit the needs of the manufacturing processes [11]. The most appropriate modern metallic materials for biomedical applications are considered to be titanium and its alloys due to their exceptional all-around qualities. They also meet the requirements of implantation materials more effectively than other competing materials like tantalum, stainless steel, Cr-Co alloys, and CP niobium [12, 13].

Shape memory alloys (SMAs) are an important class of smart or functional materials that have gained a lot of attention recently and are widely used in a variety of industries, such as biomedicine, aviation, and civil engineering [14]. One of the most important of these materials is the Ti-Ni alloy, also known as *Nitinol*, which has an equal atomic ratio of titanium (Ti) and nickel (Ni) [15-17]. This alloy has been studied as a biomaterial since its discovery by *Buehler et*

al., (1963) [15]. It is approved for long-term usage and is a substance safe for use in biomedical implants, according to the *US Food and Drug Administration (FDA)* [18]. Ti-Ni alloys have remarkable features such as shape memory effect (SME), superelasticity (SE), higher corrosion and wear resistance, as well as excellent biocompatibility in the human body's environment [19, 20]. The latter is guaranteed through the formation of an oxide layer on their surface consisting mainly of TiO_2 [21, 22].

The corrosion resistance of nitinol becomes extremely important for applications in the human body, as the amount and toxicity of corrosion products directly impact the alloy's biocompatibility [23]. A lot of research has shown that Ti-Ni is very biocompatible and resistant to corrosion, But, the high nickel concentration of the alloy and the possibility of corrosion-induced disintegration are concerning [24-27]. Human tissue contains ions such as hydroxide and chloride, proteins, water, and dissolved oxygen, all of which produce an environment that is aggressive to the metals or alloys used for implantation [26]. The release of nickel ions from an implant into body fluids and tissue frequently results in corrosion, perhaps in the form of pitting, which decreases the implant's mechanical performance and sets off adverse cellular reactions [27]. In addition, the wear resistance of implants is very important because the debris released from metallic implants causes adverse cellular responses and the implant's failure.

Additionally, one of the main challenges in designing titanium implants is to reduce the modulus of elasticity to be close to that of the bone. The elasticity modulus of Ti-Ni alloys is smaller than that of conventional materials such as Co-Cr alloys and stainless steel. But, it is still higher than the elastic modulus of bone, which is around 30 GPa. This difference can lead to a "stress shielding" phenomenon, where the implant takes too much load, which can weaken the adjacent bone and loosening of the implant.

Thus, current research is mainly focused on improving and developing these materials' performance during the design stage to accommodate the harsh circumstances of the human body. In this work, Ti-Ni alloys were produced using powder metallurgy, which provides special techniques for producing and solidifying metal powders, such as cold pressing, hot isostatic pressing (HIP), and sintering. One popular method for creating nanocrystalline materials with uniform structures is mechanical alloying (MA). To obtain the required material attributes, this

novel technique uses a high-energy ball mill. Several factors, such as grinding environment, ball-to-powder ratio (BPR), rotational speed, and milling time, influence the reduction of particle size in planetary ball milling. According to earlier research, the most important factor in MA that significantly affects the characteristics of materials is the milling time [27-29].

However, no studies have been conducted on the optimization of the milling/grinding time of Ti_{50}-Ni_{50} alloys. The main objective of this work is to determine the effects of milling times on the structural, mechanical, tribological, and electrochemical properties of Ti_{50}-Ni_{50} alloys produced using a high-energy ball milling technique. By optimizing grinding durations, this research attempts to improve the performance of Ti_{50}-Ni_{50} alloys, specifically in terms of corrosion and wear resistance for applications like total hip implants through the attempt to address the issues of nickel ion release and wear debris by developing alloys with improved properties to endure the harsh environment of the human body.

This work consists of a general introduction that situates the subject, five chapters, and a general conclusion, summarizing the main results obtained.

The ***first chapter*** focuses on a bibliographical study of biomaterials, exploring their different classes, and their desired characteristics for use in medicine. It also includes an overview of total hip prostheses, their components, fixation, friction couples, and associated problems. Furthermore, the chapter discusses titanium alloys and their choices as biomaterials, with a particular emphasis on the Ti-Ni alloy, which is the most appealing biomaterial for orthopedic implants due to its tribological and electrochemical performance in the biomedical field. Furthermore, the methods used to fabricate these materials were highlighted.

In the ***second chapter***, we outline the steps of the experimental methods of elaboration of the Ti-Ni alloy as well as the parameters involved in the elaboration process of our samples. We also describe the primary characterization methods used in this investigation.

The ***third chapter*** presents the results with their interpretations of the structural analysis of the Ti-Ni alloy, using scanning electron microscopy and X-ray diffraction to determine the evolution of the formed phases, changes in crystallite size, lattice parameters, particle size, and pore size distribution, as well as their morphology. This chapter also discusses the results of mechanical

properties including the hardness, Young's modulus, relative density, relative porosity, and surface roughness of HIPed and sintered samples.

In the ***fourth chapter***, we discuss the results obtained on the tribological behavior of the samples (i.e., coefficient of friction (COF), wear rate).

The ***fifth chapter*** presents the discussion of the results of the electrochemical behavior obtained through the use of three methods: the monitoring of the evolution of open-circuit potential (OCP), potentiodynamic polarization (PD), and electrochemical impedance spectroscopy (EIS) technique.

We closed this thesis manuscript with a general conclusion that summarizes the main results obtained from our study with prospects for future work.

BIBLIOGRAPHIC REFERENCES

[1]M.T. Mohammed., "*Nanocomposites in total hip joint replacements*". Nanotechnology and Advanced Materials Research Unit, Faculty of Engineering, University of Kufa, Najaf, Iraq, (2019), 221-252. https://doi.org/10.1016/B978-0-12-813740-6.00012-0.

[2]M. Fellah, N. Hezil, D. Bouras, M. Ali Habeeb, F. Hamadi, N. Bouchareb, S. E. Laouini, A. Perez Larios, O. Aleksei, and G.A. El-Hiti., "*Microstructural and photocatalytic properties of nanostructured near-β Ti-Nb-Zr alloy for total hip prosthesis use*". Kuwait Journal of Science, 51 (2024), 100276. https://doi.org/10.1016/j.kjs.2024.100276.

[3] M. Fellah, N. Hezil, D. Bouras, N. Bouchareb, A. Perez Larios, A. Obrosov, G.A. El-Hiti, and S. Weiß., "*Investigating the effect of Zr content on electrochemical and tribological properties of newly developed near β-type Ti-alloys (Ti–25Nb-xZr) for biomedical applications*". Journal of Science Advanced Materials and Devices, 9 (2024), 100695. https://doi.org/10.1016/j.jsamd.2024.100695.

[4] M. Kaur, and K. Singh., "*Review on titanium and titanium based alloys as biomaterials for orthopaedic applications*". Materials Science and Engineering C, 102 (2019), 844-862. https://doi.org/10.1016/j.msec.2019.04.064.

[5] M. Fellah, N. Hezil, F. Hamadi, M. Abdul Samad, A.Alburaikan, H.A.E. Khalifa, and A. Obrosov., "*Effect of Fe content on physical, tribological and photocatalytical properties of Ti-6Al-xFe alloys for biomedical applications*". Tribology International, 191 (2024), 109146. https://doi.org/10.1016/j.triboint.2023.109146.

[6] N.B. Pradeep, M.M. Rajath Hegde, G.C. Manjunath Patel, K. Giasin, D.Y. Pimenov, and S. Wojciechowski., "*Synthesis and characterization of mechanically alloyed nanostructured ternary titanium based alloy for bio-medical applications*". Journal of Materials Research and Technology, 16 (2022), 88-101. https://doi.org/10.1016/j.jmrt.2021.11.101.

[7] R.P. Verma., "*Titanium based biomaterial for bone implants: A mini review*". Materials Today Proceedings, 26 (2020), 3148-3151. https://doi.org/10.1016/j.matpr.2020.02.649.

[8] M. Niinomi, M. Nakai, and J. Hieda., "Review Development of new metallic alloys for biomedical applications". Acta Biomaterialia. 8 (2012), 3888-3903. https://doi.org/10.1016/j.actbio.2012.06.037.

[9] Y. Li, C. Yang, H. Zhao, S. Qu, X. Li, and L. Yuanyuan., "*New developments of Ti-based alloys for biomedical applications*". Materials, 7 (2014), 1709-1800. https://doi.org/10.3390/ma7031709.

[10] C. Salvo, C. Aguilar, R. Cardoso-Gil, A. Medina, L. Bejar, and R.V. Mangalaraja., "Study on the microstructural evolution of Ti-Nb based alloy obtained by high-energy ball milling". Journal of Alloys and Compounds, 720 (2017), 254-263. https://doi.org/10.1016/j.jallcom.2017.05.262.

[11] M. Sarraf, E.R. Ghomi, S. Alipour, S. Ramakrishna, and N.L. Sukiman., "*A state-of-the-art review of the fabrication and characteristics of titanium and its alloys for biomedical application*". Bio-Design and Manufacturing, 5 (2021). http://dx.doi.org/10.1007/s42242-021-00170-3.

[12] G. Senopati, R. Abdul Rahman Rashid, I. Kartika, and S. Palanisamy., "*Recent development of low-cost β-Ti alloys for biomedical applications: A Review*". Metals, 13 (2023), 194. https://doi.org/10.3390/met13020194.

[13] Y. Li, C. Yang, H. Zhao, S. Qu, X. Li, and Y. Li., "*New developments of Ti-based alloys for biomedical applications"*. Materials, 7 (2014), 1709-1800. https://doi.org/10.3390/ma7031709.

[14] B. Zhen-zhen, G. Shun, X. Fu, and Z. Xin-qing., " *Development of NiTiNb in-situ composite with high damping capacity and high yield strength* ". Progress in Natural Science: Materials International, 21 (2011), 293-300. http://dx.doi.org/10.1016/S1002-0071(12)60060-4.

[15] J. Zhu, Q. Zeng, and T. Fu., "*An updated review on TiNi alloy for biomedical applications*". Corrosion Reviews, (2019), 1-14. https://doi.org/10.1515/corrrev-2018-0104.

[16] N. Bouchareb, M. Fellah, N. Hezil, F. Hamadi, A. Montagne A. Obrosov, K. Yadav, and G.A. El-Hiti., "*Effect of milling time on structural, physical and photocatalytical properties of Ti-Ni alloy for biomedical applications*". The International Journal of Advanced Manufacturing Technology, 131 (2024), 3539-3553. https://doi.org/10.1007/s00170-024-13207-5.

[17] N. Bouchareb, N. Hezil, F. Hamadi, M. Fellah., "*Effect of milling time on structural, mechanical and tribological behavior of a newly developed Ti-Ni alloy for biomedical applications*". Material Today Communication, 38 (2024), 108201. https://doi.org/10.1016/j.mtcomm.2024.108201.

[18] M.F. Maitz., "*Surface modification of Ti-Ni alloys for biomedical applications*". Leibniz Institute of Polymer Research Dresden, Germany.

[19] J. Witkowska, J. Kaminski, T. Plocinski, M. Tarnowski, and T. Wierzchon., "*Corrosion resistance of NiTi shape memory alloy after hybrid surface treatment using low-temperature plasma*". Vacuum, 137 (2017), 92-96. http://dx.doi.org/10.1016/j.vacuum.2016.12.034.

[20] M. Fellah, N. Hezil, M.Z Touhami, M.A. Hussien, A. Montagne, A. Mejias, A. Iost, S. Kossman, T. Chekalkin, A. Obrosov, S. Weiss., "*Effect of Sintering Temperature on Mechanical and Tribological Behavior of Ti–Ni Alloy for Biomedical Applications*". In: The Minerals, Metals & Materials Society (eds) TMS 2020 149th Annual Meeting and Exhibition Supplemental Proceedings. The Minerals, Metals and Materials Series. Springer, Cham (2020), 1701-1710. https://doi.org/10.1007/978-3-030-36296-6_157.

[21] S.G. Anikeev, M.I. Kaftaranova, V.N. Hodorenko, S.D. Ivanov, N.V. Artyukhova, A.V. Shabalina, S.A. Kulinich, G.V. Slizovsky, A.V. Mokshin, and V.E. Gunther., "*TiNi-based*

material with shape-memory effect for surgical treatment of diseases of small intestine in newborn and young children". Journal of Functional Biomaterials, 14 (2023), 1-20. https://doi.org/10.3390/jfb14030155.

[22] S.E. Kulkova, A.V. Bakulin, Q.M. Hu, and R. Yang., "*Study of nickel segregation at the tini-titanium oxide interface"*. Materials Science Forum, 738-739 (2013), 269-273. http://dx.doi.org/10.4028/www.scientific.net/MSF.738-739.269.

[23] A.A.M. Soltan, ˙I. Esen, S. Ali Kara, and H. Ahlatçı., "*Examination of the corrosion behavior of shape memory NiTi material for biomedical applications*". Materials, 16 (2023), 3951. https://doi.org/10.3390/ma16113951.

[24] C. Trepanier, T.K. Leung, M. Tabrizian, L.H. Yahia, J.G. Bienvenu, J.F. Tanguay, D.L. Piron, and L. Bilodeau., "*Preliminary investigation of the effects of surface treatments on biological response to shape memory NiTi stents*". Journal of Biomedical Materials Research, 48 (1999), 65-71. https://doi.org/10.1002/(sici)1097-4636(1999)48:2%3C165::aid-jbm11%3E3.0.co;2-#.

[25] J. Ryhanen, E. Niemi, W. Serlo, E. Niemelä, P. Sandvik, H. Pernu, and T. Salo., "*Biocompatibility of nickel-titanium shape memory metal and its corrosion behaviour in human cell cultures*". Journal of Biomedical Materials Research, 35 (1997), 451-457. https://doi.org/10.1002/(sici)1097-4636(19970615)35:4%3C451::aid-jbm5%3E3.0.co;2-g.

[26] R. Venugopalanl, and C. Trepanier., "*Assessing the corrosion behaviour of Nitinol for minimally-invasive device design*". Minimally Invasive Therapy and Allied Technologies, 9 (2000), 67-74. http://dx.doi.org/10.3109/13645700009063052.

[27] M. Fellah, N. Bouchareb, N. Hezil, N. Merah, Y. Alashkar, M. Imran, O. Aleksei, and S. Weiss., "*Electrochemical analysis of mechanically alloyed Ti50%-Ni50% alloy for bone implants use*". Journal of Alloys and Compounds, 1010 (2025), 178046. https://doi.org/10.1016/j.jallcom.2024.178046.

[28] K. Toualbia, M. Fellah, N. Hezil, H. Milles, and Z. Djafia., "*Effect of milling time on structural, mechanical and tribological properties of nanostructured HIPed near type Ti-15Mo alloys*". Tribology International, 197 (2024), 109731. http://dx.doi.org/10.1016/j.triboint.2024.109731.

[29] F. Yi, X.L. Cai, L. Zhou, M.J. Yu, Z. Li, and Q.W. Jiang., "*Effect of milling time on properties of Ti-48at%Al composite powder prepared by high energy milling*". Key Engineering Materials, 609-610 (2014), 185-190. http://dx.doi.org/10.4028/www.scientific.net/KEM.609-610.185.

CHAPTER I

BIBLIOGRAPHIC STUDY

I. INTRODUCTION

The number of individuals in need of orthopedic prostheses has increased dramatically, due to the increasing world population and life expectancy. In orthopedic repairing, the most used devices are metallic, ceramic, and polymer [1]. Stainless steel, Co-Cr alloys, and titanium alloys are some of the materials that are most frequently utilized in the biomedical field [2]. However, among the materials listed, Titanium and its alloys (such as Ti-Ni alloy) are the most utilized materials in the medical field due to their special properties, including low density, specific strength, biocompatibility, and exceptional oxidation resistance [3].

The first chapter is a bibliographic study, which is divided into four parts. In the first part, we describe biomaterials (definition, desired characteristics of biomaterials for use in medicine, and their different classes…). The second part consists of some notions about total hip prosthesis and their problems. The next section provides an overview of titanium alloys, a description of the Ti-Ni study alloy, and an explanation of why these materials were selected for use as biomaterials. In the last part, we described nanomaterials and the methods used in the elaboration of Ti-Ni alloys.

I.1 BIOMATERIALS

I.1.1 Introduction

A class of non-living materials known as "biomaterials" is of great research interest today, they are used to enhance or replace (completely or partially) a tissue, an organ, or a bodily function in order to preserve or improve the lives of people suffering from severe functional problems. These materials are used in numerous branches of medicine such as orthopedics, neurology, ophthalmology, and dentistry, etc. Desired characteristics in biomaterials for use in medicine are: biocompatibility, the non-toxicity of biomaterials or their products during degradation, and mechanical continuity with the surrounding bone tissue [4].

I.1.2 Definition of biomaterials

The definition of biomaterials is "substances that are inserted into or used in conjunction with the body and are created with characteristics that closely resemble those of the biological system, be stable enough for the intended use, have the right levels of bioactivity, and are designed to partially or entirely replace the functions of diseased, damaged, or dysfunctional

tissues and organs" [5]. It should be noted that the prefix "bio" in the definition of biomaterials means "biocompatible," not "biological" or "biomedical" [6].

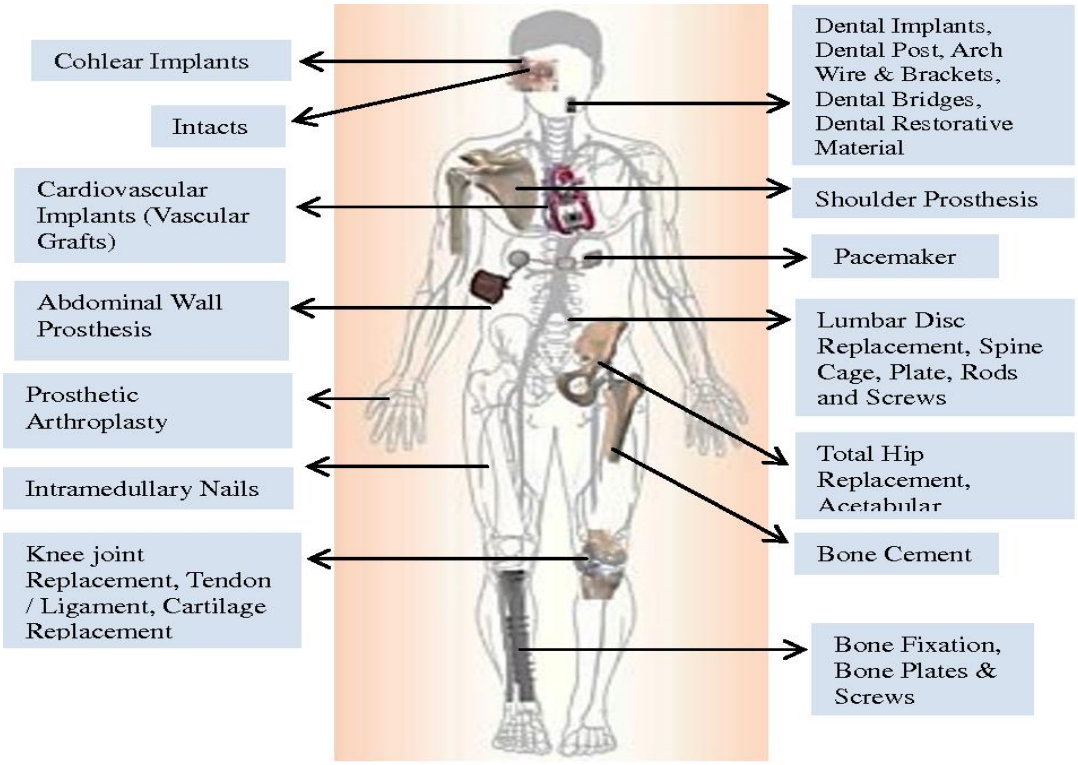

Figure I.1: The major applications of biomaterials in the human body [7].

I.1.3 Historical development of biomaterials

Although the term "biomaterial" was coined in the middle of the 20th century, however, the usage of biomaterials dates back far further [8]. The first recorded use of biomaterials for medical purposes was the use of linen sutures in ancient Egypt in 3000 BC [8]. It is also widely known that Europeans used catgut as a suture material during the middle Ages [9]. The heads of huge, biting ants were used to clamp the margins of wounds together in South Africa and India [10]. Metallic sutures have their origins in Ancient Greece, when Galen of Pergamon, a physician, surgeon, and philosopher, reported the use of golden wires as ligatures in the second century AC. Through the ages, other metals have been used including lead and silver. Similar to modern-day dentists, the ancient Mayans made artificial teeth from seashells that successfully underwent osseointegration [11, 12]. In addition, the Chinese crafted bamboo rods to resemble natural teeth that were placed in jaws similar to modern dental implants [13]. Iron has more recently been used to make artificial teeth in Europe [14]. Furthermore, *Gaspare Tagliacozzi* and other innovative plastic surgeons used autogenous skin

flaps to successfully reconstruct missing noses in the sixteenth century [15]. The following Figure I.2 lists significant dates in the development of biomaterials:

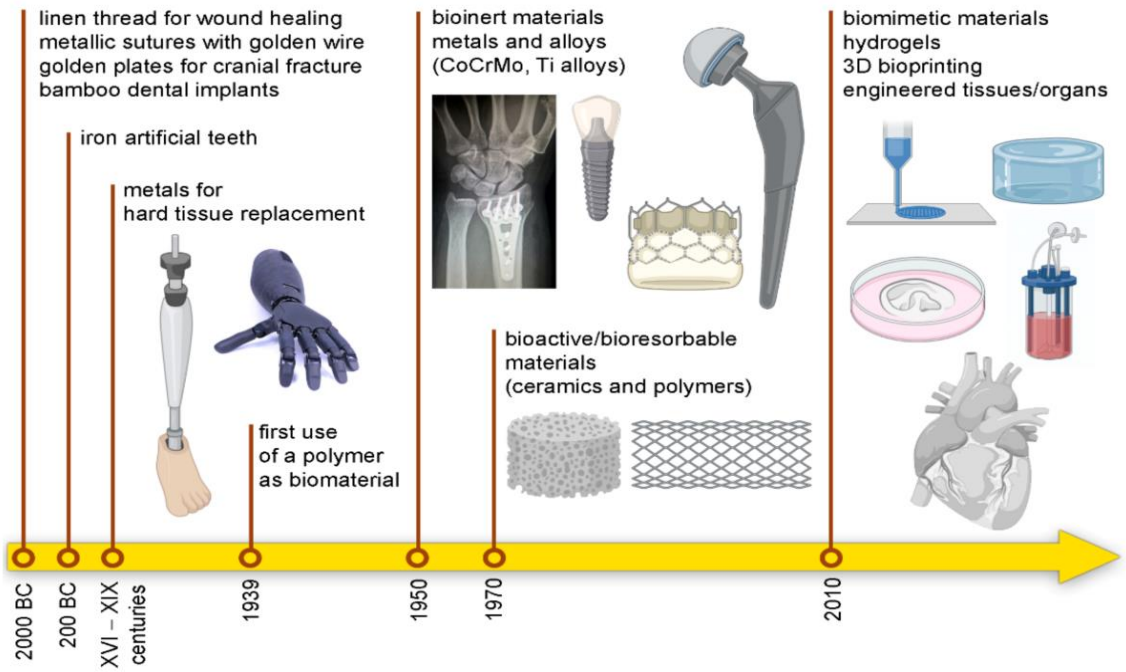

Figure I.2: The history of biomaterials: from replacement to regeneration [16].

Major advancements in biomaterials occurred in the eighteenth and nineteenth centuries. The success of using materials inside a biological system is greatly influenced by the biocompatibility of the materials, which researchers have begun to understand. The first method for fixing bone fractures with metal wire was introduced in 1775 by Toulouse doctors *Lapuyade and Sicre. H. S. Levert* conducted research on the biocompatibility of metal implants (gold, silver, lead, and platinum) and bone fixation plates in dogs in the middle to late 1800s. *Adolf Fick* created the first functional glass contact lens in 1888 although *Leonardo Da Vinci* had outlined the idea much earlier, in 1508 [8].

I.1.4 Desired properties in biomaterials for medical applications

Materials used in the manufacture of prosthetics implanted within the living human body that is in direct contact with the body's tissue should contain specific sets of qualities, some of which are listed below:

I.1.4.1 Biocompatibility

The ability of a biomaterial to interact with human body tissues without endangering those tissues is the single most crucial characteristic that sets it apart from other materials [17].

Biocompatibility was defined by *Williams* in 2008 as: "the capacity of a biomaterial to carry out its intended function in relation to a medical therapy without causing any unfavorable local or systemic effects in the recipient or beneficiary of that therapy " [18]. In general, the factors influencing biocompatibility are illustrated in Figure I.3.

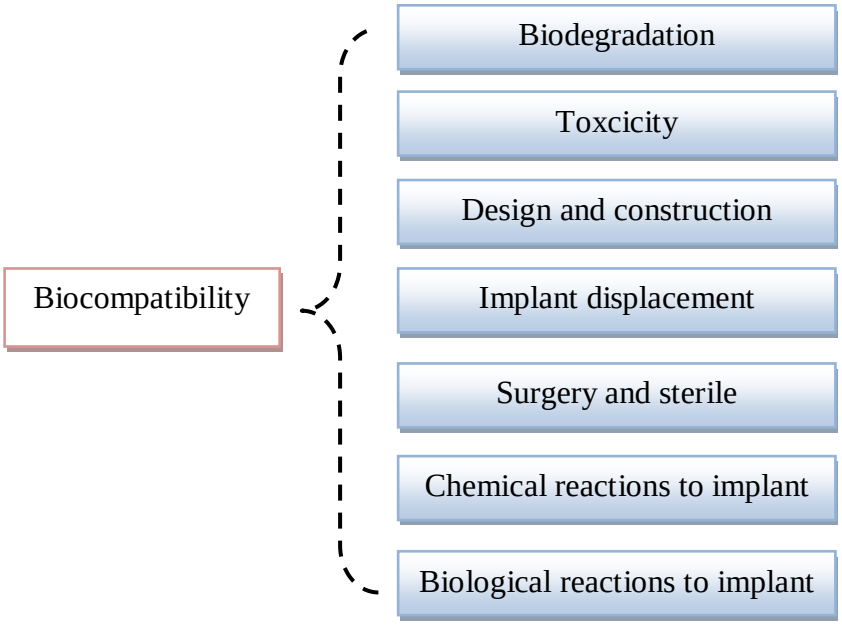

Figure I.3: Schematic presentation of variables affecting biocompatibility [18].

In medical practice, two categories of biocompatibility exist are: structural biocompatibility and surface biocompatibility.

- ✓ ***Structural biocompatibility***: The interplay between the structure of the biomaterial and the characteristics of the biological system. According to these interactions, a biomaterial has a certain capacity to carry out a specific task inside a medical device [19].
- ✓ ***Surface biocompatibility***: Describes the implant's compatibility (topographically and chemically) with the cells around it [19].

I.1.4.2 Mechanical properties

To increase the implant's service life and prevent loosening, the material should have a low modulus together with high strength to avoid the need for revision surgery [20]. Additionally, by matching the biomaterials' modulus of elasticity to the bone, which ranges from 4 to 30 GPa, it is possible to eliminate stress shielding [20, 21].

I.1.4.3 Non-toxic

The toxicity is caused by the elements that release out of the biomaterials into the biological system. For that, a biomaterial should be non-toxic to fulfill its function in the environment of the live body without adversely affecting other cells, organs, or the organism as a whole [22]. There are two different types of toxicity: genotoxic (which can change the DNA of the genome) and cytotoxic (which damages individual cells). Implant rejection and other major health issues may result from failing to meet the biocompatibility and nontoxic requirements [20, 21].

I.1.4.4 High corrosion resistance

The implants consisting of a biomaterial with low corrosion resistance release undesirable metal ions into the body, leading to hazardous reactions result, which may necessitate revision surgery. Thus, a desirable property of biomaterials is excellent corrosion resistance [21].

I.1.4.5 High wear resistance

The material should have a high wear resistance and low friction coefficient when sliding against body tissues. The implant may become loose due to an increase in friction coefficient or a decrease in wear resistance. Additionally, the wear debris produced might lead to inflammation that harms the bone supporting the implant [20, 21].

I.1.4.6 Osseointegration

Osseointegration defined as "A direct structural and functional connection between organized, living bone and the surface of a load-carrying implant" [20]. Successful osseointegration is greatly influenced by the surface's roughness, chemistry, and topography. Implant loosening is caused by the implant surface's failure to osseointegrate with the surrounding bone [20].

I.1.4.7 Long fatigue life

The fatigue strength is related to the response of the material to repeated cyclic loads. The major issues of implant loosening, stress-shielding, and eventual implant failure are caused by fatigue fracture, which is a problem that is frequently reported for hip prostheses [23].

I.1.5 The main classes of biomaterials

Biomaterials used to solve human health problems are classified by their nature into: Natural materials, metals, polymers, ceramics, and composite materials.

I.1.5.1 Natural materials

Natural biomaterials may come from humans, animals, or plants. They are mostly restorative materials with a structure comparable to the native tissue they are meant to replace. They also contain a variety of components that aid in tissue regeneration, repair, and rebuilding. Three different forms of biopolymers make up the majority of natural biomaterials [8]:

- Proteins: chains of amino acids (silk, collagen, elastin, and fibrin).
- Polysaccharides: chains of sugar (chitin, glycosaminoglycans).
- Polynucleotides: chains of nucleotides (DNA, RNA).

I.1.5.2 Metals

Among the first biomaterials employed for biomedical applications were metals and metal alloys. They are primarily utilized in surgery (instruments), stomatology (prostheses, dentures...), and orthopedics (joints, plates, screws...) [24]. The following metals and alloys are most frequently used in medical device applications:

I.1.5.2.1 Stainless steel

In the early stages of total hip replacement (THR), stainless steel was a popular implant material since it is simple to produce and inexpensive. The chromium found in stainless steel aids in preventing corrosion through the formation of an oxide layer on the surface. To ensure passivation, chromium must be present at a minimum of 12 %. Molybdenum provides resistance against pitting corrosion which is a localized form of corrosion responsible for producing cavities in the material. The lower carbon content of stainless steel prevents intergranular corrosion [25]. Table I.1 below provides an example from ASTM F138 for the chemical composition of stainless steel 316L, the most popular steel alloy utilized in implant manufacturing [25].

Table I.1: The chemical composition of 316L stainless steel according to ASTM F138 [25].

Element (wt. %)									
Alloy	**C**	**Mn**	**P**	**S**	**Si**	**Cr**	**Ni**	**Mo**	**Fe**
316L	0.03	2.00	0.03	0.01	0.75	17.00-19.00	13.00-15.5	2.00-3.00	Balance

I.1.5.2.2 Cobalt-chromium based alloys

Cobalt-based alloys contain chromium and, almost always, molybdenum [19]. In general, the Co-Cr-Mo and Co-Ni-Cr-Mo alloys are the two main categories of cobalt-chromium alloys. The Co-Cr-Mo alloy has long been utilized in dentistry, and just recently in the creation of artificial joints and the Co-Ni-Cr-Mo alloy, which is now employed to create the stems of prostheses for strongly pressured joints like the knee and hip [26].

I.1.5.2.3 Titanium and titanium alloys

Since the 1950 s, titanium (Ti) and titanium alloys have been among the materials most frequently employed in biomedical applications [27]. Titanium and its alloys have superior properties for use as implant biomaterials compared to stainless steel and cobalt-based alloys, such as reduced elastic modulus, superior biocompatibility, and higher corrosion resistance. The first-generation titanium alloys, (α+β) Ti-6Al-4V, and pure titanium CP-Ti; have been introduced some time ago, but more recently, the second-generation titanium alloys, the β-titanium alloys; have attracted a lot of attention [28]. (It will be detailed in the third part of the chapter).

I.1.5.2.4 Noble metals

Since ancient times, noble metals have been used as biomaterial [29]. Metals such as gold, silver, and platinum have high corrosion resistance. Their cost, high density, and low mechanical resistance make them less preferred materials for medical components [30].

Gold was among the earliest materials utilized for dental implants. It is a comparatively inert substance that is somewhat poisonous, highly malleable, and has great electrical conductivity. Silver is applied as a coating to surgical tools, burn treatment equipment, and stethoscope

diaphragms. Whereas, Platinum possesses outstanding biocompatibility, corrosion resistance, and electrical stability. It serves as an electrode in hearing aids as well as being utilized in pacemakers as electrodes to stabilize the cardiac rhythm by releasing electrical impulses [30].

I.1.5.3 Synthetic polymers

By definition, a polymer is an organic or inorganic macromolecule created by the repeated removal of basic units called monomers attached by covalent bonds [31]. Many different types of polymers have been used in the medical industry. Their uses include tracheal tubes, kidney, liver parts, heart components, dentures, hip and knee joints, and facial prostheses. Additionally, polymeric biomaterials are included while creating medical adhesives, etc [32]. A variety of polymers has been used for orthopedic applications, such as:

- ✓ ***Poly (methyl methacrylate), PMMA***

PMMA; is a rigid, fragile polymer, that turns out to be unsuitable for the majority of therapeutic uses. It is utilized in bone cement and dentures. The effectiveness of PMMA cement, which is prepared intra-operatively by blending the powdered polymer with monomeric methyl methacrylate to create dough that can be implanted in the bone, is a key factor in the success of many joint prostheses [33].

- ✓ ***Ultra high molecular weight polyethylene (UHMWPE)***

UHMWPE is one of the most popular polymer choices for orthopedic implants because it possesses the highest mechanical strengths, lowest wear rates, and best biocompatibility [33]. There are various factors that affect the mechanical characteristics of polymers, including the composition, molecular weight, and structure of the macromolecular chains [33, 34]. The wear resistance of UHMWPE can be improved by increasing crystallinity and cross-linking density. Even though cross-linking increases wear resistance, it also reduces tensile strength, fracture toughness, and resistance to fatigue crack propagation. Whereas, increased crystallinity improves elastic modulus; and resistance to fatigue and fracture [33].

I.1.5.4 Ceramics

Ceramics are polycrystalline materials characterized by their hardness, their low density, stiffness, mechanical resistance to corrosion and wear. It can be divided into five groups of biomaterials [7]. They are:

- ✓ ***Alumina (Al_2O_3):*** The primary sources of alumina or aluminum oxide are: Bauxite and corundum. It is employed in load-bearing hip prostheses and dental implants due to their great corrosion resistance, good biocompatibility, high strength, and good wear resistance [7, 35].
- ✓ ***Pyrolytic Carbon:*** due to the high compatibility of carbonaceous materials with bone and other tissue as well as the mechanical similarities between carbon and bone, it is used as a material for orthopedic implants [7].
- ✓ ***Zirconia (ZrO_2):*** is a biomaterial that has high mechanical strength and fracture toughness. It is currently being used in clinical settings for total hip replacement (THR) in making THR ball heads [7].
- ✓ ***Calcium phosphate ceramics*:** available in various physical forms. Their porosity is one of their primary properties. The development of an apatite layer that resembles bone on the surface of calcium phosphate materials is a crucial prerequisite for their bioactivity and ability to bind to real bone [7].
- ✓ ***Bioglass and Glass Ceramics*:** have the particularity of undergoing a Surface modification once implanted in the body allowing them for filling bone defects and binding to them [7].

I.1.5.5 Composite biomaterials

Composites are substances created by mixing two or more substances or phases in order to benefit from the distinctive qualities of each component. To prevent degradation at constituent contacts, it is imperative that every component of the composite be biocompatible [36]. The most effective composite biomaterials are utilized in dentistry as dental cement or restorative materials. Carbon-carbon and carbon-reinforced polymer composites are of tremendous interest in bone repair and joint replacement due to their low elastic modulus [37]. However, composite materials are often employed to create prosthetic limbs because of their low density/weight and excellent strength, which makes them the perfect choice for these applications [37].

I.1.6 Advantages and disadvantages of the biomaterials

The advantages; and disadvantages of various types of biomaterials are depicted in the following Table I.2.

Table I.2: The advantages and disadvantages of the biomaterials.

Material type	Advantages	Disadvantages	Ref
Natural biomaterials	Abundance, low cost, mechanical properties similar to tissues.	Degradable, evoke immune responses, cannot resist high processing temperatures.	[5]
Metals	High tensile and compressive strength, high resistance to wear.	Corrosion, high density, difficulty in processing, difficulty in producing complex shapes, release ions in the biological fluids	[5]
Synthetic Polymers	No corrosion, density similar to soft tissues, ease of processing, ability to form complex shapes, malleable.	Low strength, low resistance to impact, low resistance to wear	[5]
Ceramics	Inert, corrosion resistance, high biocompatibility, low thermal and electrical conductivity.	Difficult manufacturing, low impact strength, reproducibly.	[38]
Composites	Inert, corrosion resistant, superior biocompatibility	Difficult to reproduce during fabrication.	[38]

I.1.7 Medical applications of biomaterials

Nowadays, biomaterials are used in many therapeutic fields in order to preserve the integrity and comfort of life of persons suffering from severe functional problems.

- ✓ ***Cardiovascular***

Biomaterials are employed in the repair of heart valves, endovascular stents, vascular grafts, stent grafts, and other cardiovascular grafts [39].

- ✓ ***Orthopedic surgery***

Orthopedic implant devices are one of the most popular biomaterials application fields. The structure of freely moveable joints, such as the hip, knee, shoulder, ankle, and elbow, is impacted by osteoarthritis and rheumatoid arthritis [40]. The pain in such joints, particularly weight-bearing joints such as the hip and knee, can be considerable, and the effects on ambulatory function are quite devastating. It is possible to replace these joints with prostheses to relieve pain and movement recovery [40].

- ✓ ***Ophthalmology***

Several disorders that affect the eye's tissues can cause impaired vision and, in the long run, blindness. For example, cataracts cause cloudiness in the lens. This may be replaced with a synthetic (polymer) intraocular lens to preserve and restore vision [40].

- ✓ ***Dental applications***

In the mouth, bacterially controlled diseases can easily damage the tooth and the supporting gum tissues [40]. Extensive tooth loss results from dental caries, and the breakdown of teeth brought on by the metabolic activity in plaque (a mucus-based film that traps bacteria on the surface of the teeth) [40]. A multitude of materials can be used to repair or reconstruct teeth in their whole as well as individual tooth parts [40].

- ✓ ***Wound healing***

Fracture fixation devices are a key subset of wound-healing technologies. These include bone plates, screws, nails, rods, wires, and other devices used for fracture treatment [39].

- ✓ ***Aesthetic surgery***

Utilized biomaterials for aesthetic surgery in: artificial skin, tissue glues, and materials and implants for cosmetic surgery [41].

- ✓ ***Other applications***

Other uses for biomaterials include drug delivery, the implantation of organs like breasts, and the creation of artificial organs such as kidneys, heart-lung machines, etc [42].

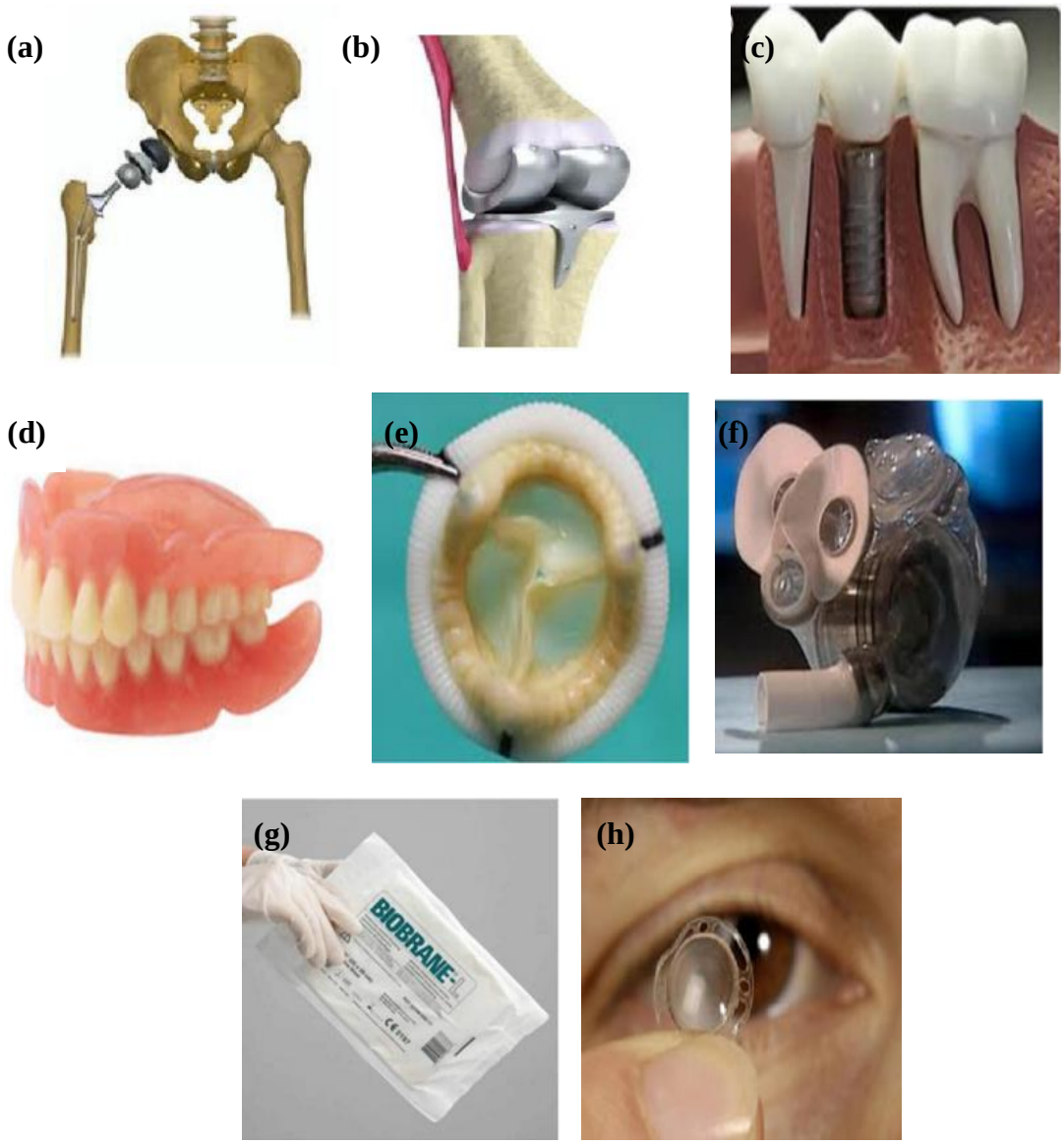

Figure I.4: Examples of some biomedical applications of biomaterials [42]: a) Hip joint prosthesis; b) Knee prosthesis; c) Dental implant; d) Tooth gums; e) Heart valve; f) Artificial heart; g) Biosynthetic wound dressing Biobrane; h) Artificial cornea.

I.1.8 Conclusion

Maintaining the safety and comfort of the life of people with acute functional problems is a major challenge for every community and a critical issue. Therefore, the need for biomaterials in all areas of health is increasing exponentially. In recent times scientists are keen to develop new biomaterials with the aim of helping patients to improve their lives and that is through enhancing their properties which enable them to bind to body tissue without causing any unfavorable effects.

I.2 TOTAL HIP REPLACEMENT AND THEIR PROBLEMS

I.2.1 Introduction

One of the most weight-bearing joints in our body is the hip; it is composed of two halves, namely: a ball (femoral head) at the top of our thighbone (femur) and it fits into a rounded socket (acetabulum) in our pelvis. There is a group of tissues called ligaments that connect the ball to the socket and provide stability to the joint [43]. Rheumatoid arthritis, osteoarthritis, fractures, dislocations, and sometimes accidents can all cause injury to the hip joint. This could result in a hip fracture and a person being permanently disabled [43].

In several situations, it becomes necessary to replace the damaged joint with an artificial one. A hip prosthesis is an artificial joint that is inserted surgically and is created to serve the same purposes as the natural one. " **Total Hip Arthroplasty** " is the name given to the surgical procedure [44].

I.2.2 The history of total hip replacement (Arthroplasty)

Artificial limbs have been used since ancient times where the first attempt to replace a femoral head with ivory in Germany by *Gluck* in 1890 [45]. However, the treatment was not as successful as anticipated and did not become widely used [46]. In 1938, *Philip Wiles* created the first total hip replacement, which had a stainless steel cup and head. The head was fastened using a stem, which was attached to the neck of the femur by a bolt, and the cup was fixed using screws. The clinical results of this development were unknown as a result of World War II's interference [47].

Over time, metal-on-metal implants were introduced by [48], [49], and [50]. The results from such implants were impractical due to implant loosening and high wear of prosthesis components caused by high frictional torque [51]. The first metal-on-polymer total hip replacement was implanted by Sir *John Charnley* in 1958, and the first polymer to articulate with a stainless steel head was polytetrafluoroethylene (PTFE). Additionally, *Charnley* utilized ultra-high molecular weight polyethylene (UHMWPE) as prosthesis in 1961. This procedure was termed "Low Friction Arthroplasty" because it provided low interfacial friction against a metal head [52]. The clinical results have encouraged the use of the *Charnley* prosthesis and are still being used to date in less active elderly patients [53]. *Boutin* created the first ceramic-on-ceramic (CoC) total hip replacement in France in the early 1970 s. Due to

ceramics' outstanding wear resistance, flawless surface finish, and high degree of inertness, ceramic-on-ceramic hip prostheses was widely used in Europe [54].

I.2.3 Definition of total hip replacement

Total hip replacement (arthroplasty) is a surgical technique that relieves the pain and disability brought on by osteoarthritis, fractures, dislocations, congenital abnormalities, and other hip-related issues [43]. Artificial materials are surgically inserted into the hip joint to replace the diseased cartilage and bone [43]. The total hip replacement technique and components position are shown in Figure I.5.

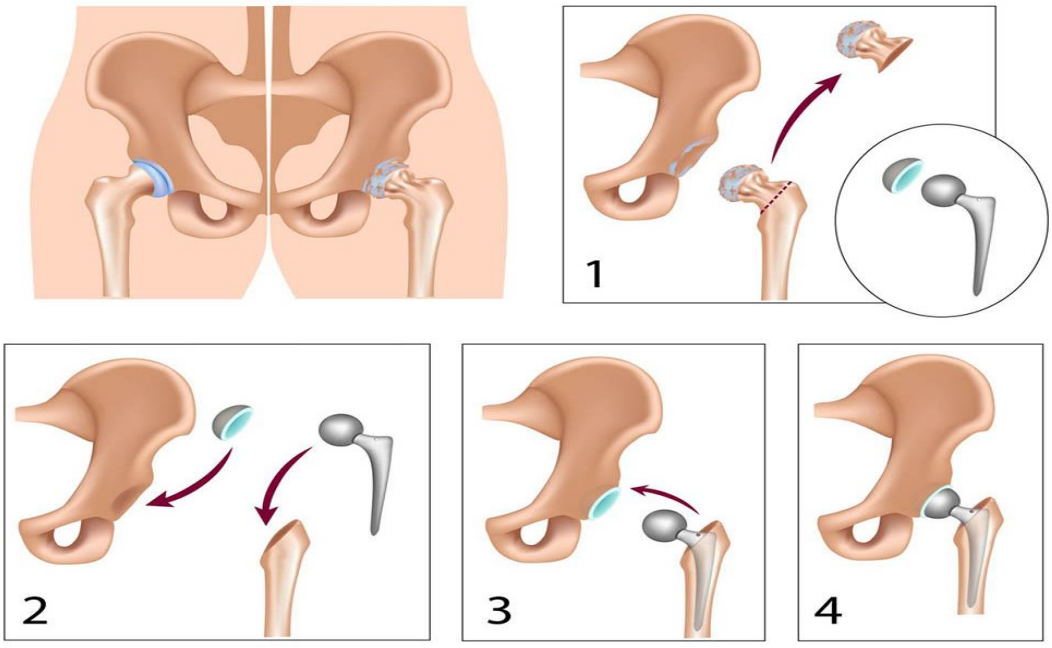

Figure I.5: Surgery details for total hip replacement [55].

I.2.4 Components of total hip prosthesis

Total hip prosthesis includes four components: the femoral head, the femoral stem and the two layers of the acetabular cup.

I.2.4.1 The femoral head

The femoral head (ball) has a taper junction that connects it to the stem's neck [56], and it comes in a variety of diameters that are frequently correlated with the size of the cup [57]. Its diameter plays an important role in determining the range of motion of the artificial joint and its stability against dislocation [56].

I.2.4.2 The femoral stem

The femoral stem is the portion of the prosthesis. After the femoral neck has been removed and the femur's medullary canal has been drilled and reamed, the stem is put into the medullary canal [56]. A uniform load transfer from the prosthesis to the lower limb is ensured by the tight fixation of the femoral stem to the femoral bone [56]. The stem is fixed either by press-fitting against the walls of the medullary canal or by a surrounding layer of bone cement that is injected into the canal before the stem is inserted [56].

I.2.4.3 The acetabular cup-liner

The acetabular cup's liner, sometimes referred to as the insert or socket, is the femoral head's counterpart [56]. It typically has a hollow that is half spherical and mimics the tribological surface that the femoral head wears down [56].

I.2.4.4 The acetabular cup-shell

The shell provides the outer face of the acetabular cup, which must be cemented into the pelvis using either bone cement or press-fitting [56]. Its fixation can be improved by using screws that are put into the pelvis bone [56].

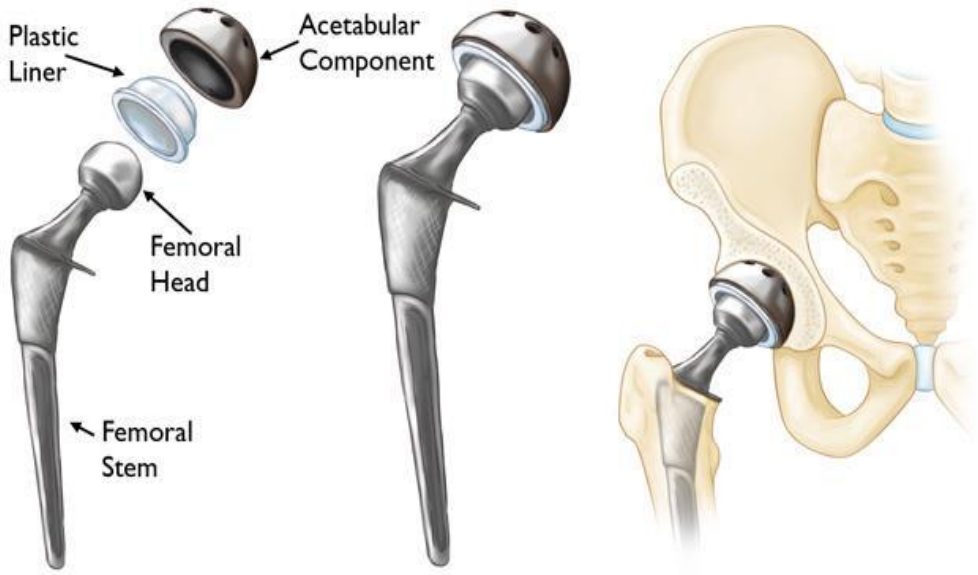

Figure I.6: Components of a total hip replacement [58].

I.2.5 Implantable material systems for THR

The femoral stem and ball of total hip prosthesis fit into the cup or acetabular component and move about it. Each of the components (ball and the liner) can be made from a wide range of materials.

I.2.5.1 Metal-on-Metal (MoM)

Metallic prosthetics are stronger and more durable. However, because of wear, corrosion, and unfavorable reactions with host tissues, causes complications in the human body [59]. In most cases, MoM bearing systems for hip implants are made of Co-Cr-based alloys. (Co-Cr-Mo) alloy system is the most popular form of Co-based alloy utilized in orthopedic implants as femoral and acetabular components. However, the wear of the parts used for more than 30 years is affecting these bearing materials [60]. Therefore, it is essential to increase the life expectancy of the MoM hip joints for younger, more active patients to more than 30 years. Some researchers examined the tribological behavior of Co-Cr alloys modified with various boron additions. They noticed an improvement in wear resistance and hardness with increasing boron content [60].

I.2.5.2 Ceramic-on-Ceramic (CoC)

The Ceramic-on-Ceramic is better than MoM and MoP implants because they show lesser wear [59]. Al_2O_3 and ZrO_2, two common ceramics, have better biocompatibility and greater mechanical strength. As a result, the implant's lifespan is increased by these improved wear properties [59].

I.2.5.3 Metal-on-Polymer (MoP)

Recently, several total joint replacements have utilized MoP-bearing combination materials as a bearing couple, such as Co-Cr alloy on UHMWPE. UHMWPE wear debris, however, has the potential to trigger an inflammatory reaction, which could then result in bone resorption and ultimately aseptic loosening of the implant with complete failure [60]. In addition, the metal ions produced have the potential to cause poisoning. To reduce wear debris, various bearing combinations such as MoM, CoC, and ceramic-on-PE have been created [60].

I.2.5.4 Ceramic-on-Polymer (CoP)

A good mix of two dependable materials is ceramic on UHMWPE, whereas the polyethylene bearing's wear rate can be significantly decreased by the firm, ultra-smooth surface [21]. Ceramic-on-polyethylene implants have potential wear at a rate of about 0.05 mm each year, i.e., 50 % less than metal on polyethylene [21].

I.2.6 Fixation strategies: cemented and uncemented prostheses

The stem and acetabular cup parts of the THA can be fixed to the bone by using bone cement (cemented fixation) or by press-fitting against the bone (uncemented fixation).

I.2.6.1 Uncemented total hip arthroplasty (Cementless)

Direct press-fit contact between implant components and surrounding bone is a distinctive feature of uncemented THA where bone integration is made easier by the intimate surface contact between the implant and bone [56, 61]. Uncemented components' surfaces include porous coatings or a porous surface finish to encourage long-term osteointegration; these pores are meant to be filled by freshly formed trabecular bone tissue [56, 61]. Common coating techniques include Plasma-sprayed hydroxyapatite, Ti-sintered beads, or plasma-sprayed Ti that encourage incorporation into the bone tissue they are hosting. Uncemented THA is preferably used for younger patients since their bone tissue is physiologically more active and they can be candidates for additional replacement surgery. So, using the cemented method will complicate surgery due to the presence of cement and cement debris [56, 61].

I.2.6.2 Cemented total hip arthroplasty

Cemented prostheses are frequently placed in elderly patients who have weaker bones or reduced bone density and cannot withstand extensive rehabilitation [62]. As bone cement, polymethylmethacrylate (PMMA) is the material of choice [56, 61].

The cement purpose is to affix the implant to the bone and distribute the load evenly throughout the joint between the two. Notably, cement acts as filler and does not cling to either the implant or the bone, but rather relies on tight mechanical interlock between the prosthesis and the irregular surface a bone surface [63]. Smooth surfaces are required on cemented stems and acetabular cups to prevent stress concentrations that could cause the

PMMA layer to break. Furthermore, they must be rigid enough to prevent mechanical loading of cement by elastic deformation of the metal [64].

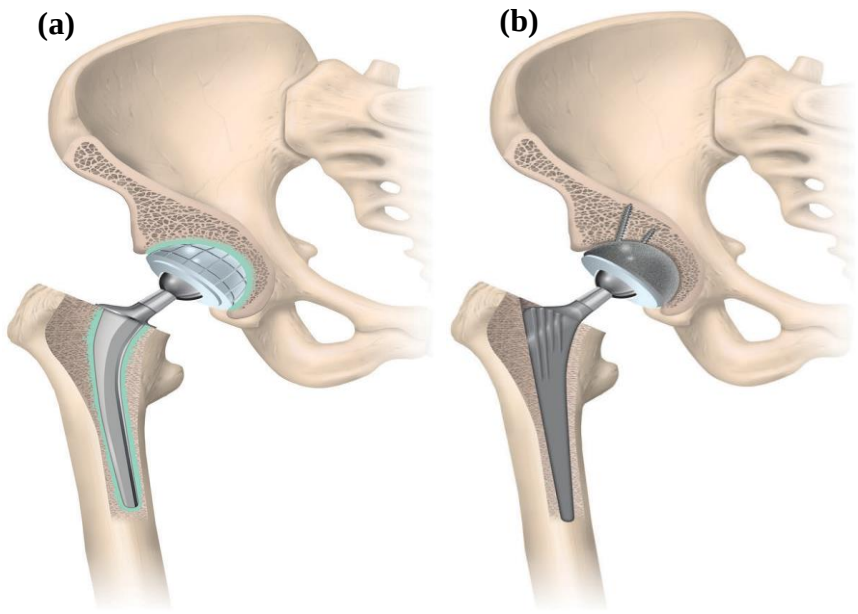

Figure I.7: Types of conventional total hip replacement: a) cemented; b) uncemented [65].

I.2.7 Total hip arthroplasty surgical indications

There are numerous reasons why a natural joint can fail, and in order to restore joint functionality and relieve pain, joint replacement surgery is ultimately necessary. The most popular causes that harm and deteriorate natural joints are:

I.2.7.1 Osteoarthritis

Weight-bearing joints like the hips, knees, spine, and ankles are all affected by osteoarthritis, a type of degenerative joint disease [66]. The loss of the collagen structure and the amorphous portion of the matrix is what leads to the degeneration of the articular hyaline cartilage lining, which in turn causes either a localized lesion or a specific type of erosion resulting in pain and decreased movement [66].

Figure I.8: Hip in a healthy state (left) and hip with osteoarthritis (Right) [55].

I.2.7.2 Acetabular dysplasia and protrusion

Hip dysplasia can be a congenital is caused by a defective acetabulum or developmental deformation typically takes a major trauma to tear the ligaments and dislocate the hip such as car collisions and falls from significant heights [67].

I.2.7.3 Rheumatoid arthritis

Rheumatoid Arthritis is a chronic inflammatory joint disease that frequently results in cartilage degradation and bone degeneration, leaving patients disabled [68].

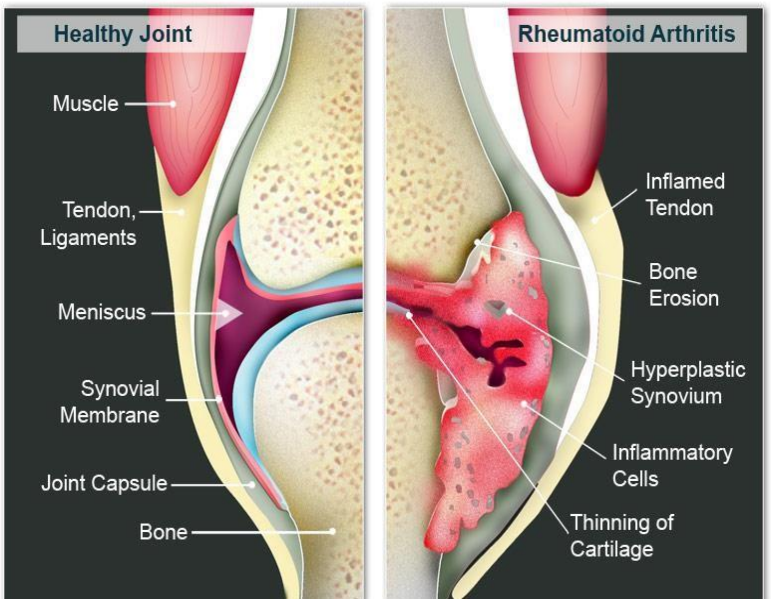

Figure I.9: Image showing contrast between a joint free of rheumatoid arthritis and one that has the disease [55].

I.2.7.4 Avascular necrosis

Avascular necrosis is a result of the shortage of bone irrigation, either temporarily or permanently. With the lack of blood supply, the bone tissue dies and loses its properties [69]. It primarily affects the joints at the shoulder, knee, and hip. Consequently, the bone strength diminishes and the neck of the femur becomes more susceptible to fracture [69].

I.2.8 Complications of the total hip prosthesis

Despite the success of THR, problems may arise and can have a negative impact resulting in poor functional results. The main problems that can occur after a total hip implant are:

I.2.8.1 Aseptic loosening

Implant loosening is the most frequent cause of total hip arthroplasty revision. It may be mechanical or biological in nature where mechanical loosening is caused by loads that are too great for the prosthetic material or the area where it meets the bone [70]. This issue may be made more likely by excessive loading brought on by usage, poor prosthetic design, and inappropriate insertion technique. The cause of biological loosening is bone resorption, which is mediated by cells that are triggered by the presence of cement, polyethylene, or metal particulate-wear debris [70]. Untreated loosening increases the chance of periprosthetic fracture and dislocation, which is frequently painful [71].

Figure I.10: Radiography of an example of aseptic loosening of the femoral stem in a THA [67].

I.2.8.2 Dislocation

Dislocation is characterized by a lack of contact between the acetabulum and the component of the femoral head (Fig. I.11) [67]. It is a common early (within the first year) problem following THA, while it can also happen years after the initial surgery as a result of trauma or acetabular cup wear that increases instability [72]. When the hip is in flexion and internal rotation, the dislocation is posterior; however, can also be anterior by the hip extending and rotating externally [72].

The surgeon must have the necessary skill to properly position the prosthetic components following THA to avoid dislocation [73]. Additionally, choosing the right prosthesis is crucial. For instance, implants with a head diameter of 22 mm have a high risk of dislocation [73]. Prosthesis with a sizable head appears to be the best option for elderly individuals who are more susceptible to dislocation [73].

Figure I.11: Radiography of an example of implant dislocation in a THA [67].

II.2.8.3 Wear

The wear phenomenon is an unfavorable gradual loss of material used to construct a hip arthroplasty component that slowly erodes over time due to frequent movement and contact [74]. There are several mechanisms that contribute to wear, but the following four are crucial:

- ✓ ***Adhesive wear*:** is the result of the material moving from one surface to another surface through shearing of solid welded junctions of asperities. On the surface, it leaves troughs, holes, pits, or other irregularities [75].
- ✓ ***Abrasive wear*:** is the result of hard particles or protuberances sliding along a soft solid surface [75].
- ✓ ***Fatigue/Delamination wear*:** is the name for wear brought on by fracture resulting from surface fatigue due to cyclic loading. It results in a series of pits or voids [75].
- ✓ ***Corrosive wear*:** is due to a chemical reaction between the surface and the environment [76].

I.2.8.4 Fracture

Fractures are classified according to when they occur into two categories: intraoperative and postoperative fractures. Inserting an uncemented component is frequently related to intraoperative fracture. In an uncemented THA, as large a component as possible should be inserted into the medullary canal of the femur or into the acetabulum [73]. The idea is to press-fit an uncemented component into the bone, however doing so increases the risk of the bone breaking, especially for those who are elderly or have severe osteoporosis. Wires cerclages can be used to quickly fix a femur that has only cracked and not broken into fragments. Trauma from a fall or a car accident might result in a postoperative fracture, which is challenging to cure due to the prosthetic stem's presence [73]. Figure I.12 illustrates a stem breakage as an example.

Figure I.12: Radiograph of an example a broken femoral stem in a THA [67].

I.2.9 Conclusion

The total hip prosthesis is an ideal solution for patients who suffer from severe pain and functional problems in the joints. Although the success of total hip replacement in improving people's lives, problems may arise and can have a negative impact resulting in poor functional results.

The major problem is that hip prostheses contain metal and are likely to release metal particles in patients who wear them through friction and corrosion that manifest at the implant-bone interface which leads to toxicity and inflammation thus the implant is damaged. Therefore, must the development of biomaterials to reduce problems of total hip prosthesis and improve their properties to enhance the lives of people suffering.

I.3 GENERALITY ON THE MATERIAL STUDIED

I.3.1 Introduction

The study of nanostructured materials has grown in popularity in recent years. This is due to recent advances in materials synthesis and characterization techniques, as well as the realization that these materials have a variety of interesting and unexpected mechanical, physical, and chemical properties with a variety of potential technological applications [77].

Especially, nanostructured Ti-based biomaterial alloys are widely used in the biomedical field; they are the most attractive biomaterials for orthopedic implants (hip prostheses).

I.3.2 Generality of Titanium

Titanium is now one of the most important metals in the industry. It was first discovered in England by *Gregor* in 1790, but it did not receive a name until *Klaproth* named it the Titans in 1795 [78]. Chemically, titanium is the transition element in group IV and period 4 of Mendeleev's periodic table with an atomic weight of 47.9 and an atomic number of 22. Titanium, as a transition element, has an incompletely filled d shell in its electronic structure [78].

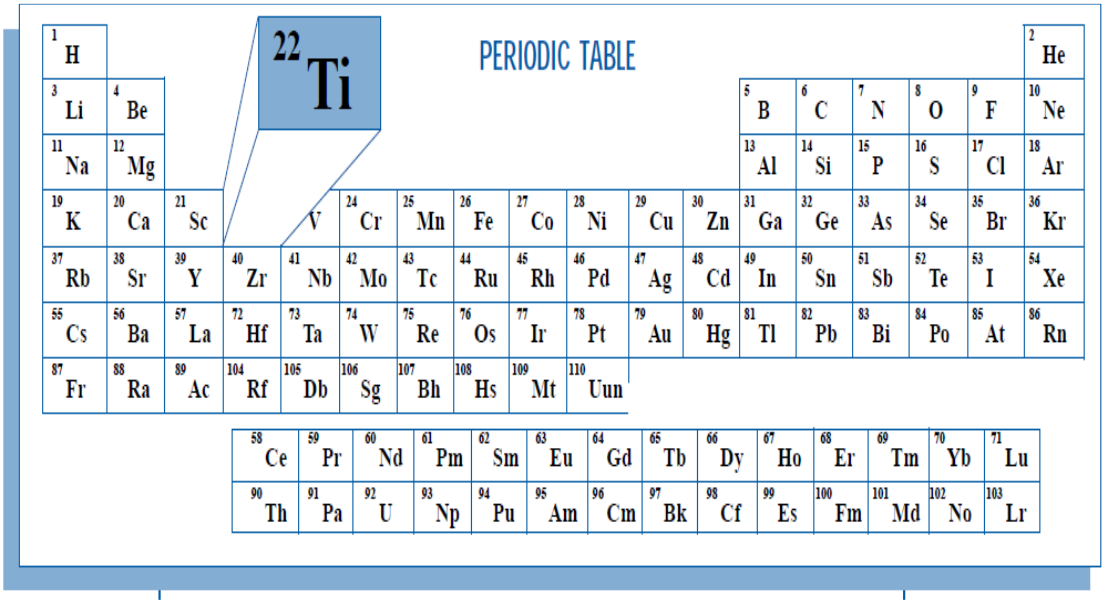

Figure I.13: Titanium location in periodic table [79].

Titanium is present in the earth's crust at a concentration of about 0.6 %, making it the fourth most abundant structural metal after aluminum, iron, and magnesium [80], but it is not found naturally in the metallic state due to its high reactivity in the presence of oxygen. As a result,

titanium-rich ores are scarce and mostly comprised of oxygen, iron, and carbon. Rutile (97-98.5 % TiO_2) and ilmenite (a mixture of titanium and iron oxides with a maximum titanium content of 30 %) are the two main ores mined for titanium production [81].

The increased use of titanium and its alloys as biomaterials is due to their superior biocompatibility and excellent corrosion resistance due to the thin surface oxide layer, as well as good mechanical properties, such as a certain elastic modulus and low density, which give these metals mechanical properties similar to those of bones [82]. Table I.3 shows some important properties of titanium compared to other metallic materials.

Table I.3: Selected physical properties of titanium, compared to some metals [83].

	Ti	**Ni**	**Al**	**Fe**
Density [g/cm^3]	4.5	8.9	2.7	7.9
Melting point [°C]	1670	1455	660	1538
Thermal conductivity [W/mK]	15-22	72-92	221-247	68-80
Elastic modulus [GPa]	115	200	72	215
Reactivity with oxygen	Very high	Low	High	Low
Corrosion resistance	Very high	Medium	High	Low
Metal price	Very high	High	Medium	Low

I.3.3 Crystal structure of Titanium

Titanium transitions from one crystalline form to another through an allotropic transformation [84]. At low temperatures (Below 882 ± 2 ºC), It has a hexagonal-close-packed structure (hcp), called α titanium (α-phase), whereas at high temperatures (above 882 ± 2 ºC) the stable structure is body-centered cubic (bcc), which is referred to as β titanium (β-phase). The corresponding transformation temperature is known as the β-transus temperature and its value for pure titanium is 882±2 °C [84]. The two crystallographic forms of titanium are given in Figure I.14.

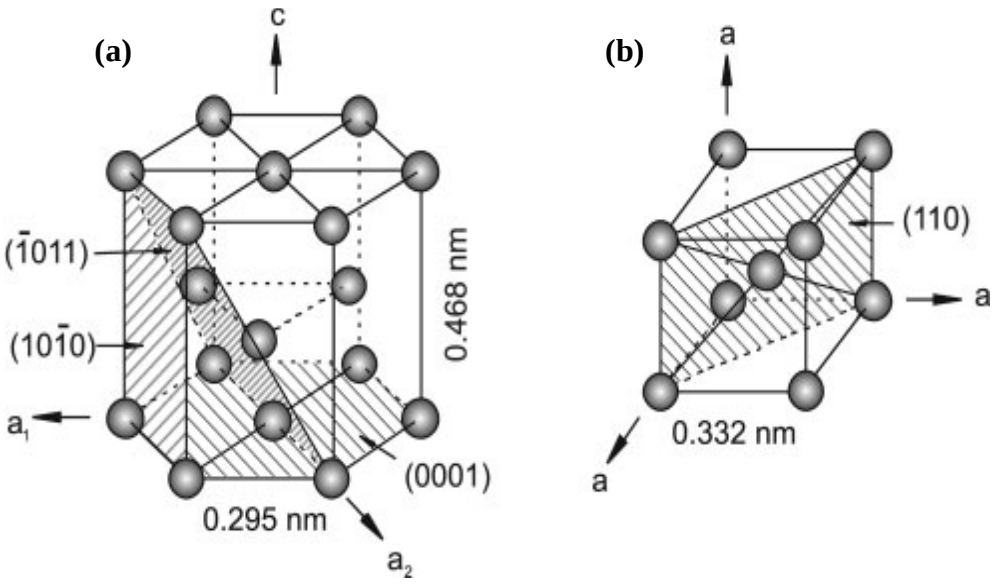

Figure I.14: Crystal structures of titanium: a) hexagonal close-packed (α-phase); b) body centered-cubic (β-phase) [84].

In general, the existence of the two different crystal structures and the corresponding allotropic transformation temperature is of central importance since they are the basis for the large variety of properties achieved by titanium and its alloys [84].

I.3.4 Allotropic transformation

The allotropic transformation β ↔ α of titanium is of martensitic type, according to the mechanism proposed by *Burgers* in 1934 for the zirconium [85]. One can pass from the cubic form centered to the hexagonal form by a weak displacement (less than an interatomic distance), of a few atoms and by a slight rearrangement of these, without any diffusion (Fig. I.15) [85]. Bürger's relations between these two phases α and β are characterized by:

$$\{110\}_{\beta} // \{0001\}_{\alpha} \text{ and } [111]_{\beta} // [11\bar{2}0]_{\alpha}$$

The bcc → hcp transformation in titanium would be the result of athermic germination (via a shearing mechanism involving atomic displacements at short distances) and followed possibly, in the case of slow cooling, by a thermally activated growth [85].

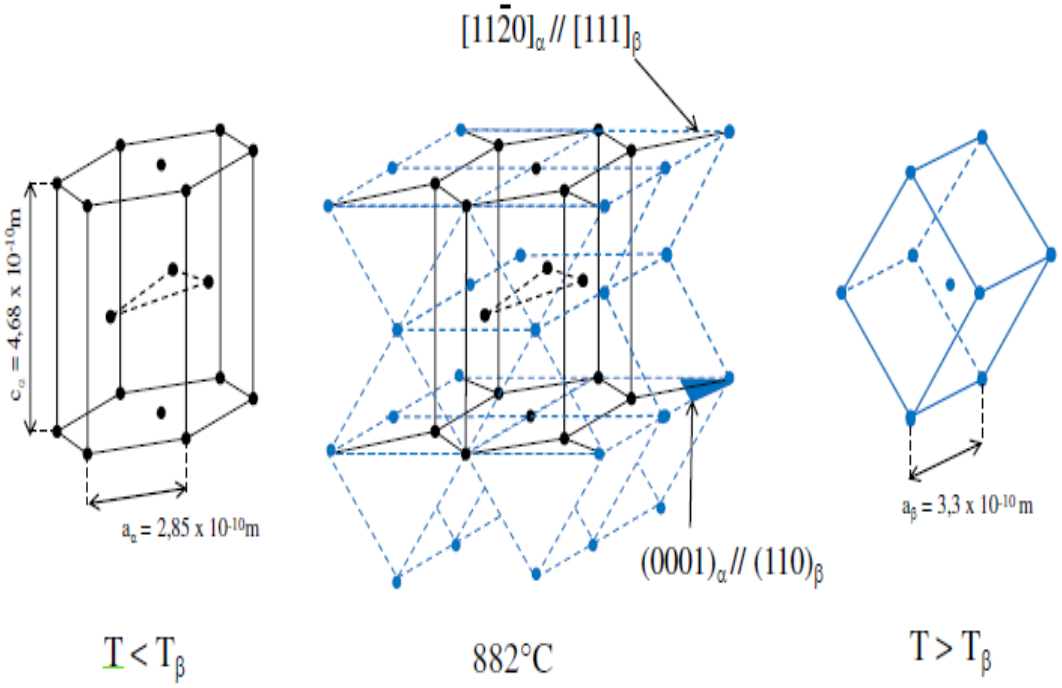

Figure I.15: Schematic representation of allotropic transformation β → α in titanium [86].

I.3.5 Titanium alloys

I.3.5.1 Alloying elements of titanium

Titanium is the transition element; it can combine with other elements to form solid solutions either by insertion or substitution in the lattice according to the nature of the elements of addition [87]. This results in a diverse range of titanium alloys. These elements will modify the stability domains of the β and α phase and thus influence the value of the β-transus temperature [87].

The alloying elements for titanium alloys based on their influence on stabilizing α or β phases are classified into 3 categories: α-stabilizers, β-stabilizers and neutral elements [83] (Table I.4):

I.3.5.1.1 The α-stabilizers

Stabilize the α-phase to higher temperatures, and increase the β-transus temperature [88]. Titanium can have substitutional alloying elements like Al which is the only one that forms a solid substitution solution, as well as interstitial elements such as C, N, and O [89].

I.3.5.1.2 The β-stabilizers

Stabilizes the β-phase to lower temperatures [88], and decrease the β-transus temperature [89]. They are classified into two types: namely β-isomorphous and β-eutectoid.

- ✓ ***β-isomorphous*:** Like Mo, Ta and V, they are much more important because of their much higher solubility in titanium [84].
- ✓ ***β-eutectoid*:** Among β-eutectic elements are Fe, Mn, Cr, Co, Ni, Cu, Si, and H, these elements can lead to the formation of intermetallic compounds [84].

I.3.5.1.3 Neutral elements

Sn and Zr are considered neutral elements because they have no effect on the β-transformation temperature [90].

Table I.4: Influence of different addition elements on the β transus of titanium [91].

Categories		Phase diagram	Insertion	Substitution
α-stabilizers		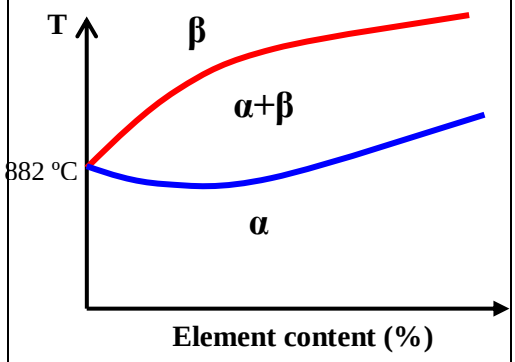	O, N, B, C	Al
β-stabilizers	Isomorphous	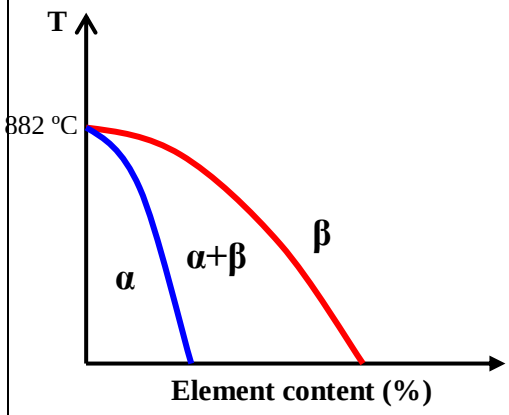		Mo, V, Nb, Ta
	Eutectoid	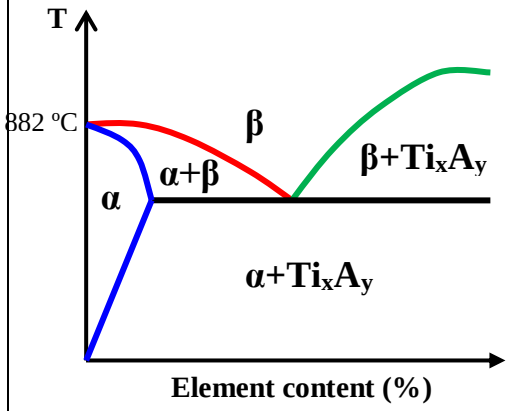	H	Mn, Fe, Cr, Co, W, Ni, Cu, Au, Ag, Si
Neutral		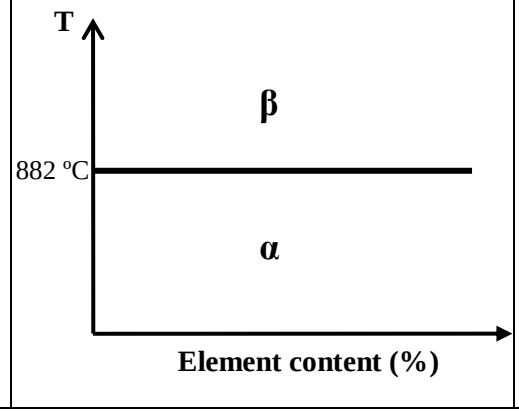		Sn, Zr

I.3.5.2 Classification of Titanium alloys

Titanium alloys can be classified into five main classes which depend mainly on the alloying additions and phases present in the microstructures [92]. Figure I.16 depicts a schematic binary phase diagram demonstrating the effect of both α and β stabilizing elements.

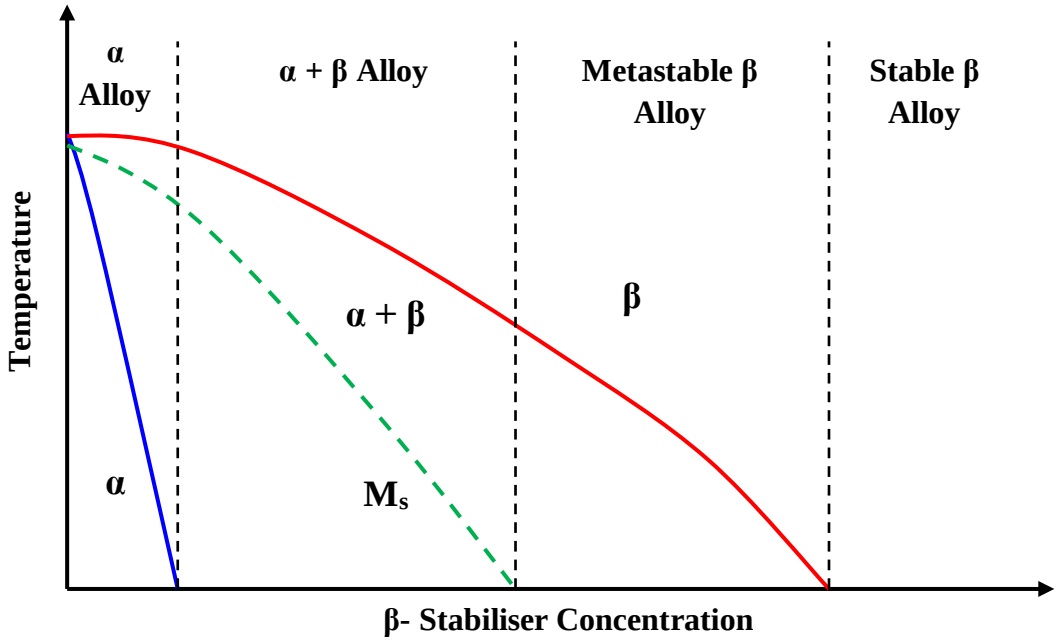

Figure I.16: Classification of Ti alloys according to their composition chemical.

I.3.5.2.1 Alpha alloys (α)

These are single-phase alloys that have been reinforced by the inclusion of neutral alloying components or α stabilizer such as aluminum and tin [92]. The important characteristic of these alloys is that they have acceptable strength, toughness, and weldability but are less forgeable than β alloys [93]. α alloys are suitable for cryogenic applications due to the absence of a ductile-brittle transformation, which is a property of the bcc structure [93].

I.3.5.2.2 Near α alloy

Near α alloys, which small additions of β stabilizers (1 to 2 %) improve strength and workability and are an excellent compromise between the higher strength of α+β alloys and the creep resistance of simple α alloys [92]. This class includes the most widely used commercial high-temperature Ti alloys for aero-engine applications [92].

I.3.5.2.3 (α+ β) alloys

These alloys have a higher concentration of beta stabilizers (4 to 6 %) [92]. Heat treatment of beta alloys can result in a wide range of microstructures and mechanical property combinations. The alloy Ti-6Al-4V is an example of α + β type alloy [89, 94]. Because of its high availability, excellent workability, and enhanced mechanical behavior at low temperatures, this alloy is the most common composition among titanium alloys, and it is still widely used as a biomaterial, primarily in orthopedic implant devices [89, 94].

I.3.5.2.4 Metastable β alloys

Metastable β alloys, often known as near β-alloys, have 10-15 % β-stabilizers and a small amount of α-stabilizers. This source indicates that these alloys can be heat treated by aging, resulting in a very fine α phase dispersed in the β matrix [83]. β stabilizers promote phase retention in metastable circumstances at ambient temperature. These alloys can also be hardened to a strength level greater than 1400 MPa and optimize strength and toughness [83].

I.3.5.2.5 β alloys

A significant addition (30 %) of β stabilizers results in the retention of β as a stable phase at room temperature [89]. Because of their high densities and low ductility, beta alloys are used for highly specialized burn-resistance and corrosion-resistance applications [89].

I.3.5.3 Titanium alloys properties

For the application of titanium alloys in medical sectors like orthopedics and orthodontics, as well as in cardiovascular and reconstructive procedures, they must have great mechanical properties (low density, low Young's modules), high biocompatibility, and superior corrosion resistance [95-99].

I.3.5.3.1 Corrosion of titanium and its alloys

Corrosion resistance is one of a metallic material's primary features used in the environment of the human body [100]. The performance of an implant is directly related to its ability in functioning in aggressive body fluids [89]. These liquids often contain several acids and a specific quantity of NaCl. In normal conditions, its pH is 7; however, it may be altered due to immune system response, like in the case of an infection or inflammation [89]. The implant

component may lose its integrity in the case of corrosion, which would fail. Furthermore, the discharge of corrosion products may trigger harmful biological processes [89].

Titanium is regarded as a stable metal with excellent corrosion resistance than copper and stainless steel [95], this good corrosion resistance is due to the formation of a thin oxide layer on its surface, which separates the metal from its environment [101-103].

The thickness of passive films formed on these metals is 4 to 6 nm, which protects them from corrosion and slows down the release of titanium ions [104]. This oxidation layer consists of a mixture of TiO_2, TiO, and Ti_2O_3 oxides, the most stable being titanium dioxide (TiO_2) [104].

I.3.5.3.2 Biocompatibility

One of the most crucial elements affecting the biocompatibility of metal implants is corrosion behavior [100]. This is due to the fact that the metal ions that corrosion releases have a variety of negative effects [98, 104]. Among the biomaterials, titanium is considered to have excellent biocompatibility, manifested in various applications: orthopedic devices (hip and knee joint, fixation plates on the bone, screws), dental implants, maxillofacial surgery, etc [105, 106]. It has high mechanical strength and a modulus of elasticity that makes it compatible with bone structures [104].

I.3.5.3.3 Wear resistance

Generally, the wear resistance of titanium alloys is less than that of other biomaterials like Co-Cr alloys and alumina [107]. The titanium alloys used in biomedical applications need to have better wear resistance. The wear mechanisms for titanium alloys are roughly grouped into abrasive wear and adhesion wear [107].

Orthopedic implants malfunction when worn debris gets into the surrounding tissues, causing tissue injury, inflammation, and impaired implant functionality [91]. Replacement is usually necessary for this, involving costly revision surgery that has a lower success rate than the original procedure [91]. Moreover, the formation of wear debris at the interface between the orthopedic implant and the human body is made worse by the presence of foreign materials such as metal beads, cement particles, or hydroxyapatite from coatings [91]. Therefore, in order to better adapt to the harsh circumstances found inside the human body, extensive

scientists concentrate on creating and improving the tribological performance (wear rate, coefficient of friction (COF)) of these materials during the design stage [108-111, 2].

I.3.5.3.4 Young's modules

The resistance of a material to deforming under stress is known as the elastic modulus (Young's modules). According to Wolff's law, the bone will adjust to the load it is placed under and vice versa [112]. This means that if an orthopedic biomaterial has a much larger elastic modulus than what it is replacing, the surrounding bone will suddenly be placed under much less stress than it typically endures. As a result, this causes bone atrophy, an increase in osteoclast activity, and finally aseptic loosening (a major cause of implant failure), this tendency is frequently referred to as "*stress shielding*" [112]. The kind of bone (cancellous or cortical) affects the elastic modulus of bone. Although titanium has a larger elastic modulus than that of the outer cortical bone it replaces in total hip arthroplasties, its elastic modulus is still lower than many of the other metals used in orthopedics [112].

I.3.6 An overview about the study alloy Ti-Ni SMAs (Nitinol)

Shape memory alloys (SMAs) are one among many varieties of smart materials. SMAs are relatively new kind of metals that will show unique ability of "retaining" its set shape and a practical phenomenon of shape shift. Deformation occurs at a relatively low temperature, whereas shape memory effect (SME) occurs on heating [113]. Among the various SMA_S alloys is the Ti-Ni which is used in various applications especially, in the area of health [114].

The Ti-Ni or Nitinol is a group of titanium-based intermetallic compounds with almost equal amounts of titanium and nickel. It was discovered by *William J. Buehler* and his coworkers in the *Naval Ordnance Lab (NOL)* in 1963, which is why this alloy is more commonly known as "nitinol" where "niti" refers for nickel-titanium and "nol" means to Naval Ordnance Lab (NOL) [115].

The atomic structure of nitinol is a three-dimensional symmetric grid, with each atom of nickel surrounded by four atoms of titanium (Fig. I.17). The atomic forces that bind these atoms create a unique crystal structure that can exhibit a transition between two phases [116]. The first phase, known as the austenite phase, is a high-temperature, stronger state. The second phase, the martensite phase, is a low-temperature, unstable, weak phase [116]. The transformation between the two phases gives nitinol its unique physical properties [116].

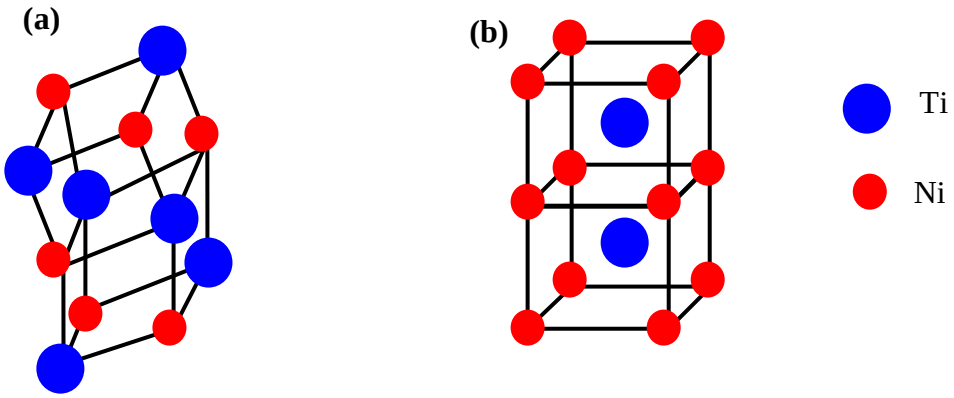

Figure I.17: Atomic structure of nitinol: a) Martensite; b) Austenite.

The Ti-Ni Shape memory alloys (SMAs) have received a lot of interest lately because of their desirable properties:

- ✓ ***Shape memory effect (SME):*** is the result of a material changing from one crystal form to another as it is cooled or heated over a range of typical transformation temperatures [117]. In Nitinol, the change is from an ordered cubic crystal structure (austenite) to a monoclinic crystal phase (martensite) [117].
- ✓ ***Superelasticity (pseudo-elasticity):*** Superelasticity (or pseudo-elasticity) refers to the ultra high elastic behavior of the alloy under stress: typical reversible strains of up to 10 % elongation can be achieved in a superelastic Nitinol wire as compared to 0.5 % reversible strain in a steel wire, for example [118]. The superelastic behavior appears in the austenitic phase when stress is applied to the alloy and the alloy changes from the austenitic phase to the martensitic phase [118].
- ✓ ***Low elastic modulus:*** The elastic modulus of Ti-Ni alloy has been found to range from 20 GPa to 50 GPa for martensite and 40 GPa to 90 GPa for austenite, which is substantially closer to that of natural bone (≈30 GPa) [117]. The low modulus is advantageous in the orthopedic field because it transfers the necessary stress to neighboring bone without causing bone resorption, thus avoid loosening of implants and giving implants a longer service period to prevent revision surgery [117].
- ✓ ***Good corrosion resistance and biocompatibility*:** Numerous in *vitro* and in *vivo* experiments show that Ti-Ni alloy has excellent corrosion resistance and biocompatibility, mostly because a passive dense titanium-oxide layer forms on its surface (TiO_2) [117].

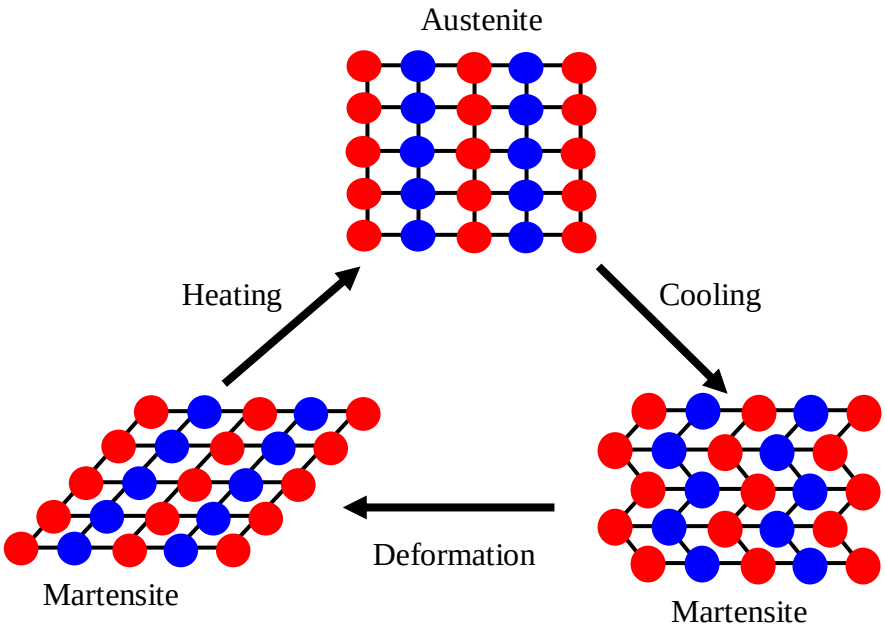

Figure I.18: Schematic illustration of shape memory effect.

I.3.7 Phase diagram of Ti-Ni

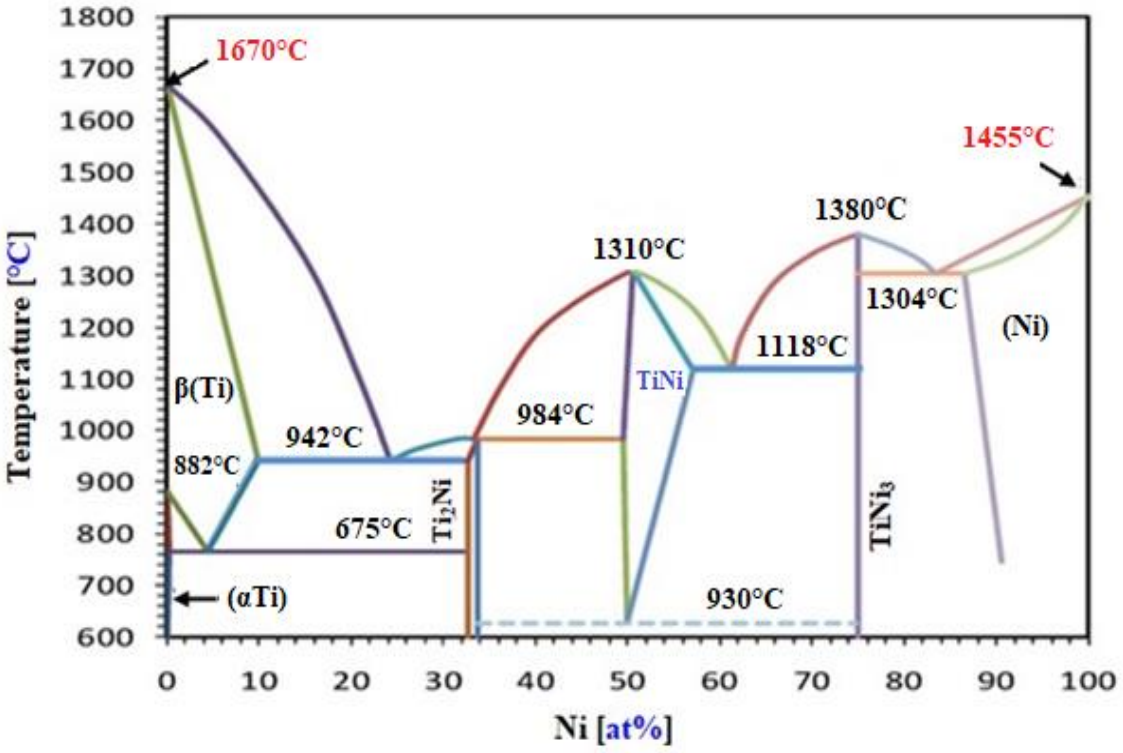

Figure I.19: Phase diagram of a Ti–Ni alloy [119].

The phase diagram of the Ti-Ni alloy system is crucial for improving the properties of alloys during heat treatment (Fig. I.19). It presents four phases of equilibrium are: Ti_2Ni, TiNi, $TiNi_3$, and Ti_3Ni_4 [120].

- The TiNi phase has a B2 (CsCl) type ordered structure with a lattice constant of 0.3015 nm at room temperature. The B2 phase retains upon quenching or slow cooling to room temperature. This is the phase that plays an essential role in the martensitic transformation and the associated shape memory effects.
- The Ti_2Ni phase is cubic with space group Fd3m. The lattice constant is 1.132 nm and the unit cell contains 96 atoms.
- The $TiNi_3$ phase has the hexagonal DO_{24} type ordered structure. The lattice constants are a = 0.51010 nm, c = 0.83067 nm and c/a = 1.6284
- The Ti_3Ni_4 has a rhombohedral structure with space group R3. The lattice constant is a = 0.670 nm [120].

I.3.8 Biomedical applications of Ti-Ni alloy

Ti-Ni alloy is important biomaterials due to its unique characteristics, including shape memory effect, superelasticity, excellent resistance corrosion and biocompatibility, etc. It has been widely used in the biomedical field:

✓ ***Applications of Nitinol as arch wire***

For more than 20 years, dental professionals have utilized nitinol as an orthodontic arch wire. Nitinol can be utilized in orthodontics because of its large strain recovery capacity and due to the generation of stresses that are useful for the alignment of teeth in the orthodontic process. It has better pitting resistance than stainless steel when used as orthodontic arch wire in saliva solution [115].

✓ ***Applications of Nitinol in stent***

These alloys can be employed as stents and blood clot filters in cardiovascular treatments because they change shape following phase transformation [115].

✓ ***Applications of Nitinol as guided wire and in endoscopes***

Guided wire is a thin metal wire. It is inserted through a minor cut or a natural hole. The risk of harm is decreased by using Ti-Ni shape memory alloy in guided wire [115]. Endoscopes are one of the most complex medical devices that use shape memory alloys. The introduction

of nitinol shape memory alloy significantly improved the flexibility and control of endoscopes [115].

- ✓ ***Applications of Nitinol in orthopedics***

In orthopedic surgery, a Ti-Ni shape memory alloy is an excellent choice of material. It has been used for bone plates to determine and fix fracture spine in scoliosis device (for example, in higher shoulder) operation. Ti-Ni can also be utilized as an implant since its elastic modulus is too similar to that of human bone [115, 121, 122]. Figure I.20 shows some of the biomedical applications of nitinol [115].

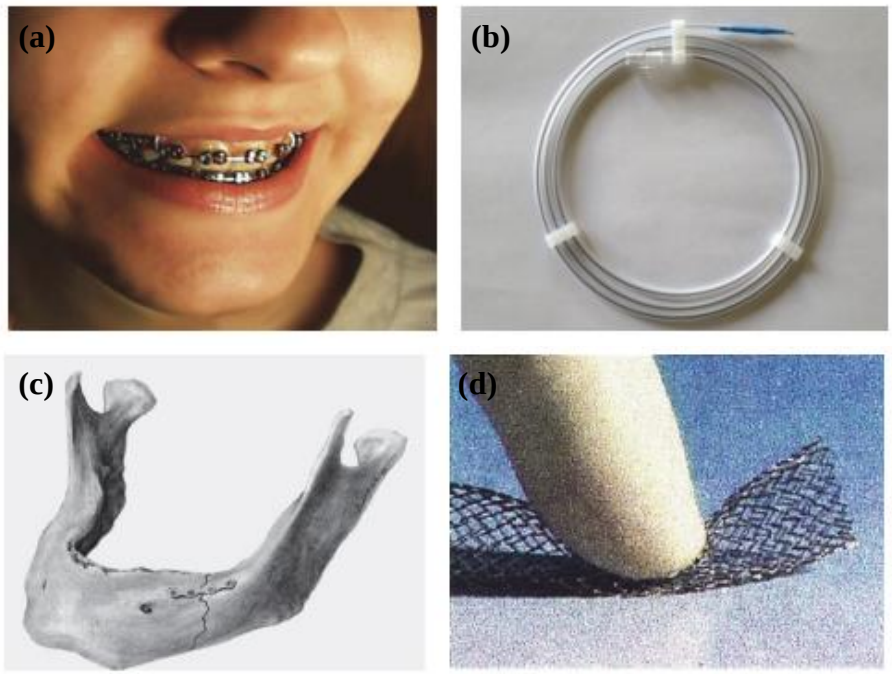

Figure I.20: Biomedical applications of nitinol: a) Orthodontic arch wire; b) Guided wire; c) Bone fixation; d) Stent [115].

I.3.9 Conclusion

Shape memory alloys are fascinating materials that open up a wide range of uses. One of the most these materials is Ti-Ni alloys; which have attracted increasing attention as smart materials for a variety of applications particularly in the field of orthopedics due to their excellent properties.

I.4 NANOMATERIALS

I.4.1 Introduction

Over the past century, "nanotechnology" has experienced significant growth. And today, nanotechnology is a major topic of research in many different fields [123]. Nanotechnology is generally understood to be the study, manipulation, and reorganization of matter on the order of nanometers (i.e., less than 100 nm) to produce materials with essentially novel properties and capabilities [124]. The Greek word "Nanos" or the Latin word "nanus," which both imply "dwarf," are the origins of the word "nano" [123].

The "nanomaterials" are the fundamental and essential components of nanotechnology. Due to their outstanding electrical, optical, magnetic, and catalytic capabilities, they have been receiving a lot of attention. It is well recognized that the shapes, sizes, and morphologies of nanomaterials greatly affect their characteristics and prospective uses; as a result, current research has focused heavily on the controlled synthesis of nanostructured materials with unique morphologies [124].

I.4.2 Properties of nanomaterials

The characteristics of nanomaterials are notably different from other materials due to two main factors: Quantum effects and an increased relative surface area [125]. Some of the properties of nanomaterials are listed below:

- ✓ ***Thermal conductivity***

Nanomaterials have a very high thermal conductivity because covalent bonds vibrate and it is also due to minimum defects in the structure. Its thermal conductivity is 10 times greater than the metal [125].

- ✓ ***Mechanical properties***

The bonds between atoms affect mechanical properties like hardness, elasticity, and ductility. Changes in these properties are brought on by imperfections in the crystal structure and impurities. The carbon nanotubes are 20 times stronger than steel [126].

- ✓ ***Electrical properties***

The electrical properties of nanomaterials vary between metallic to semiconducting materials. It is based on the nanoparticles' diameter. This high electrical conductivity is caused by the structure's little flaws [125].

- ✓ ***Optical properties***

The optical characteristics of nanomaterials are among their most interesting and beneficial features, these characteristics are affected by several factors such as feature size, shape, surface characteristics, doping, and interactions with the environment or other nanostructures [127]. Applications based on nanoparticles' optical characteristics include lasers, optical detectors, sensors, imaging, display, solar cell, photocatalysis, and biomedicine [127].

I.4.3 Classification of nanomaterials

Nanomaterials can be classified according to their origin, their dimensions, and their constitutive materials.

I.4.3.1 Classification of nanomaterials according to dimensionality

Based on their dimensionality, nanomaterials are divided into four classes [128]:

- ✓ ***Zero-dimensional nanomaterials (0D):*** have all their dimensions in the nanoscale i.e., sized below 100 nm (e.g. Spheres, and nanorods, etc).
- ✓ ***One-dimensional nanomaterials (1D):*** are materials with one dimension not in the nanoscale while the other two dimensions are in the nanoscale (e.g. metallic, ceramic, nanotube, and nanofibers, etc).
- ✓ ***Two-dimensional nanomaterials (2D):*** contain only one dimension in the nanoscale while the other two are not (e.g. thin films).
- ✓ ***Three-dimensional nanomaterials (3D):*** materials have a range of dimensions beyond 100 nm (e.g. polycrystals, pillars, etc).

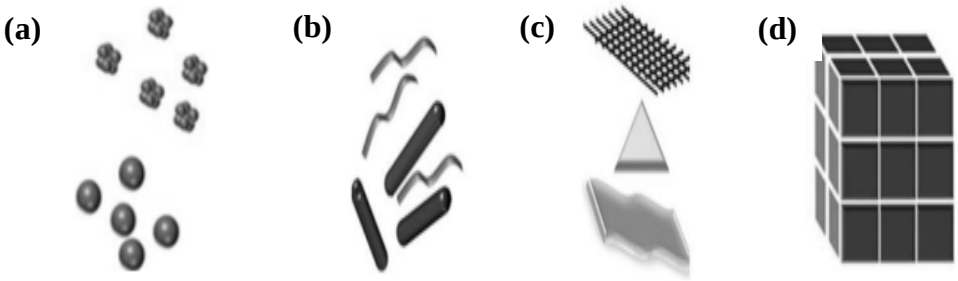

Figure I.21: Dimensionality-based classification of nanomaterials: a) 0 D Spheres and Clusters; b) 1 D Nanofibers, Wires; c) 2 D thin Films, Plates; d) 3 D Nanomaterials [129].

I.4.3.2 Classification of nanomaterials according to origin

Nanomaterials can be classified according to their origin on: natural and synthetic.

I.4.3.2.1 Natural nanomaterials

Inorganic nanomaterials can be found naturally in soils, erupting volcanoes, forest fires, sandstorms, and other natural phenomena. For instance, some types of clay are made of stacked nanoplates that are 1 nm thick and 70 to 150 nm wide [130]. Some nanomaterials can also be found naturally in living things, such as ferritin, a protein that stores iron, and calcium hydroxyapatite, a hard nanocrystalline substance that makes up bones [130]. Additionally, nanomaterials are produced accidentally through human action. This includes, for example, internal combustion engines, power plants, incinerators, and jet engines, etc [130].

I.4.3.2.2 Synthetic (engineered) nanomaterials

An extensive variety of chemical components are used in the production of nanomaterials, for example, semiconductors, metals, carbon, metal oxides, and polymers [130]. They are created for certain purposes; and come in a large variety of forms: spheres, wires, fibers, rods, tubes, shells, and plates, etc [130].

I.4.3.3 Classification of nanomaterials according to constitutive materials

Nanomaterials are now categorized as carbon-based, metal-based, dendrimers, and composites depending on their construction [131].

I.4.3.3.1 Carbon-based nanomaterials

Generally, the primary element in this kind of nanomaterial is carbon; it can be seen in morphologies like spheres, ellipsoids, or hollow tubes [132].

I.4.3.3.2 Metal based nanomaterials

Metal-based nanomaterials are metal-based substances that are generally included nanogold, nanosilver, quantum dots, and metal oxides like Titanium dioxide [131].

I.4.3.3.3 Dendrimers

Dendrimers are branched components that form polymers [131]. They are fewer than 10 nm in size, contain structures and enclose internal cavities [133]. Dendrimers are used in biomedicine for things like cancer treatment, pain control, and other things [131].

I.4.3.3.4 Composite-based nanomaterials

A polyphase solid substance called a nanocomposite [132]. They could consist of any mix of metal-based, carbon-based, or organic-based nanoparticles with any form of metal, ceramic, or polymer bulk materials [132].

I.4.4 Fabrication methods of nanomaterials

The methods used to create the nanomaterials can be divided into two categories:

I.4.4.1 Bottom-up methods

Bottom-up or constructive method is the build-up of material from atom to clusters to nanoparticles. The following are the most typical bottom-up techniques for manufacturing nanomaterials: Sol-gel, spinning, chemical vapour deposition (CVD), pyrolysis and biosynthesis [134, 135].

I.4.4.2 Top-down methods

The top-down or destructive method is the reduction of bulk material to nanometric scale particles [134, 135]. The most commonly used bottom-up methods are: High-energy ball milling, mechanochemical synthesis, and severe plastic deformation [136-138].

I.4.5 Processes used in the elaboration of Ti-Ni alloys:

I.4.5.1 Elaboration of the powders

Several techniques are used for the synthesis of the alloys. Among them is: High-energy ball milling (mechanical process).

I.4.5.1.1 High-energy ball milling

High-energy ball milling is also called mechanical alloying [139]. It is a method for creating nanostructured materials in powder form with an average particle size of less than 100 nm [140], which involves placing a powder mixture in a ball mill and subjecting it to high-energy collisions from the balls [139]. The main of most frequent types of mills for high-energy milling are shown in Figure I.22.

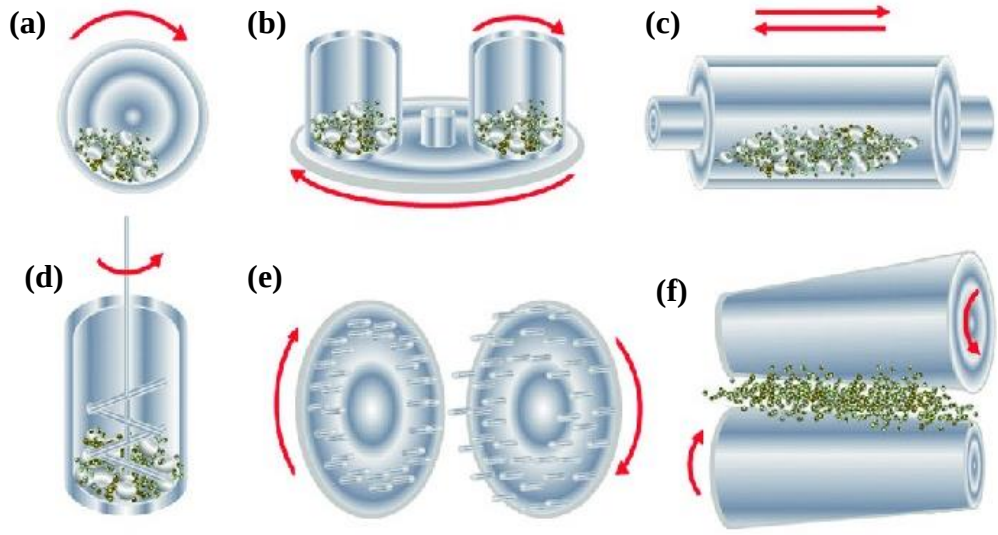

Figure I.22: Types of mills for high-energy milling: a) ball mill; b) planetary mill; c) vibration mill; d)-attritor (stirring ball mill); e) pin mill; f)-rolling mill [141].

I.4.5.1.2 Planetary ball milling

The planetary mill is one of the high-energy ball mills, which is used for efficient and precision milling. Thus, elastic/plastic deformation occurs during the collisions of the powder particles between two colliding balls [142, 143].

I.4.5.1.2.1 Principle

The planetary mill is composed of a disc on which is fixed the jars; the disc turns in one direction and jars in the opposite direction [144]. The ball-powder motion inside the ball mill is shown in Figure I.23.

When the jar and the disc spin in opposite directions produced centrifugal forces. These act on the grinding balls and material inside the jar. As the jar and the disc rotate in opposite directions, the centrifugal forces act alternately in the same and opposite directions [144, 145]. This causes the grinding balls to run down the inside wall of the vial (friction effect on the powder) and then they fly to the other side of the jar hitting the powder (impact effect). The interplay between these forces is responsible for the size reduction of particles and at the same time the microstrains produced in them [144, 145].

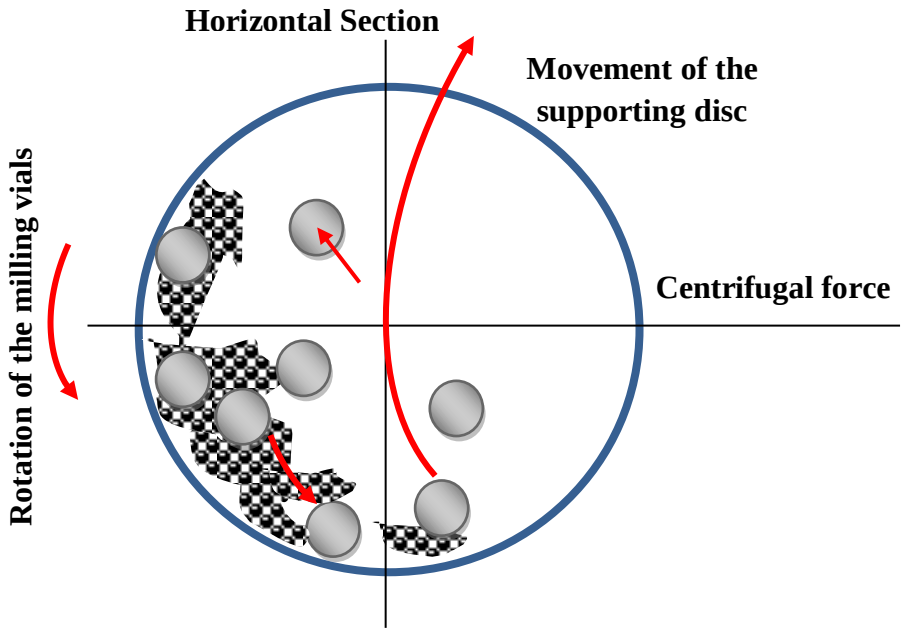

Figure I.23: The ball-powder motion inside the planetary ball mill.

I.4.5.1.2.2 Parameters influencing the nature of the product in the planetary ball milling

The primary variables that affect particle size reduction in planetary ball milling are rotation speed, ball size, ball-to-powder weight ratio, milling medium, milling time, etc. Because of the variety of the powder materials, the selection of parameters varied substantially [146].

- ✓ ***Milling time***

In the ball milling process, the milling time is a crucial variable for the phase formation, microstructural distribution, and homogeneous distribution of components [147-149]. It affects the composites' physicochemical-mechanical characteristics as well. With longer milling times, the size of the nanomaterial reduces [147-149].

- ✓ ***Ball-to-powder weight ratio***

The ball-to-powder ratio is a fundamental parameter of milling operations. It can vary from a value as low as 1:1 to as high as 220:1 [144]. This has a significant effect on the time required to achieve a particular phase in the powder being milled. With the increase in this ratio, the shorter the time required [144].

- ✓ ***The milling atmosphere***

The contamination of the powder is the main consequence of the milling atmosphere. In general, inert gases (Ar, He) are used to avoid contamination [144].

- ✓ ***Milling speed***

The size of the grain boundaries and the particle size are substantially impacted by milling speed. With the increase in milling speed, there was a consequent reduction in the size of the particles [147]. Low milling speeds also resulted in minimum surface imperfections and roughness, whereas high milling speeds led to more strain hardening and thermal softening [147].

- ✓ ***Ball size***

The size of the balls used for milling has a greater impact on the crystal size, yield of production, and energy consumption [147]. The efficiency of the milling increases with smaller diameter balls (sized 10 mm or lesser) [147].

I.4.5.2 Powder metallurgy

Powder metallurgy is a process for developing a solid material from powders metallic without going through fusion but using thermal and/or mechanical techniques [150]. This method

generally includes compression of the powder and then sintering [150]. It can be characterized by the following three keywords: powder, pressure, and temperature. The different manufacturing methods on which it is based make it possible to obtain porous or non-porous parts of various shapes, sizes, and masses [151].

I.4.5.2.1 Methods of shaping from powders

A common technique for creating semi-finished components from powder is compaction [152]. This stage aims to put the obtained powder mixture into the molds and bring them to the required shape and size [153]. Powder compacts can be produced via uniaxial pressing and hot isostatic pressing.

I.4.5.2.1.1 Uniaxial pressing

Uniaxial pressing is the most popular technique for compaction for creating PM components. The compaction cycle is consists in the following three steps [152]:

- ✓ Filling the matrix with the powder.
- ✓ Compacting the powder.
- ✓ Ejecting the powder compact from the matrix.

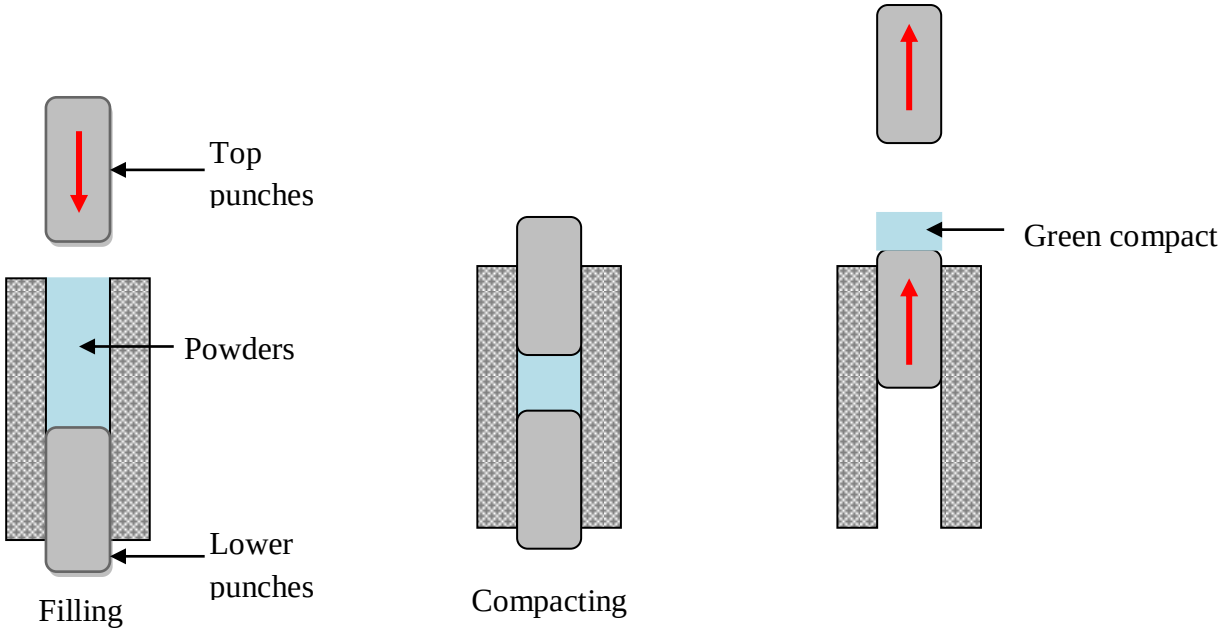

Figure I.24: The different steps of powder compression.

I.4.5.2.1.2 Hot isostatic pressing

Hot isostatic pressing (HIP), is a manufacturing technique in which a work piece (often powder) is simultaneously subjected to high temperature and pressure, causing the powder to consolidate [154]. An inert gas, such as argon or nitrogen, is employed as the pressure medium [154].

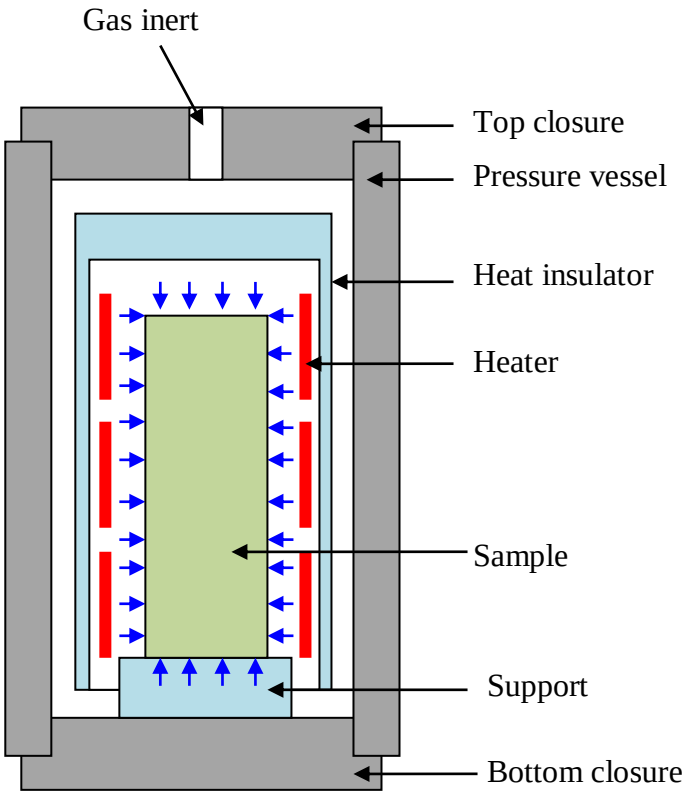

Figure III.25: A schematic representation of HIP equipment.

I.4.5.2.2 Sintering

Sintering is the process of compressing and shaping an object into a solid mass under pressure or heat without melting it to the point of liquefaction [155, 100]. As a result of the process, the porous structure in the piece disappears and it gains strength and stiffness stably [153]. There are two categories of sintering processes: liquid-phase sintering and solid-state sintering. Liquid-phase sintering happens when a liquid phase is present in the powder compact during sintering, while solid-state sintering occurs when the powder compact is densified wholly in a solid state at the sintering temperature [156].

I.4.6 Conclusion

Nanotechnology and research in this area are increasing in popularity every day for improving our lives, especially in the biomedical field.

Mechanical alloying, pressing, and sintering are critical processes in the production of materials with good mechanical properties, good biocompatibility, as well as high resistance to corrosion and wear making them suitable for biomedical uses.

I.5 CONCLUSIONS

We have reported in this chapter some of the general aspects relating to biomaterials, total hip prostheses and their problems, as well as the materials of the study. In addition, we have described all methods utilized in the production of our alloys including, high energy ball milling, pressing, and sintering.

A total hip prosthesis also known as a total hip arthroplasty (THA), is generally considered an ideal solution for those with extensive hip joint damage brought on by degenerative illnesses, fractures, or osteoarthritis.

The mechanisms responsible for the loosening of the total hip prosthesis are mechanical, i.e. related to the problems of friction, resistance to wear, corrosion, design of parts, and also the biological factor. In this context, this study aims to improve the mechanical, tribological, and electrochemical properties of total hip prostheses made of one of the titanium alloys which nanostructured Ti_{50}-Ni_{50} alloys enabling them to bind to body tissue without causing any unfavorable effects.

I.6 BIBLIOGRAPHIC REFERENCES

[1] M.C. Rossi, F.C. Stievani, J.P.H. Pfeifer, L.G. Martinez, V.A. Borrás, M.J. Saekid, and A.L.G. Alves., "*Evaluation of the physical and biological properties of Ti-34Nb-6Sn/Mg alloy obtained by powder metallurgy for use as biomaterial*". Materials Research, 25 (2022), 1-15. https://doi.org/10.1590/1980-5373-MR-2021-0233.

[2] N. Hezil, L. Aissani, M. Fellah, M. Abdul Samad, A. Obrosov, Ch. Timofei, and E. Marchenko., "*Structural, and tribological properties of nanostructured α + β type titanium alloys for total hip*". Journal of Materials Research and Technology, 19 (2022), 3568-3578. http://dx.doi.org/10.1016/j.jmrt.2022.06.042.

[3] O.E. Falodun, S.R. Oke, P.A. Olubambi, J.O. Dirisu, and R. Sule., "*Microstructural characteristics and wear behavior of sintered Ni-modifed Ti-xTiB$_2$ composites*". Journal of The Institution of Engineers (India): Series D, 105 (2023). https://doi.org/10.1007/s40033-023-00484-9.

[4] Z. Miljana, A.B. Krstić, H.Z. Stanković, R.B. Ljupković, M.S. Ranđelović, and A.R. Zarubica., "*Different types of biomaterials: structure and application: A Short review*". Advanced technologies, 9 (2020), 69-79. http://dx.doi.org/10.5937/savteh2001069R.

[5] V. Hasirci, and N. Hasirci., "*Fundamentals of biomaterials*". Springer Science+Business Media, LLC, part of Springer Nature. (2018), 338.

[6] Q. Chen, and G.A. Thouas., "*Metallic implant biomaterials*". Materials Science and Engineering: R: Reports, 87 (2015), 1-57. http://dx.doi.org/10.1016/j.mser.2014.10.001.

[7] N.R. Patel, and P.P. Gohil., "*A Review on Biomaterials: scope, application and human anatomy significance*". International Journal of Emerging Technology and Advanced Engineering, 2 (2012), 91-101.

[8]I. Kulinets., "*Biomaterials and their applications in medicine*". In book: Regulatory Affairs for Biomaterials and Medical Devices, (2015), 1-10. http://dx.doi.org/10.1533/9780857099204.1.

[9] E. Gentleman, M.D. Ball, and M.M. Stevens., "*Medical sciences-vol.II-biomaterials*". Available online: https://www.eolss.net/ ebooklib/home.aspx, (2021).

[10] B.D. Ratner, and G. Zhang., "*A history of biomaterials. In biomaterials science. An introduction to materials in medicine, 4th ed*"; Ratner, B.D., Hoffman, A.S., Schoen, F.J., Lemons, J.E., Eds.; Elsevier Academic Press: London, UK, (2020).

[11] A. Bobbio., "*The first endosseous alloplastic implant in the history of man*". Bulletin of the History of Denttistry, 20 (1972), 1-6.

[12] R. Anjard., "*Mayan dental wonders* ". Journal of Oral Implantology, 9 (1981), 423-426.

[13] F. Ali., "*History of dental implants, in memoriam: Dr. Per-Ingvar Branemark, the man who made people smile*". International Journal of Advance Research, Ideas and Innovations in Technology, 5 (2019), 123-124.

[14] E. Crubézy, P. Murail, L. Girard, and J-Pierre Bernadou., "*False teeth of the Roman world*". Nature Cell Biology, 391 (1998), 29-30.

[15] C.F. Barker, and J.F. Markmann., "*Historical overview of transplantation*". Cold Spring Harbor Perspectives in Medicine, 3 (2013), a014977. https://doi.org/10.1101/cshperspect.a014977.

[16] S. Todros, M. Todesco, and A. Bagno., " Review *biomaterials and their biomedical applications:from replacement to regeneration*". Processes, 29 (2021), 1-20. https://doi.org/10.3390/pr9111949.

[17] D.F. Williams., "*On the mechanisms of biocompatibility*". Biomaterials, 29 (2008), 1-13. https://doi.org/10.1016/j.biomaterials.2008.04.023.

[18] R. Shelton., "*Biocompatibility of dental biomaterials*". Woodhead Publishing Series in Biomaterials (1st Edition), (2017), 135. http://dx.doi.org/10.1016/B978-0-08-100884-3.00005-9.

[19] L. Gabriel., "*Methods and technique for bio-system's materials behavior analysis*". PhD Thesis, University of Politècnica of València, (2013).

[20]M. Hussein, A. Mohammed, and N. Al-Aqeeli., "*Wear characteristics of metallic biomaterials*". Materials, 8 (2015), 2749-2768. https://doi.org/10.3390/ma8052749.

[21] N. Bouchareb, N. Hezil, F. Hamadi, M. Fellah., "*Effect of milling time on structural, mechanical and tribological behavior of a newly developed Ti-Ni alloy for biomedical applications*". Material Today Communication, 38 (2024), 108201. https://doi.org/10.1016/j.mtcomm.2024.108201.

[22] S.K. Kiran, and S. Ramakrishna., "*An introduction to biomaterials science and engineering*". World Scientific, (2021), 412.

[23] S.H. Teoh., "*Fatigue of biomaterials: A review*". International Journal of Fatigue, 22 (2000), 825-837.

[24] S. Andreia., "*Films minces de dioxyde de Titane déposés sur Titane par MOCVD: microstructure et biocompatibilité*". PhD Thesis, University of Toulouse, (2008).

[25]ASTM F138-13a, in Standard Specification for Wrought 18Chromium-14Nickel2.5Molybdenum Stainless Steel Bar and Wire for Surgical Implants (UNS S31673). 2013, ASTM International: West Conshohocken, PA.

[26] J.B. Park, J.D. Bronzino., "*Biomaterials principles and applications*". CRC Press LLC. (2003), 250.

[27] M. Sarraf, E.R. Ghomi, S. Alipour, S. Ramakrishna, N.L. Sukiman.," *A state-of-the-art review of the fabrication and characteristics of titanium and its alloys for biomedical applications*". Bio-Design and Manufacturing, 5 (2022), 371-395. https://doi.org/10.1007/s42242-021-00170-3.

[28] A. Verstrynge, J.V. Humbeeck, and G. Willems., "*In-vitro evaluation of the material characteristics of stainless steel and beta-titanium orthodontic wires*". American journal

of orthodontics and dentofacial orthopedics, 130 (2006), 460-470. https://doi.org/10.1016/j.ajodo.2004.12.030.

[29] S. Medici, M. Peana, V.M. Nurchi, J.I. Lachowicz, G. Crisponi, and M.A. Zoroddu., "*Noble metals in medicine: latest advances*". Coordination Chemistry Reviews, 284 (2015), 329-350. https://doi.org/10.1016/j.ccr.2014.08.002.

[30] A.J Festas, A. Ramos, and J.P Davim., "*Medical devices biomaterials-A review*". Proceedings of the Institution of Mechanical Engineers Part L Journal of Materials Design and Applications, 234 (2020), 218-228. http://dx.doi.org/10.1177/1464420719882458.

[31] P. Weiss., "*La chimie des polymères*". umvf.univ-nantes.fr/odontologie/.../cours.pdf, (2010).

[32] T.J. Adrian A. Mishra, I. Park, Y.J. Kim ,W.T. Park, and Y.J. Yoon., "*Polymeric biomaterials for medical implants and devices*". ACS Biomaterials Science and Engineering, 2 (2016), 454-472. https://doi.org/10.1021/acsbiomaterials.5b00429.

[33] A. Aherwar., "*Review current and future biocompatibility aspects of biomaterials for hip prosthesis*". In AIMS Bioengineering, 3 (2016), 23-43. http://dx.doi.org/10.3934/bioeng.2016.1.23.

[34]Y.D. Siraparapu, S. Bassa, and P.D. Sanasi., "*A review on recent applications of biomaterials*". International Journal of Science and Research, (2013), 70-75.

[35] S. Anu, and S. Gayatri., "*Clinical application of bio ceramics*". American Institute of Physics, 1728 (2016), 020538. https://doi.org/10.1063/1.4946589.

[36]K. Mudali., "*Corrosion of bio implant*". Sadhana, 28 (2003), 601-637. http://dx.doi.org/10.1007/BF02706450.

[37] J.R. Davis., "*Handbook of materials for medical devices*". ASM International, (2003), 317.

[38] N. Nikita, W. Kamlesh, and U. Milind., "*An overview on biomaterials: pharmaceutical and biomedical applications*". Journal of Drug Delivery and Therapeutics, 11 (2021), 154-161. http://dx.doi.org/10.22270/jddt.v11i1-s.4723.

[39] P. Balakrishnan., "*Fundamental biomaterials: metals*". Woodhead Publishing Series in Biomaterials, (2018). https://doi.org/10.1016/C2016-0-03502-7.

[40] L. Raja, M.O. Reddy, M.Thaidun, and P.G. Reddy., "*Biomaterials and its applications*". Journal of information and computational Science, 10 (2020), 90-94.

[41] B.M. Elnedhir., "*Comportement mécanique du ciment orthopédique sous chargement dynamique* ". PhD Thesis, University of Djillali Liabes-Sidi Bel Abbes, (2018).

[42] G.M. Raghavendra, K. Varaprasad, and T. Jayaramudu., "*Biomaterials: Design, Development and biomedical applications* ". In book: Nanotechnology Applications for Tissue Engineering, (2015), 21-44. http://dx.doi.org/10.1016/B978-0-323-32889-0.00002-9.

[43] M. Sivasankar, S. Arunkumar, V. Bakkiyaraj, A. Muruganandam, and S. Sathishkumar., "*A review on total hip replacement*". International research journal in advanced engineering and technology, 2 (2016), 589-642. http://dx.doi.org/10.13140/RG.2.2.13686.80969.

[44] M. Merola, and S. Affatato., "*Materials for hip prostheses: a review of wear and loading considerations*". Materials, 12 (2019), 1-24. https://doi.org/10.3390%2Fma12030495.

[45] S. Affatato., "*Perspectives in total hip arthroplasty advances in biomaterials and their tribological interactions*". Woodhead Publishing (2014), 164.

[46] R.A. Brand, J.J. Callaghan, and R.C. Johnston., "*Total hip reconstruction*". Department of Orthopaedic Surgery the University of Iowa, 11 (1991), 19-42.

[47] P. Wiles., "*The surgery of the osteo-arthritic hip* ". Clinical Orthopaedics and Related Research, 45 (2003), 3-16. http://dx.doi.org/10.1097/01.blo.0000096822.67494.2d.

[48] M. Jayaraman, U. Meyer, M. Bühner, U. Joos, and H.P. Wiesmann., "*Influence of titanium surfaces on attachment of osteoblast-like cells in vitro* ". Biomaterials, 25 (2004), 625-631. https://doi.org/10.1016/s0142-9612(03)00571-4.

[49] E. Haboush.,"*A new operation for arthroplasty of the hip based on biomechanics, photoelasticity, fast-setting dental acrylic, and other considerations*". Bull Hosp Joint Disease, 14 (1953), 242-277.

[50] S. Robert, and M. Derkash., "*History of the association of bone and joint surgeons*". Clinical Orthopaedics and Related Research, 337 (1997), 306-309. https://doi.org/10.1097/00003086-199704000-00035.

[51] P.S. Walker, and B.L. Gold., "*The tribology (friction, lubrication and wear) of all-metal artificial hip joints*". Wear, 17 (1971), 285-299. https://doi.org/10.1016/0043-1648(71)90032-9.

[52] J. Charnley., "*Arthroplasty of the hip. A new operation*". Lancet, 277 (1961), 1129-1132. https://doi.org/10.1016/S0140-6736(61)92063-3.

[53] J. Charnley., "*Long-term results of low-friction arthroplasty*". Hip, (1982), 42-49.

[54] P. Bizot, R. Nizard, S. Lerouge, F. Prudhommeaux, and L. Sedel ., "*Ceramic/ceramic total hip arthroplasty*". Journal of Orthopaedic Science, 5 (2000), 622-627. https://doi.org/10.1007/s007760070017.

[55] K. Darshil., *"Method for characterising and quantifying volumetric edge-wear in ceramic-on-ceramic hip arthroplasty devices*". PhD Thesis, University of Huddersfield, (2018).

[56] U. Holzwarth, and G. Cotogno., "*Total hip arthroplasty: state of the art, prospects and challenges*". Luxembourg: Publications Office of the European Union, (2012), 60. http://dx.doi.org/10.2788/31286.

[57]AAHKS. American Association of hip and knee surgeons. *"What are hip and knee replacements implants made of* ?" (2018).

[58]S.T. Jensen., "*Evaluation of dual mobility total hip arthroplasty in elderly patients with femoral neck fracture or hip osteoarthritis*". PhD Thesis, University of Aarhus, (2019).

[59] S.S Das, and P. Chakraborti., "*Development of biomaterial for total hip joint replacement*". IOP Conference Series: Materials Science and Engineering, 377 (2018), 1-7. http://dx.doi.org/10.1088/1757-899X/377/1/012177.

[60] M.T. Mohammed., "*Nanocomposite in total hip joint replacements*". Applications of Nanocomposite Materials in Orthopedics, (2019), 221-252. http://dx.doi.org/10.1016/B978-0-12-813740-6.00012-0.

[61] E. Tamjid, M. Rezaei, Y. Akhtari, A. Ehsandoost, and B. Samavati., "*A Review on total hip joint arthroplasty: prosthesis design and clinical trials*". Journal of Applied Tissue Engineering, 5 (2018), 7-24.

[62] M.H. Stone, R . Wilkinson, and I. G. Stother., "*Sorne factors affecting the strength of the cement-metal interface*". Journal of Bone and Joint Surgery, 71 (1989), 217-221. https://doi.org/10.1302/0301-620x.71b2.2925738.

[63] R. Vaishya, M. Chauhan , and A. Vaish., "*Bone cement*". Journal of Clinical Orthopaedics and Trauma, 4 (2013), 157-163; https://doi.org/10.1016/j.jcot.2013.11.005.

[64] I.D. Learmonth, C. Young, and C. Rorabeck., "*The operation of the century: total hip replacement*". Lancet, 370 (2007), 1508-1519. https://doi.org/10.1016/S0140-6736(07)60457-7.

[65] G. Chatziagaorou., "*Periprosthetic femoral fracture after total hip replacement. Incidence, risk factors and treatment*". PhD Thesis, University of Gothenburg, (2020).

[66] P.J. Bills., "*The development of a geometric methodology for the determination of volumetric wear in total joint replacements and development of a total knee replacement joint using new and novel measurement techniques*". PhD Thesis, University of Huddersfield, (2007).

[67] D. Moreira .," *A total hip replacement toolbox: from CT-Scan to patient-specific FE analysis*". PhD Thesis, University of Ghent, (2017).

[68] J.S. Smolen, D. Aletaha, and I.B McInnes., " *Rheumatoid arthritis*". Lancet, 388 (2016), 2023-2038; https://doi.org/10.1016/s0140-6736(16)30173-8.

[69] S. Agarwala, D. Jain, V.R. Joshi, A. Sule., "*Efficacy of alendronate, a bisphosphonate, in the treatment of AVN of the hip. A prospective open label study*". Rheumatology, 44 (2005), 352-359. https://doi.org/10.1093/rheumatology/keh481.

[70] S.S Jorge, and H.E. Jergesen, "*Total hip arthroplasty* ". Western Journal of Medicine, 162 (1995), 243-249.

[71] V. Lindgren.,"*Complications after total hip arthroplasty-register-based stuadies on surgical approach and infections* " PhD Thesis. (2014).

[72] K.G. Seagrave, A. Troelsen , H. Malchau , H. Husted , and K. Gromov., "*Acetabular cup position and risk of dislocation in primary total hip arthroplasty*". Acta Orthopaedica, 88 (2017), 10-17. https://doi.org/10.1080/17453674.2016.1251255.

[73] S. Susumu., "*Complications of total hip arthroplasty and their prevention and management*". Japan Medical Association Journal, 44 (2001), 165-170.

[74] M.A. McGee, D.W. Howie, K. Costi, D.R. Haynes, C.I. Wildenauer, M.J. Pearcy, and J.D. McLean., "*Implant retrieval studies of the wear and loosening of prosthetic joints: a review* ". Wear, 241 (2000), 158-165. https://doi.org/10.1016/S0043-1648(00)00370-7.

[75] A. Devaraju., "*A critical review on different types of wear of materials*". International Journal of Mechanical Engineering and Technology, 6 (2015), 77-83.

[76] A.Tsujimoto, W.W. Barkmeier, N.G. Fischer, K. Nojiri, Y. Nagura, T. Takamizawa, M. A. Latta, and M. Miazaki, " *Wear of resin composites: current insights into underlying mechanisms, evaluation methods and influential factors*". Japanese Dental Science Review, 54 (2018), 76-87. https://doi.org/10.1016%2Fj.jdsr.2017.11.002.

[77] K. Niespodziana, K. Jurczyk, and M. jurczyk., "*The synthesis of titanium alloys for biomedical applications*". Reviews on Advanced Materials Science, 18 (2008), 236-240.

[78] L. Xuanyong, P.K. Chu, and C. Ding., "*Surface modification of titanium, titanium alloys, and related materials for biomedical applications*"; Materials Science and Engineering R, 47 (2004), 49-121. https://doi.org/10.1016/j.mser.2004.11.001.

[79] Titanium alloy guide.

[80] G. Lütjering, and J.C. Williams., "*Titanium*". 2nd edition, Springer-Verlag Berlin Heidelberg (2003), (2007), 431.

[81]M. Berthaud., "*Étude du comportement de l'alliage de titane Ti6242S à haute température sous atmosphères complexes : applications aéronautiques*". PhD Thesis, University of Burgundy France-Comte, (2018).

[82] J. Gegner., "*Tribology: fundamentals and advancements*". InTech open, (2013), 332.

[83] C. Veiga, J.P. Davim, and A.J.R. Loureiro., "*Properties and applications of titanium alloys*". Reviews on Advanced Materials Science, 32 (2012), 133-148.

[84] C. Leyens, and M. Peters., "*Titanium and titanium alloys - fundamentals and applications*". Wiley-VCH, (2003), 513.

[85] H. Jousset., " *Viscoplasticité et microstructures d'un alliage de titane : Effets de la température et de la vitesse de déformation*". PhD Thesis, University of Paris School of Mines, (2008).

[86] C.F-Miche., "*Evaluation par nanoindentation des propriétés mécaniques locales d'alliages de titane superélastiques et à mémoire de forme*". PhD Thesis, Rennes, INSA, (2014).

[87] E. Bertrand., "*Elaboration et caractérisation d'alliages biocompatibles Ti-Ta-Nb présentant des propriétés superélastiques et à mémoire de forme*". PhD Thesis, Rennes, INSA, (2011).

[88] R.R. Boyer., *"Titanium and its alloys: metallurgy, heat treatment and alloy characteristics*". In book: Encyclopedia of Aerospace Engineering, (2010), 1-11. http://dx.doi.org/10.1002/9780470686652.eae198.

[89] M..J. Jackson , J. Kopac, M. Balazic, D. Bombac, M. Brojan, and F. Kosel ., *"Titanium and titanium alloy applications in medicine".* In book: Surgical Tools and Medical Devices, (2016), 475-517. http://dx.doi.org/10.1007/978-3-319-33489-9_15.

[90] S.F. Jawad, C.D. Rabadia, M.A. Khan, and S.J. Khan., "*Effect of alloying elements on the compressive mechanical properties of biomedical titanium alloys a systematic review".* American Chemical Society, 7 (2022), 29526-29542. https://doi.org/10.1021/acsomega.2c02096.

[91] W. Abd-Elaziem, M.A. Darwish, A. Hamada, and W.M. Daoush "*Titanium-based alloys and composites for orthopedic implants applications: a comprehensive review*". Materials and Design, 241 (2024), 112850. https://doi.org/10.1016/j.matdes.2024.112850.

[92] V.A. Joshi., "*Titanium alloys an atlas of structures and fracture features* ". CRC Press Taylor and Francis Group (1st Edition), (2006), 248. https://doi.org/10.1201/9781420006063.

[93] A. Zhecheva, W. Sha, S. Malinov, and A. Long.,*" Enhancing the microstructure and properties of titanium alloys through nitriding and other surface engineering methods* ". Surface and Coatings Technology, 200 (2005), 2192-2207. https://doi.org/10.1016/j.surfcoat.2004.07.115.

[94] M. Fellah, N. Hezil, T. Mohamed, M. Abdul Samad, A. Obrosov, D.O. Bokov, E. Marchenko, A. Montagne, A. Iost, A. Alhussein., "*Structural, Tribological and Antibacterial Properties of (α+β) based Ti-Alloys for Biomedical Applications*". Journal of Materials Research and Technology, 9 (2020), 14061-14074. https://doi.org/10.1016/j.jmrt.2020.09.118.

[95] M.S. Baltatu, C.A. Tugui, M.C. Perju, M. Benchea, M.C. Spataru, A.V. Sandu, and P. Vizureanu., "*Biocompatible titanium alloys used in medical applications*". Revista De Chimie, 70 (2014), 1302-1306. https://doi.org/10.37358/RC.19.4.7114.

[96] M. Fellah, N. Hezil, M. Abdul Samad, R. Jellabi, A. Montagne, A. Mejias, S. Kossman, A. Iost, A. Purnama, A. Obrosov, and S. Weiss., "*Effect of Molybdenum Content on Structural, Mechanical, and Tribological Properties of Hot Isostatically Pressed β-Type Titanium Alloys for Orthopedic Applications*". Journal of Materials Engineering and Performance, 28 (2019), 5988-5999. https://doi.org/10.1007/s11665-019-04348-w.

[97] M. Fellah, N. Hezil, M.A. Hussein, M. Abdul Samad, M.Z. Touhami, A. Montagne, A. Iost, A. Obrosov, and S. Weiss., "*Preliminary investigation on the bio-tribocorrosion behaviour of porous nanostructured β-type titanium based biomedical alloy*". Materials Lettres, 257 (2019), 126755. https://doi.org/10.1016/j.matlet.2019.126755.

[98] M. Fellah, N. Hezil, M. Z. Touhami, A. Obrosov, S. Weiß, E.B. Kashkarov, A.M. Lider, A. Montagne, and A. Iost., "*Enhanced Structural and Tribological Performance of Nanostructured Ti–15Nb Alloy for Biomedical Applications*". Results in physics, 15 (2019), 102767. https://doi.org/10.1016/j.rinp.2019.102767.

[99] M. Fellah, N. Hezil, D. Leila, M. Abdul Samad, R. Djellabi, S. Kosman, A. Montagne, A. Iost, A. Obrosov, and S. Weiss., "*Effect of sintering temperature on structure and tribological properties of nanostructured Ti-15Mo alloy for biomedical applications*". Transactions of Nonferrous Metals Society of China, 29 (2019) 2310-2320. https://doi.org/10.1016/S1003-6326(19)65137-X.

[100] M. Fellah, N. Bouchareb, N. Hezil, N. Merah, Y. Alashkar, M. Imran, O. Aleksei, and S. Weiss., "*Electrochemical analysis of mechanically alloyed Ti50%-Ni50% alloy for bone implants use*". Journal of Alloys and Compounds, 1010 (2025), 178046. https://doi.org/10.1016/j.jallcom.2024.178046.

[101] A.M. Khorasani M. Goldberg, E.H. Doeven, and G. Littlefair., "*Titanium in biomedical applications—properties and fabrication: a review*". American Scientific Publishers, 5 (2015), 593-619. http://dx.doi.org/10.1166/jbt.2015.1361.

[102] N. Bouchareb, M. Fellah, N. Hezil, F. Hamadi, A. Montagne A. Obrosov, K. Yadav, G.A. El-Hiti., "*Effect of milling time on structural, physical and photocatalytical properties of Ti-Ni alloy for biomedical applications*". The International Journal of Advanced Manufacturing Technology, 131 (2024) 3539-3553. https://doi.org/10.1007/s00170-024-13207-5.

[103] N. Bouchareb, N. Hezil, F. Hamadi, M. Fellah., "*Effect of milling time on structural, mechanical and tribological behavior of a newly developed Ti-Ni alloy for biomedical applications*". Material Today Communication, 38 (2024), 108201. https://doi.org/10.1016/j.mtcomm.2024.108201.

[104] B. Abida., " *Oxydation du titane sous l'action d'un rayonnement électromagnétique: etude des mécanismes d'insertion des éléments chimiques*". PhD Thesis, University of Guelma, (2021).

[105] M. Fellah, N. Hezil, K. Abderrahim, M. Abdul Samad, A. Montagne, A. Mejias, A. Iost, S. Kossman, T. Chekalkin, A. Obrosov, and S. Weiss., "*Investigating the Effect of Sintering Temperature on Structural and Tribological Properties of a Nanostructured Ti–20Nb–13Zr Alloy for Biomedical Applications*". In: Li J. et al. (eds) Characterization of Minerals, Metals, and Materials 2020. The Minerals, Metals & Materials Series. Springer, Cham, (2020), 619-629. https://doi.org/10.1007/978-3-030-36628-5_61.

[106] M. Fellah, L. Aissani, A. Iost, A. Zairi, A. Montagne, and A. Mejias., "*Comportement à l'usure et au frottement de deux biomatériaux AISI 316L et Ti6Al7Nb pour prothèse totale de hanche*". Matériaux and Techniques, 106 (2018), 1-10. https://doi.org/10.1051/mattech/2018051.

[107] M. Niinomi., "*Mechanical biocompatibilities of titanium alloys for biomedical applications*". Journal of the mechanical behavior of biomedical materials, 1 (2008), 30-42. https://doi.org/10.1016/j.jmbbm.2007.07.001.

[108] M. Fellah, N. Hezil, D. Bouras, N. Bouchareb, A.P. Larios, A. Obrosov , G. A. El-Hiti, and S. Weiß., "*Investigating the effect of Zr content on electrochemical and tribological properties of newly developed near β-type Ti-alloys (Ti–25Nb-xZr) for biomedical applications*". Journal of Science: Advanced Materials and Devices, 9 (2024), 100695. https://doi.org/10.1016/j.jsamd.2024.100695.

[109] M. Fellah, N. Hezil, F. Hamadi, A. Iqbal, M. Abdul Samad, A. Alburaikan, H. Abd El-Wahed Khalifa, and A. Obrosov., "*Effect of Fe content on physical, tribological and photocatalytical properties of Ti-6Al-xFe alloys for biomedical applications*". Tribology International, 191 (2024), 109146. https://doi.org/10.1016/j.triboint.2023.109146.

[110] M. Fellah, N. Hezil, D. Bouras, A. Montagne, A. Obrosov, W. Jamshed, R.W. Ibrahim, A. Iqbal, S.M El Din, and H.A. Khalifa., "*Investigating the effect of milling time on structural, mechanical and tribological properties of a nanostructured hiped alpha alumina for biomaterial applications*". Arabian Journal of Chemistry, 16 (2023), 105112. https://doi.org/10.1016/j.arabjc.2023.105112.

[111] M. Fellah, N. Hezil, M.Z. Touhami, M. Abdul Samad, A. Obrosov , D.O. Bokov, E. Marchenko, A. Montagne, A. Iost, and A. Alhussein., "*Structural, tribological and antibacterial properties of (α + β) based ti-alloys for biomedical applications*". Journal of Materials Research and Technology, 9 (2020), 14061-14074. https://doi.org/10.1016/j.jmrt.2020.09.118.

[112] J. Quinn, R. McFadden, C.W. Chan, and L. Carson., "*Review titanium for orthopedic applications: an overview of surface modification to improve biocompatibility and prevent bacterial biofilm formation*". IScience 23 (2020), 101745. https://doi.org/10.1016/j.isci.2020.101745.

[113] A.K. Rao, A. Kothari, D.L. Prakash, J.S. Hallikeri, and N.V. Shetty, "*A review on nickel titanium and it's biomedical applications*". International Research Journal of Engineering and Technology, 7 (2020), 1742-1748.

[114] L.G. Machado, and M.A. Savi., "*Medical applications of shape memory alloys*". Brazilian Journal of Medical and Biological Research, 36 (2003), 683-691. http://dx.doi.org/10.1590/S0100-879X2003000600001.

[115] A. Wadood., "*Review article brief overview on nitinol as biomaterial*". Advances in Materials Science and Engineering, 2016 (2016), 1-9. http://dx.doi.org/10.1155/2016/4173138.

[116] A. Szold., "*Nitinol: shape-memory and super-elastic materials in surgery*". Surgical Endoscopy, 20 (2006), 1493-1496. http://dx.doi.org/10.1007/s00464-005-0867-1.

[117] Y.F. Zheng, B.B. Zhang, B.L. Wang, Y.B. Wang, L. Li, Q.B Yang, and L.S. Cui., "*Introduction of antibacterial function into biomedical Ti-Ni shape memory alloy by the addition of element Ag*". Acta Materialiaia, 7 (2011), 2758-2767; https://doi.org/10.1016/j.actbio.2011.02.010.

[118] A. Biscarini, G. Mazzolai, and A. Tuissi., "*Enhanced nitinol properties for biomedical applications*". Recent Patents on Biomedical Engineering, 1 (2008), 180-196. http://dx.doi.org/10.2174/1874764710801030180.

[119] V.D. Cocco, C. Maletta, and S. Natali, "*Structural transitions in a NiTi alloy: a multistage loading-unload cycle*". Frattura ed Integrità Strutturale. 18 (2011), 45-53. https://doi.org/10.3221/IGF-ESIS.18.05.

[120] K. Otsuka, and X. Ren., "*Physical metallurgy of Ti–Ni-based shape memory alloys*". Progress in materials Science, 50 (2005), 511-678. https://doi.org/10.1016/j.pmatsci.2004.10.001.

[121] M. Fellah**, N.** Hezil, M. Abdul Samad, M.Z. Touhami, A. Montagne, A. Iost, A. Mejias, and S. Kossman., "*The Effect of Milling Time on Structural, Friction and Wear Behavior of Hot Isostatically Pressed Ti-Ni Alloys for Orthopedic Applications*". TMS 2019 148th Annual Meeting & Exhibition Supplemental Proceedings, 85 (2019), 865-875. https://doi.org/10.1007/978-3-030-05861-6_85.

[122] L. Dekhil, S. Louidi, M. Bououdina, and M. Fellah., "*Microstructural, Magnetic, and Nanoindentation Studies of the Ball-Milled Ti80Ni20 Alloy*". Journal of Superconductivity and Novel Magnetism, 32 (2019), 3623-3636. https://doi.org/10.1007/s10948-019-05145-1.

[123] L.A. Kolahalam., "*Review on nanomaterials: Synthesis and applications*". Materials Today: Proceedings. 18 (2019), 2182-2190. https://doi.org/10.1016/j.matpr.2019.07.371.

[124] X. Liu, Z. Zhong, Y. Tang, and B. Liang., "*Review on the synthesis and applications of Fe_3O_4 nanomaterials*". Journal of Nanomaterials, (2013), 1-7. https://doi.org/10.1155/2013/902538.

[125] K. Arivalagan, S. Ravichandran , K. Rangasamy, and E. Karthikeyan., "*Nanomaterials and its potential applications*". International Journal of ChemTech Research, 3 (2011), 534-538.

[126] R.M. Bachhav, and S.N. Deore., "*A review on nanomaterials*". International Journal of Science and Research, (2013), 1451-1451.

[127] A. Alagarasi., "*Chapter - Introduction to nanomaterials*". In book: Introduction to Nanomaterials, (2011).

[128] T.A. Saleh., "*Nanomaterials: Classification, properties, and environmental toxicities*". Environmental Technology and Innovation, 20 (2020), 2-10. https://doi.org/10.1016/j.eti.2020.101067.

[129] P. Sharma, and M. Bhargava., "*Applications and characteristics of nanomaterials in industrial environment*". International Journal of Civil, Structural, Environmental and Infrastructure Engineering Research and Development, 3 (2013), 63-72.

[130] P.I. Dolez., "*Nanoengineering: : global approaches to health and safety issues*". Elsevier B.V. (2015), 706.

[131] A. Bratovcic., "*Different applications of nanomaterials and their impact on the environment*". International Journal of Material Science and Engineering, 5 (2019), 1-7. http://dx.doi.org/10.14445/23948884/IJMSE-V5I1P101.

[132] J. Jeevanandam, A. Barhoum, Y.S. Chan, A. Dufresne, and M.K Danquah., "*Review on nanoparticles and nanostructured materials: history, sources, toxicity and regulations*". Beilstein Journal of Nanotechnology, 9 (2018), 1050-1074. https://doi.org/10.3762%2Fbjnano.9.98.

[133] M. Rabiee, N. Rabiee, R. Salarian, and G. Rabiee., "*Introduction to nanomaterials in medicine*". Iop Concise Physics, (2019), 110.

[134] M.M. Varma, K.T. Sunil Kumar, and I.D.Srivalli., "*A review on nanoparticles: synthesis, characterization and applications*". World journal of pharmaceutical and medical research, 7 (2021), 169-179.

[135] A.M. Ealias, and M.P. Saravanakumar., "*A review on the classification, characterisation, synthesis of nanoparticles and their application*". IOP Conference Series: Materials Science and Engineering, 263 (2017), 032019. http://dx.doi.org/10.1088/1757-899X/263/3/032019.

[136] E. Mansfield, D.L. Kaiser, D. Fujita, and M.V. Voorde., "*Metalorgy and standardization for nanotechnology: protocols and industrial innovation, first Edition*". WILEY-VCH Verlag GmbH and Co. KgaA. (2017), 626.

[137] M. Fellah, M. Abdul Samad, M. Labaïz, and O. Assala., "*Sliding friction and wear performance of the nano-bioceramic α-Al_2O_3 prepared by high energy milling*". Tribology International, 91 (2015), 151-159. https://doi.org/10.1016/j.triboint.2015.07.006.

[138] F. Hammadi, M. Fellah, N. Hezil, L. Aissani, M. Guessem, S. Mechachti, M. Abdul Samad, A. Montagne, A. Iost, W. Sabine, and A. Obrosov., "*The effect of milling time on the microstructure and mechanical properties of Ti-6Al-4Fe alloys*". Materials today communication, 27 (2021), 102428. https://doi.org/10.1016/j.mtcomm.2021.102428.

[139] A.V. Rane, K. Kanny, V.K. Abitha, and S. Thomas., "*Methods for synthesis of nanoparticles and fabrication of nanocomposites*". Synthesis of Inorganic Nanomaterials, (2018), 121-139. https://doi.org/10.1016/B978-0-08-101975-7.00005-1.

[140] M. Mhadhbi., "*Modelling of the high-energy ball milling process*". Advances in Materials Physics and Chemistry, 11 (2020), 31-44. https://doi.org/10.4236/ampc.2021.111004.

[141] P. Balaz, M. Achimovicova´, M. Bala, P. Billik, Z.C. Zheleva, J.M. Criado, F. Delogu, E. Dutková, E. Gaffet, F.J. Gotor, R. Kumar, I. Mitov, T. Rojac, M. Senna, A. Streletskii, and K.W. Ciurowa., "*Hallmarks of mechanochemistry: from nanoparticles to technology*". Chemical Society Reviews, 42 (2013), 7571-7637. https://doi.org/10.1039/C3CS35468G.

[142] H. Fouzia, M. Fellah, N. Hezil, D. Bouras, S. E. Laouini, A. Montagne, H. Abd El-Wahed khalifa, O. Aleksei, G. A. El-Hiti, and K. Yadav., "*Effect of milling time on structural, physical and tribological behavior of a newly developed Ti-Nb-Zr alloy for biomedical applications*". Advanced Powder Technology, 35 (2024), 104306. https://doi.org/10.1016/j.apt.2023.104306.

[143] M. Dahmani, M. Fellah, N. Hezil, M. Benoudia, A. Obrosov, and M. Abdul Samad., "*Structural and mechanical evaluation of a new Ti-25Nb-25Mo alloy produced by high-energy ball milling with variable milling time for biomedical applications*". International Journal of Advanced Manufacturing Technology 129 (2023), 4971-4991. https://doi.org/10.1007/s00170-023-12650-0.

[144] C. Suryanarayana., "*Mechanical alloying milling*", Progress in Materials Science, 46 (2001), 1-184. https://doi.org/10.1016/S0079-6425(99)00010-9.

[145] A.K. Nath, C. Jiten, and K.C. Singh., "*Influence of ball milling parameters on the particle size of barium titanate nanocrystalline powders*". Physica B, 405 (2010), 430-434. https://doi.org/10.1016/j.physb.2009.08.299.

[146] F.L. Zhang, M. Zhu, and C.Y. Wang., "*Parameters optimization in the planetary ball milling of nanostructured tungsten carbide/cobalt powder*". International Journal of Refractory Metals and Hard Materials, 26 (2008), 329-333. https://doi.org/10.1016/j.ijrmhm.2007.08.005.

[147] J. Joy., "*Recent developments on the synthesis of nanocomposite materials via ball milling approach for energy storage applications*". Applied sciences, 12 (2022), 36. http://dx.doi.org/10.3390/app12189312.

[148] M. Farah, M. Fellah, D. Bouras, N. Hezil, A. Becheri, B. Regis, H. Daoudi, A. Montagne, A. Tmader, A.W.K. Hamiden, "*Unraveling the role of sintering temperature on physical, structural and tribological characteristics of ball milled Co28Cr6Mo biomaterial based alloy*". Journal of Engineering Research, (2023). https://doi.org/10.1016/j.jer.2023.10.040.

[149] M. Fellah, N. Hezil, D. Bouras, A. Obrosov, M. Abdul Samad, A. Montagne, S., S. Weiß., "*Structural, Mechanical and Tribological Performance of a nano structured Biomaterial Co-Cr-Mo Alloy Synthesized Via Mechanical Alloying*". Journal of Materials Research and Technology, 25 (2023), 2152-2165. https://doi.org/10.1016/j.jmrt.2023.06.031.

[150] Y. Le Guennec, P. Dorémus, L. Lazzarotto, F. Dore, Y. Kamdem, D. Bouvard, A. Thomazic, C. Pascal, J.-M. Chaix, J. M. Auger, F. Valdivieso, and P. Goeuriot., "*La*

métallurgie des poudres appliquée aux multimatéraux". Mécanique and Industries, 10 (2009), 151-156. https://doi.org/10.1051/meca/2009042.

[151] M. Lahcene., "*Elaboration et caracterisation d'un acier a outil resistant a l'usure obtenu par la metallurgie des poudres*". PhD Thesis, University of Mohamed khider Biskra, (2019).

[152] F. lemoisson, L. froyen., "*Understanding and improving powder metallurgical processes*". Fundamentals of Metallurgy, (2005), 471-501. http://dx.doi.org/10.1533/9781845690946.2.471.

[153] E. beştek., "*Powder metallurgy processes and making metal powder*", (2020). http://dx.doi.org/10.13140/RG.2.2.21469.84967.

[154] N.L. Loh, and K.Y. Sia., *"An overview of hot isostatic pressing*". Journal of Materials Processing Technology, 30 (1992), 45-65. https://doi.org/10.1016/0924-0136(92)90038-T.

[155] N.M. Deraz., "*Sintering process and catalysis*". International Journal of Nanomaterials, Nanotechnology and Nanomedicine, 4 (2018). http://dx.doi.org/10.17352/2455-3492.000023.

[156] S.J.L. Kang., "*Sintering*: *densification, grain growth and microstructure*". Elsevier Butterworth-Heinemann (1st Edition), (2005).

CHAPTER II

MATERIALS

&

METHODS

II. INTRODUCTION

This Chapter presents the elemental powders and the different techniques used in this work. We start by the procedures employed for the synthesis of Ti_{50}-Ni_{50} alloys, which include milling by using Fritsch Pulverisette P7 planetary ball mill, pressing, and sintering. Then, we provide the various characterization techniques that are used to identify specific structural, mechanical, tribological and electrochemical properties.

The main experimental techniques utilized to examine the structural evolution, the morphology, as well as the uniformity of chemical composition of the samples are: X-ray diffraction (XRD) and scanning electron microscopy (SEM) coupled with an energy dispersive spectroscopy (EDS). The mechanical properties (Young's modulus, hardness) were determined by nanoindentation test, while the roughness was measured with a profilometer. A ball-on-plate tribometer was used to measure the samples' wear rate and friction coefficient which was operated under applied loads of 2, 10, and 20 N. Additionally, open-circuit potential (OCP) measurement, potentiodynamic polarization (PD), and electrochemical impedance spectroscopy (EIS) were used to characterize the electrochemical features of alloys.

II.1 ELABORATION OF Ti_{50}-Ni_{50} ALLOYS

II.1.1 Materials of study

Materials used to produce Ti-Ni alloys are metal powders of Ti and Ni supplied by Sigma-Aldrich, Germany (Refer Fig. II.1), their chemical compositions and characteristics are given in the Table II.1 bellow.

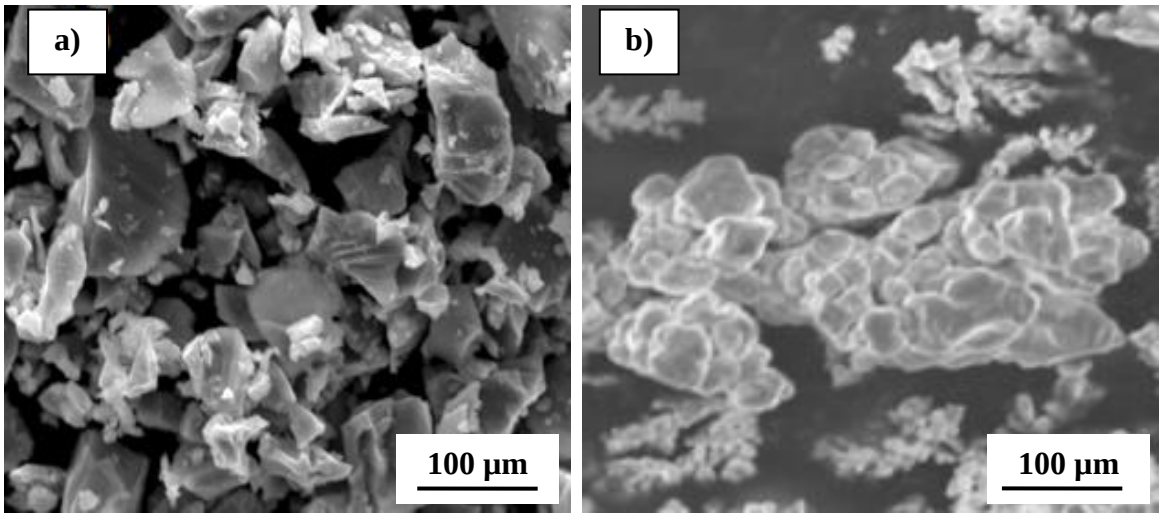

Figure II.1: SEM micrographs of as-received powders particles of pure: a) Ti, b) Ni.

Table II.1: The chemical compositions and characteristics of Ti and Ni powders.

Properties	Ti	Ni
Purity	99.98%	
Particle Size (µm)	< 50	< 55
Fe (at.%)	0.0035	0.0033
O (at.%)	0.0058	0.0031
C (at.%)	0.0036	0.0076
N (at.%)	0.0024	0.0028
H (at.%)	0.0047	0.0032
Melting point (°C)	1670	1455
Density (g/cm^3)	4.5	8.9
Production Process	Hydriding	Hydriding

II.1.2 Synthesis methods

In our study, the fabrication of the binary Ti_{50}-Ni_{50} alloys goes through the following steps:

II.1.2.1 Weighing of powders

The elementary powders of Ti and Ni were weighed using an analytical balance (Fig. II.2**)** with a chemical composition of 50 %/50 % atomic ratio (at.%).

Figure II.2: Analytical balance.

II.1.2.2 Milling process

After weighing the elemental powders, they were milled at different milling times (2, 6, 12, and 18 h) by using a high-energy Planetary Micro Mill Pulverisette P7, Fritsch GmbH, Germany; (Fig. II.3) equipped with two hardened vial (100 ml) containing agate balls (10 mm in diameter). The ball-to-powder ratio (BPR) used for this operation was 10:1, and the milling speed was 400 rpm. After every 15 minutes of grinding, the procedure was halted for 5 minutes in order to prevent an excessive increase in the temperature within the vials. The milling method was utilized to obtain powders with desired particle size and homogeneity.

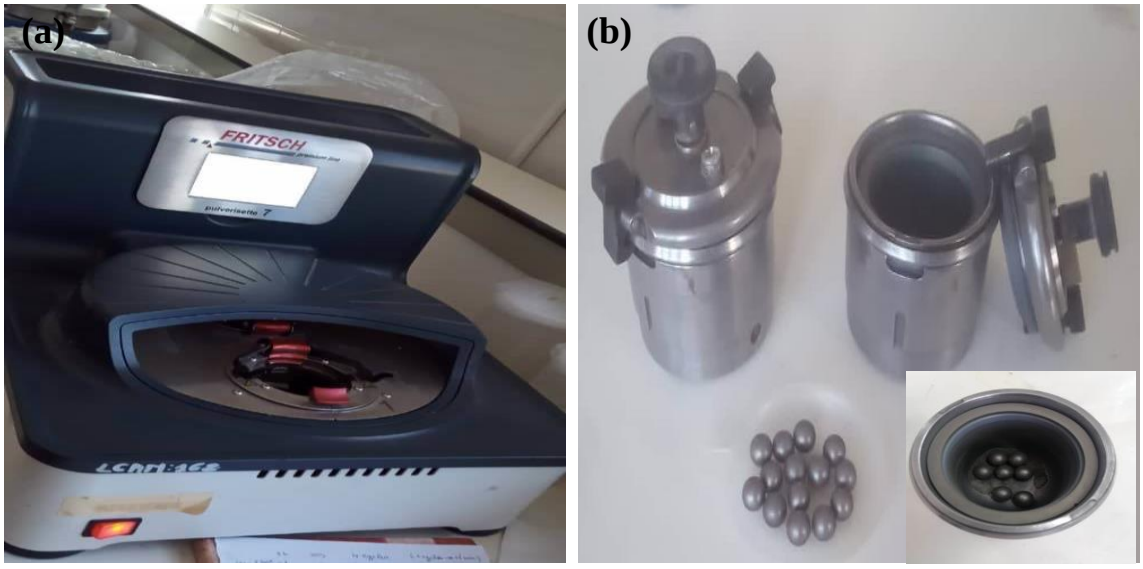

Figure II.3: a) planetary ball mill (Fritsch P7); b) hardened vials and balls.

II.1.2.3 Pressing

Compressed powders were produced by uniaxial pressing (a cold method) and hot isostatic pressing (a hot method). Firstly, the milled powders were compacted by uniaxial press into circular discs by a rigid steel die to obtain cylindrical samples with a diameter of 13 mm under the pressure of 93 MPa. After that, the samples obtained were pressed by the hot isostatic press type (Press Assembly, Germany) at 1050 °C and pressure of 150 MPa for 45 min.

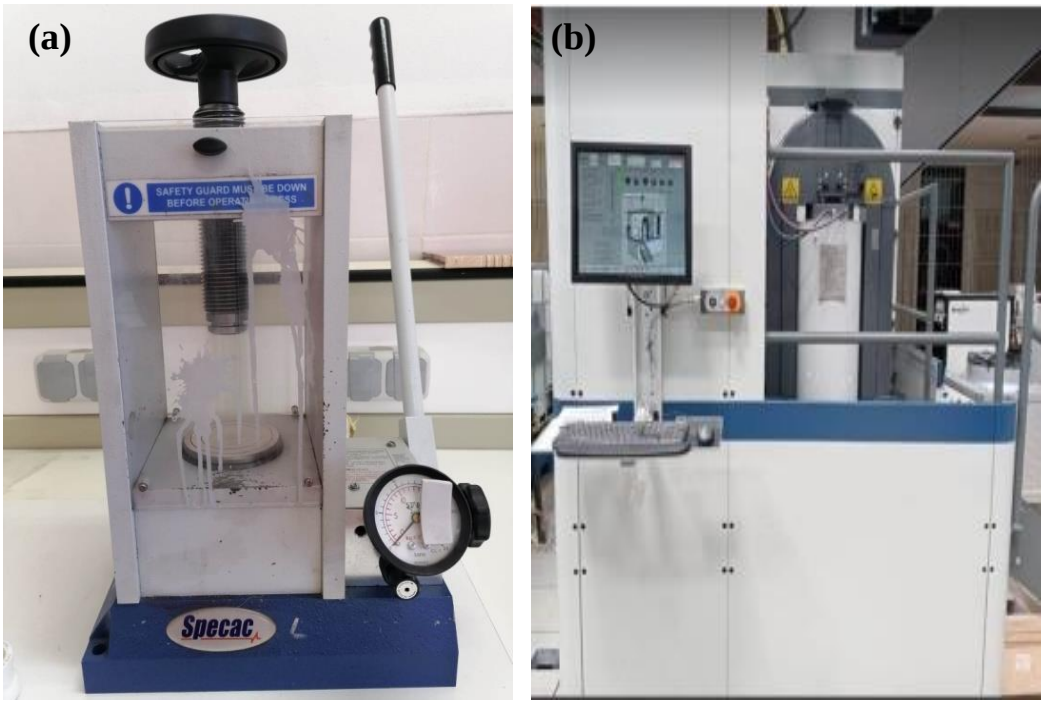

Figure II.4: Machines used in the pressing process:

a) Uniaxial press machine b) Hot isostatic pressing machine

II.1.2.4 Sintering process

The HIPed samples were sintered for 4 hours at 1250 °C under 3 × 10^{-5} mbar using the previously mentioned machine (Press Assembly; Germany), with heating and cooling rates of 20 °C/min and 5 °C/min, respectively. The pellets' sintering process cycle is shown in Figure II.5.

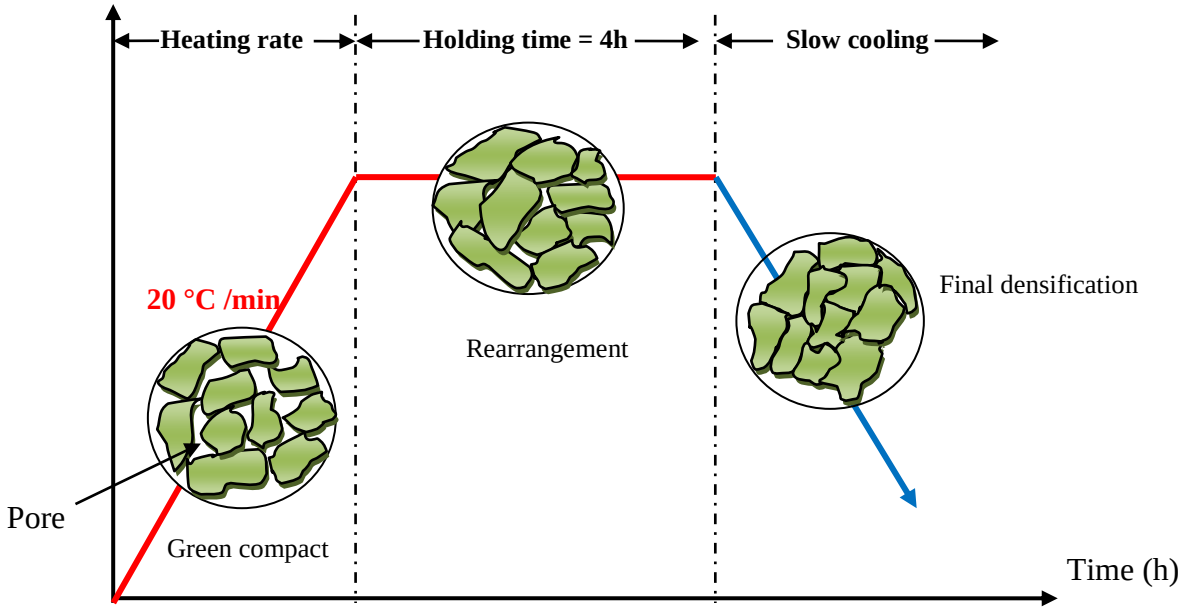

Figure II.5: Sintering process cycle of the pellet.

The synthesis procedure used to manufacture Ti_{50}-Ni_{50} alloys, which includes milling, pressing, and sintering, is summed up in Figure II.6. In addition to that, the characterization methods used were illustrated.

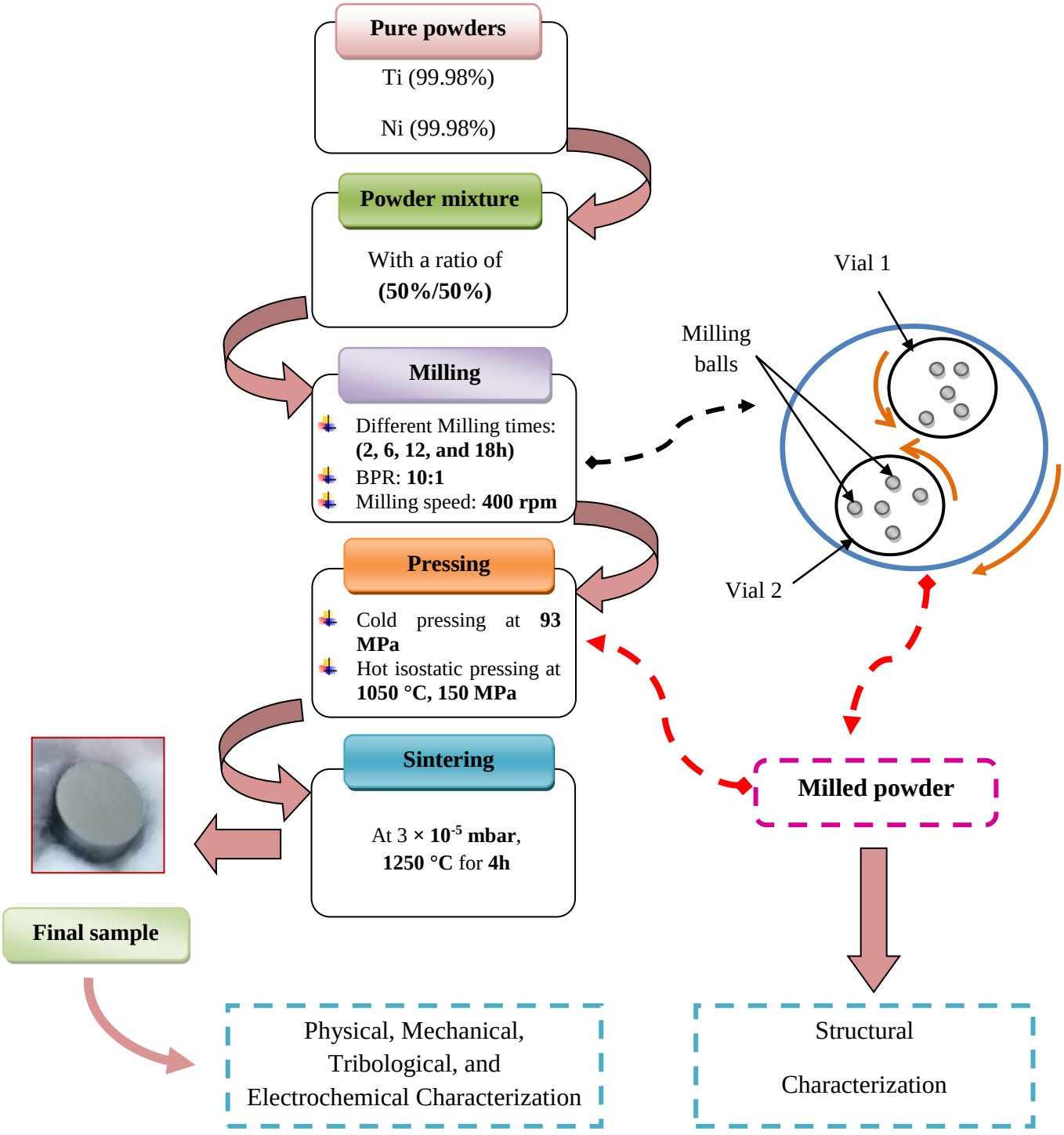

Figure II.6: An illustration diagram of the synthesis of the Ti_{50}-Ni_{50} samples.

II.2 CHARACTERIZATION TECHNIQUES

II.2.1 STRUCTURAL CHARACTERIZATION TECHNIQUES

The study of the microstructural of the Ti_{50}-Ni_{50} alloys milled at different grinding times has required the use of various characterization techniques among them: X-ray diffraction (XRD), scanning electron microscopy (SEM), and energy dispersion spectrometry (EDS). For the quantitative analysis of the microstructure and morphology of the milled Ti_{50}-Ni_{50} powders, a SEM was used which is coupled with EDS to determine the chemical composition. The formed phases and crystal structures of $Ti_{50}Ni_{50}$ alloys were identified by XRD.

II.2.1.1 X-ray diffraction

X-ray diffraction (XRD) is a powerful and widely used nondestructive technique for characterizing crystalline materials. It offers details on structures, phases, and other structural parameters, such as crystalline size and microstrain.

a) Principle

Constructive interference between monochromatic X-rays and a crystalline sample is the foundation of X-ray diffraction. A cathode ray tube produces the X-rays, which are then filtered to produce monochromatic radiation, collimated to concentrate, and pointed at the sample [1] (Fig. II.7). According to *Bragg's law*, which is presented below, incident X-ray interactions with the sample's atomic planes result in diffracted, transmitted, refracted, scattered, and absorbed beams [1, 2]:

$$2.d_{hkl}.\sin\theta = n.\lambda \quad \text{(Eq. II.1)}$$

Where: n is an integer, λ is the wavelength of the X-rays, d_{hkl} is the interplanar spacing generating the diffraction, and θ is the diffraction angle.

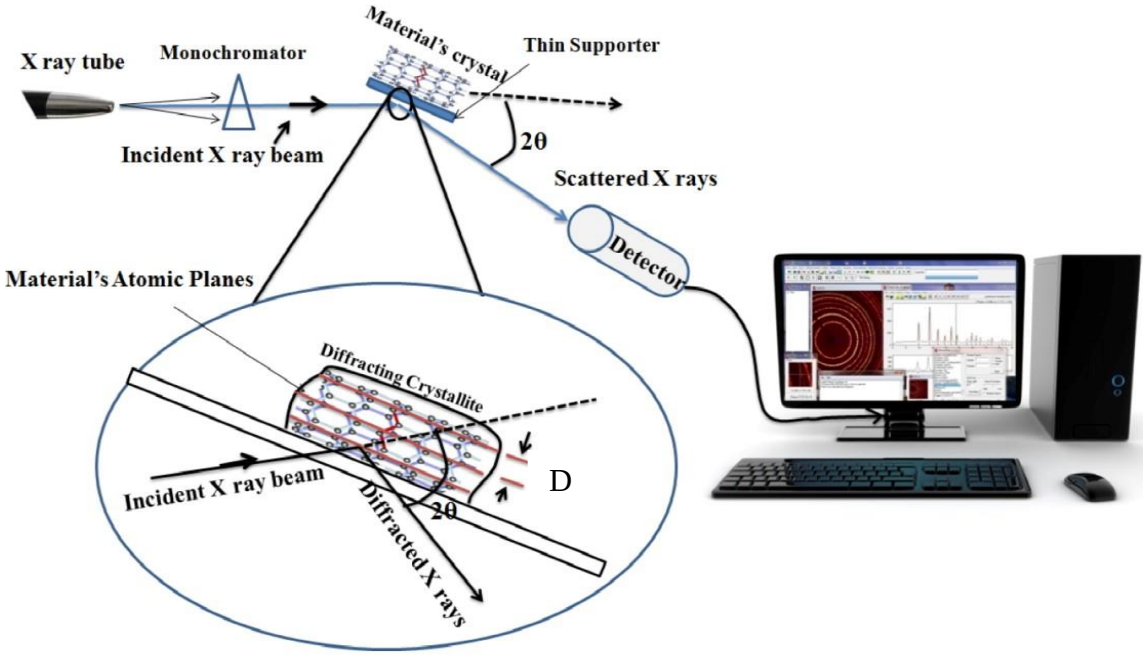

Figure II.7: Schematic diagram of basic principle of XRD [2].

b) Apparatus

Diffraction has been achieved by a diffractometer of type (XRD, Rigaku D-MAX) equipped with copper radiation Cu-K <α> (λ_{Cu} = 0.15406 nm), within the range of 20-80°, with a step of 0.02° and a scan time of 1 s/step. It was also conducted with a current of 20 mA and a voltage of 40 KV.

- **Crystallite size calculation**

The crystallites size was calculated by using Scherer formula [3, 4].

$$D = \frac{0.9.\lambda}{\beta\cos\theta} \quad \text{..... (Eq. II.2)}$$

- **Microstrain/Lattice strain calculation**

Microstrain was determined by the classical William-son–Hall, (W-H) equation, which is presented below [5, 6]:

$$\beta\cos\theta = \frac{0.9.\lambda}{D} + 4\varepsilon \sin\theta \quad \text{..... (Eq. II.3)}$$

- **Lattice parameter calculation**

The following formula was used to determine the lattice parameter (a) [7].

$$a = \frac{\lambda\sqrt{h^2+k^2+l^2}}{2\sin\theta} \quad \text{..... (Eq. II.3)}$$

Where:

D is the crystallite size, λ is the wavelength of the X-radiation used, β is the peak width at half the maximum intensity, θ is the Bragg angle, ε the internal strain (microstrain), and h, k, l are Miller indices of the diffraction planes.

II.2.1.2 Scanning electron microscopy

The scanning electron microscopy (SEM) is one of the most adaptable tools for examining and analyzing the morphology and particle size of powders.

a. Principle

The fundamental principle of SEM is an electron beam with a high energy focused on it that causes numerous interactions between electrons and the surface of the solid sample. As a result of the sample's atoms being ionized by the collision of the electron beam, low-energy secondary electrons, a backscatter of the incident beam's electrons, Auger electrons, and X-rays that are specific to the elements in the sample are released [8]. Each is gathered by a unique detector that is properly placed. Secondary electrons provide topographical information about the surface of the sample whereas Backscattered electrons allow observing chemical contrast [8]. Energy dispersion spectrometry (EDS) coupled with SEM allows the determination of the chemical composition of the analyzed sample. The regions from which various signals are detected are depicted in Figure II.8.

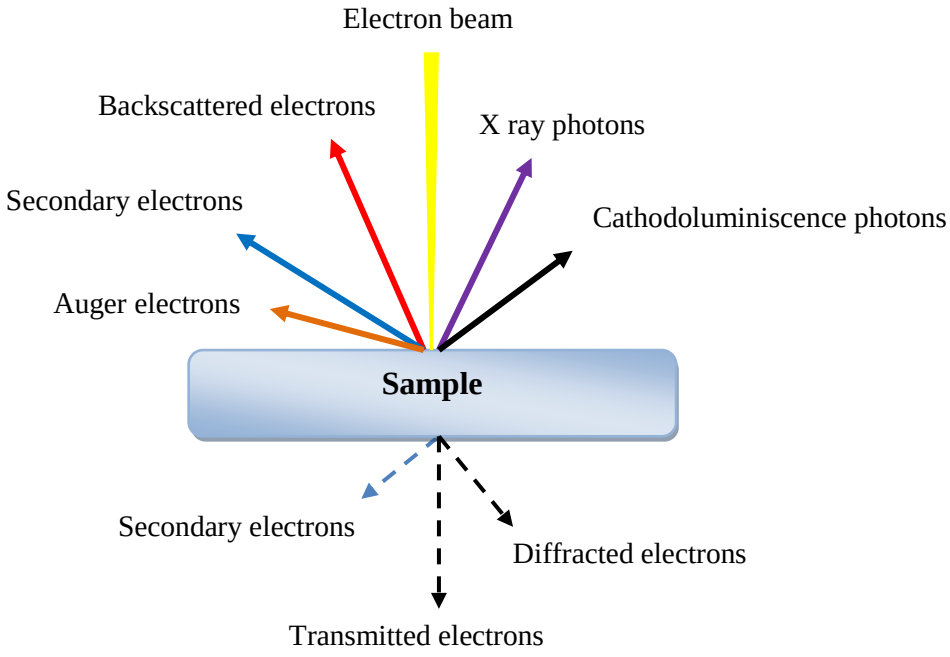

Figure II.8: The different types of signals generated.

b. Apparatus

The investigation of particle size distribution, powder shape, and particle size during planetary milling was conducted by the SEM type TESCAN MIRA, Germany (Fig. II.9).

Figure II.9: Scanning electron microscopy (SEM) machine type TESCAN MIRA, Germany.

II.2.2 MECHANICAL AND PHYSICAL CHARACTERIZATION TECHNIQUES

II.2.2.1 Density and porosity measurement

Density was measured by Archimedes Method. This technique is based on measuring the buoyancy of a body in the water by hydrostatic weighing. It describes the internal porosity of the material and not the open porosity that will be filled with water during the measurement [9].

According to Archimedes' principle, the relative density can be calculated as follows [10]:

$$\rho = \frac{W_a}{W_{a-W_w}} \rho_w \quad \text{..... (Eq. II.4)}$$

Where: ρ_w: Density of distilled water (g/cm^3), w_a: Weight of sample in air (g), and w_w: Weight of sample in water (g).

Porosity was assessed using quantitative micrograph analysis using Image-Pro Plus software, and the results were confirmed using the following relation (Eq. II.5) [11].

$$P = \left(1 - \frac{\rho_{sint}}{\rho_{th}}\right) \times 100\ \% \quad \text{..... (Eq. II.5)}$$

Where: ρ_{th} is the theoretical density of Ti-Ni (6.45 g/cm^3) and ρ_{sint} is the density of the sintered samples.

II.2.2.2 Hardness and Young's modulus

In the world of materials, hardness and Young's modulus are crucial characteristics since these properties are directly influence the performance of the parts manufactured in various applications.

- **Apparatus**

Before the tests, the samples were polished by using polishing machine Struers ROTOPOL 22 (Fig.II.10 (a)). This technique was used to remove surface flaws. It involves using abrasive paper with varying granulometry (between 800 and 4000), then followed by finishing polishing with diamond paste with granulometry 0.25 µm. After polishing the samples are cleaned for 10

minutes in an ultrasonic bath (Fig.II.10 (b)), and then rinsed with distilled water before being dried with hot air.

The nanoindentation test was used to evaluate the hardness and young modulus using a machine (Asmec, Germany Fig. II.11) with a force of 186 mN applied and a dwell time of 10 s. For every sample, six measurements were taken while keeping the distance between the two indents at least three times the indented size.

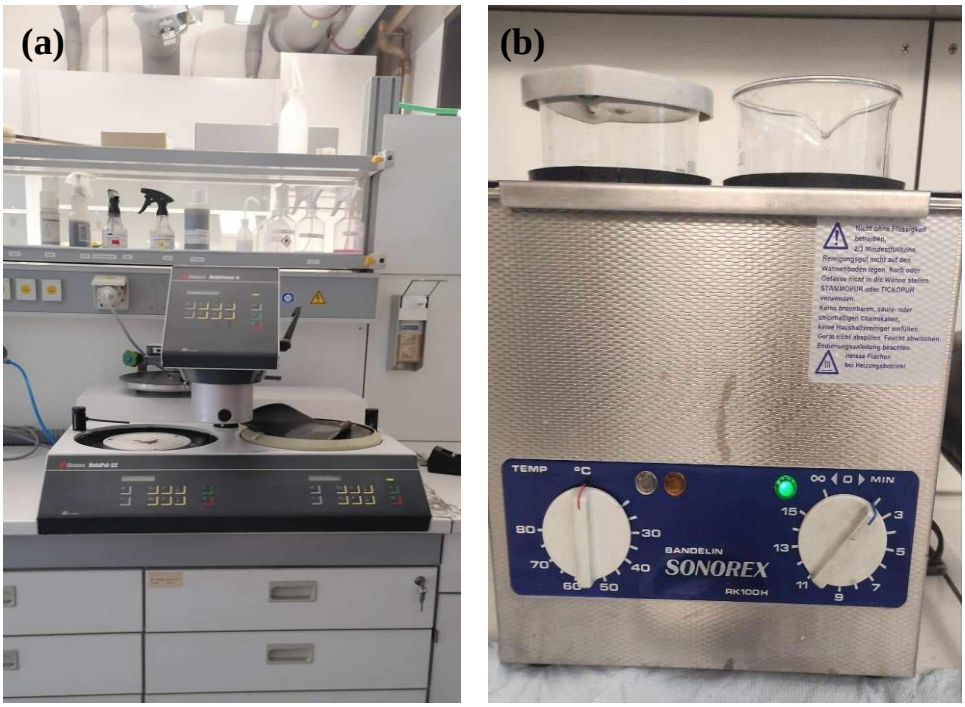

Figure II.10: (a) Polishing machine; (**b)** Ultrasonic bath.

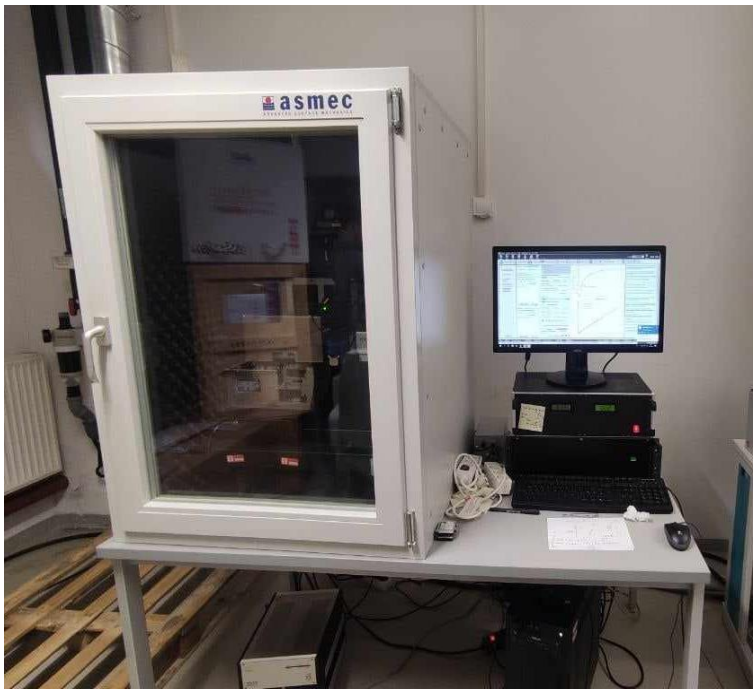

Figure II.11: Nanoindentation tester (Asmec, Germany).

II.2.2.3 Roughness analysis

Surface roughness measures how smooth a surface texture is in areas with less than three dimensions, like lines or surfaces. It has a substantial impact on manufacturing, engineering and the sciences due to its crucial role in the physical and chemical interactions between various materials [12]. There is a direct relationship between roughness, mechanical properties, and tribological behavior of the material.

Generally, roughness can be determined by measuring a number of parameters (Table II.2) [13]. Some of the most commonly used are:

Table II.2: Some of the most commonly characteristics of surface roughness parameters [13].

Parameters	Characteristics
Rp	*R*p is the maximum peak height of the roughness profile within one sampling length (Rp= r_{max}).
Rv	*Rv* is the maximum valley depth of the roughness profile within one sampling length. Previously, the parameter symbol *R*m was used in place of *R*v.
Ra	Roughness average *R*a is the arithmetic mean of the absolute values of the roughness profile ordinates.

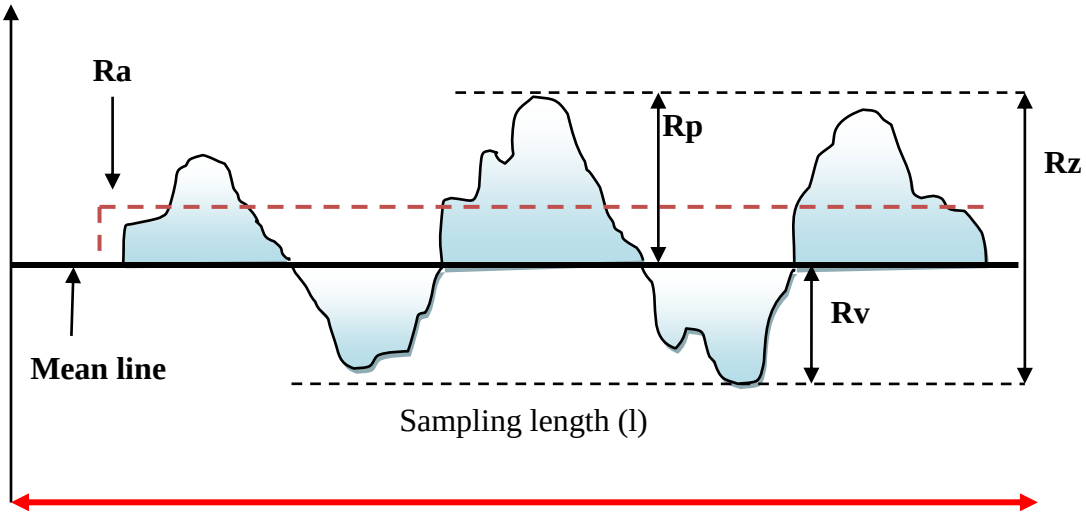

Figure II.12: Roughness measurement parameters.

The optical profilometer type VEECOeeco-Wyko q300 (MSMP) used in the measurement of the average surface roughness (Ra), which was determined utilizing ISO 4287 [14].

II.2.3 TRIBOLOGICAL CHARACTERIZATION TECHNIQUES

In the pursuit of reducing wear and minimizing friction in materials, various methods are employed to assess wear resistance. These methods include measuring the friction coefficient and wear rate, as well as analyzing the damage mechanisms of contact surfaces. The primary

wear mechanisms can be categorized as follows: abrasive wear, adhesive wear, fatigue wear and corrosion wear.

Apparatus

Ti_{50}-Ni_{50} samples were subjected to tribological testing utilizing a ball-on-plate type oscillating tribometer (Fig. II.13), in accordance with the ASTM G 133-95, ISO 7148-1:2012 and ASTM G 99 standards [15]. The experiments were conducted under wet conditions with simulated bodily fluid (Ringer's Solution Table II.3). As the counter body, an alumina ball (Al_2O_3) with the following characteristics was employed: young modulus of 310 GPa, diameter of 6 mm, density of 3.97 g/cm^3, and $HV_{0.02}$ of 2400. The tests were conducted with a stroke length of 5 mm and a sliding speed of 25 mm/s, under various normal loads of 2, 10, and 20 N. SEM was used to examine the surface morphology following each sliding wear test.

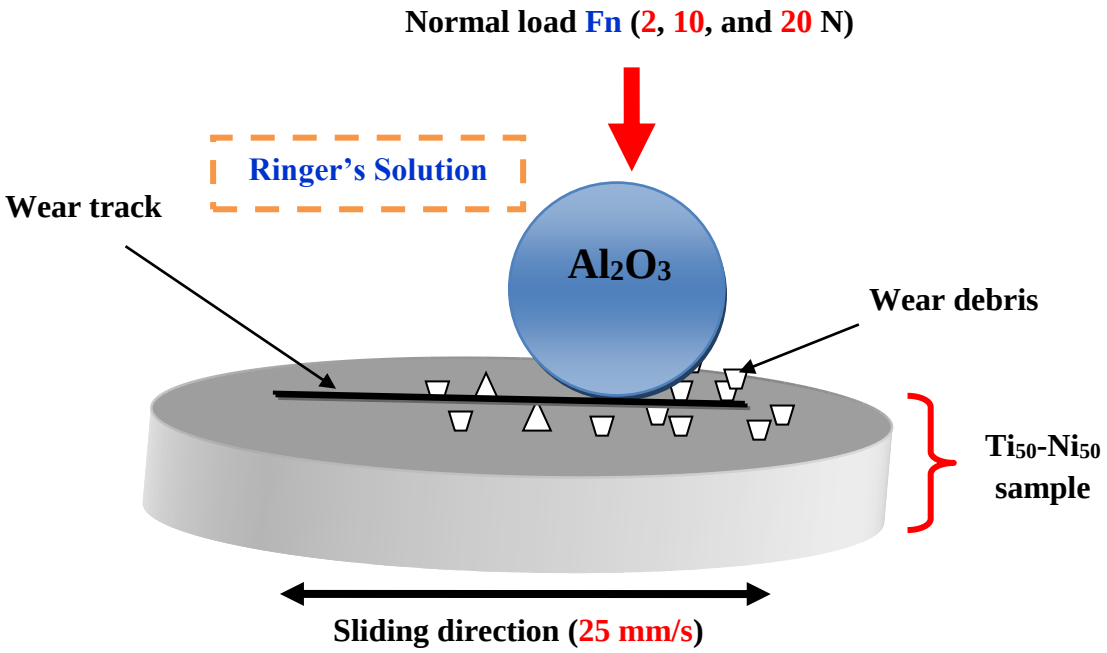

Figure II.13: Representative schematics of a ball-on-plate type oscillating tribometer.

Table II.3: The Ringer's solution's chemical composition [16].

Elements	KCl	NaCl	$C_8H_{18}N_2O_4S$	$CaCl_2$	Glucose
Chemical composition ($g.l^{-1}$)	0.19	6.43	2.38	0.27	1.80

II.2.4 ELECTROCHEMICAL CHARACTERIZATION TECHNIQUES

Electrochemical studies are essential for comprehending the behavior of materials' corrosion. Three key techniques commonly employed in this study are: Open Circuit Potential (OCP) measurement, Potentiodynamic Polarization (PD), and Electrochemical Impedance Spectroscopy (EIS).

The OCP measurements can indicate the formation of passive layers on metals, which are crucial for corrosion resistance.

By analyzing the polarization curves, researchers can calculate corrosion rates and identify critical parameters such as the corrosion potential and current density.

Electrochemical Impedance Spectroscopy (EIS) is a valuable technique used to assess the stability of passive layers formed on metal surfaces by analyzing changes in impedance parameters such as charge transfer resistance and capacitance.

a) Preparation of the work electrode

Ti_{50}-Ni_{50} materials were cut into cylindrical specimens that were 5 mm in diameter and 5 mm in thickness. They were then polished, cleaned in distilled water, coated, and left in a 1 cm^2 area for an electrochemical test. A conductor thread with an insulating coating connects the work electrode.

b) The electrolyte solution

Electrochemical tests are performed in physiological mediums simulated to the human body: Hank`s solution; their chemical composition is given in Table II.4.

Table II.4: Chemical composition of Hank's solution [17].

Elements	Hank (g/l)
NaCl	8.0
KCl	0.4
$CaCL_2$	0.14
$NaHCO_3$	0.35
$MgSO_4$ ahyder. $7H_2O$	0.1
$MgCl_2$ $6H_2O$	0.1
Na_2ClHPO_4. $2H_2O$	0.06
KH_2PO_4	0.06
Glucose	1.0

c) Mounting electrochemical

The electrochemical tests were carried out utilizing a Gamery 600-15005 potentiostat to link a cell to three electrodes, controlled by the Ec-Lab software and a microcomputer (see Fig.II.14 and 15).

- Work electrode: based on Ti_{50}-Ni_{50} alloy samples.
- Reference electrode: saturated calomel electrode (SCE).
- Auxiliary platinum electrode.

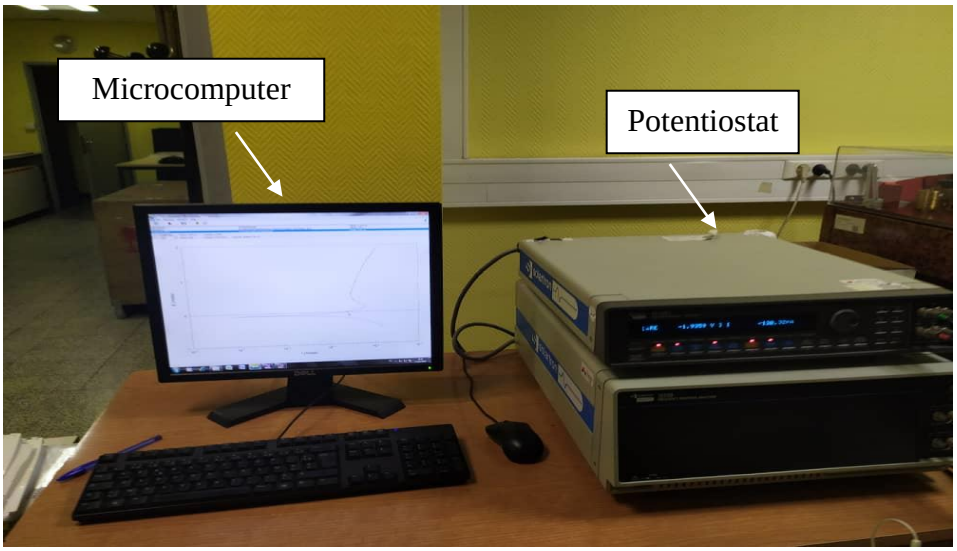

Figure II.14: The experimental device used for electrochemical measurements.

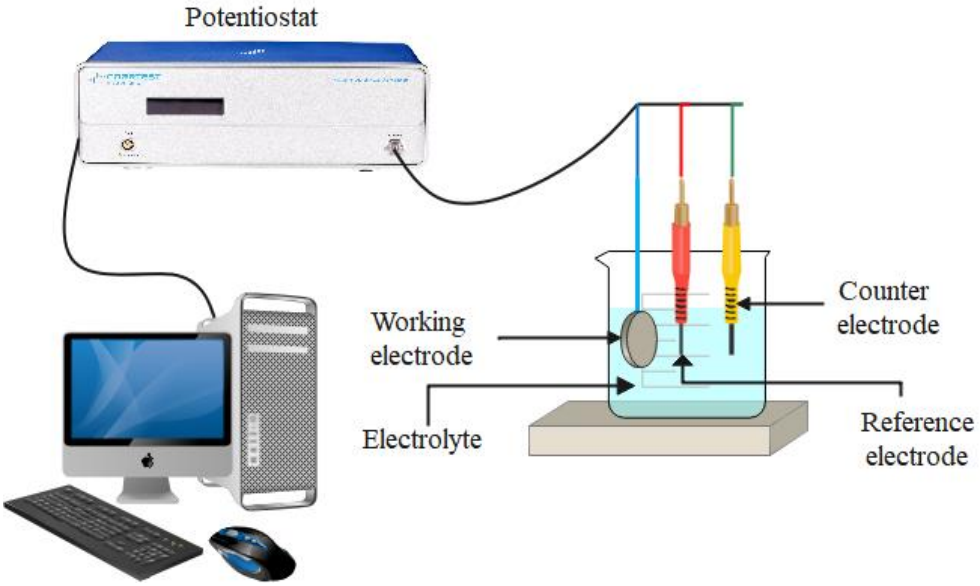

Figure II.15: Diagram of an electrochemical cell (three electrodes).

d) Test condition

The Open Circuit Potential (OCP) method was utilized to evaluate the abundance potential during a 2500-second immersion before the PD/EIS techniques were applied. The potentiodynamic polarization curves were created with a scanning range of -0.7 to 2 V (Versus SCE) and a sweeping speed of 1 mV/s. To analyze the corrosion behavior, the Tafel extrapolation method was used to compute the corrosion current density (i_{corr}), corrosion potential (E_{corr}), and corrosion rate (CR). With an amplitude of 10 mV, a frequency range of 10^{-2} to 10^{5} Hz, and a sampling rate of 10 points per decade, the EIS approach was utilized to evaluate the stability of the passive layer. Every electrochemical measurement was carried out at least three times for every sample in order to ensure the results' reliability and reproducibility.

II.3 CONCLUSIONS

In this chapter we have presented the process of elaboration of Ti_{50}-Ni_{50} alloys at different milling time from 2 h to 18 h; and the different techniques used for structural characterization, and for studying the structural, mechanical, tribological, and electrochemical properties, namely:

1. Structural and surface characterization techniques (SEM, EDS, XRD).
2. Physical and mechanical characterization techniques (Density, porosity, hardness, Young’s modulus, and roughness).

3. Tribological characterization (friction coefficient, wear rate, and volume wear).
4. Electrochemical techniques (Open circuit potential measurement, potentiodynamic polarization, and electrochemical impedance spectroscopy).

II.4 BIBLIOGRAPHIC REFERENCES

[1]A.A. bunaciu, E.G. Udriştioiu, and H.Y. Aboul-Enein., "*X-ray diffraction: instrumentation and applications*". Critical Reviews in Analytical Chemistry, 45 (2015), 289-299. http://dx.doi.org/10.1080/10408347.2014.949616.

[2]R. Das, M. Eaqub Ali, and S.B. Abd Hamid., "*Current applications of x-ray powder diffraction*". Reviews on Advanced Materials Science, 38 (2014), 95-109.

[3] M. Fellah, N. Hezil, M. Z. Touhami, A. Obrosov, S. Weiß, E. B. Kashkarove, A. M. Lidere, A. Montagne, and A. Iost., "*Enhanced structural and tribological performance of nanostructured Ti-15Nb alloy for biomedical applications*". Results in Physics, 15 (2019) 102767. https://doi.org/10.1016/j.rinp.2019.102767.

[4] M. Fellah, N. Hezil, M. Abdul Samad, R. Jellabi, A. Montagne, A. Mejias, S. Kossman, A. Iost, A. Purnama, A. Obrosov, and S. Weiss., "*Effect of Molybdenum Content on Structural, Mechanical, and Tribological Properties of Hot Isostatically Pressed b-Type Titanium Alloys for Orthopedic Applications*". Journal of Materials Engineering and Performance, 28 (2019), 5988-5999. https://doi.org/10.1007/s11665-019-04348-w.

[5] V. Mote, Y. Purushotham, and B. Dole., "*Williamson-Hall analysis in estimation of lattice strain in nanometer-sized ZnO particles*". Journal of Theoretical and Applied Physics, 6 (2012), 1-8.

[6] S. Devesa, M.P.F. Graça, and L.C. Costa., "*Williamson-hall analysis in estimation of crystallite size and lattice strain in Bi1.34Fe0.66Nb1.34O6.35 prepared by the sol-gel method*". Materials Science and Engineering B, 263 (2021). http://dx.doi.org/10.1016/j.mseb.2020.114830.

[7] X.H. Yan, J. Ma, and Y. Zhang, "*High-throughput screening for biomedical applications in a Ti-Zr-Nb alloy system through masking co-sputtering*". Science China Physics, Mechanics and Astronomy, 62 (2009), 1-9.

[8] M. Fellah., "*Etude électrochimique et tribologique de deux prothèses totales de hanche en acier AISI 316L et en alliage Ti-Al-Nb*". PhD Thesis, University of Badji Mokhtar Annaba, (2014).

[9] D. Mereib., "*Fabrication et caractérisation des matériaux composites lamellaires à matrice Ti et TA6V*". PhD Thesis, Libanaise University, (2018).

[10] K.C. Wai Jin, M.M. Anak Mathew Minggat, and R. Singh., "*Sintered properties of stainless steel-doped YTZP ceramics*". MATEC Web of Conferences, 152 (2018), 1-13. http://dx.doi.org/10.1051/matecconf/201815202012.

[11] F. Hammadi, M. Fellah, N. Hezil, L. Aissani, G. Mimanne, S. Mechachti, A.S. Mohammed, A. Montagne, A. Iost, S. Weiß, and A. Obrosov., "*The effect of milling time on the microstructure and mechanical properties of Ti-6Al-4Fe alloys*". Materials Today Communications, 27 (2021), 1-11. http://dx.doi.org/10.1016/j.mtcomm.2021.102428.

[12] J. Xu, and R.C. Buchanan., "*Surface roughness: a review of its measurement at micro -/nano-scale*". Physical Sciences Reviews, 3 (2018). http://dx.doi.org/10.1515/psr-2017-0057.

[13] A. Rudawska., "*Surface treatment methods*". Surface Treatment in Bonding Technology, (2019), 47-62. https://doi.org/10.1016/B978-0-12-817010-6.00003-5.

[14] ISO 4287, Geometrical Product Specifications (GPS)-surface Texture: Profile Method-terms, Definitions and Surface Texture Parameters, International Organisation for Standardisation, Geneva, (1997).

[15] M. Fellah, N. Hezil, M.A. Samad, M. Z. Touhami, A. Montagne, A. Iost, A. Mejias, and S. Kossman., "*The effect of milling time on structural, friction and wear behavior of hot isostatically pressed Ti–Ni alloys for orthopedic applications*". The Minerals, Metals and Materials Society. (2019), 865-875. http://dx.doi.org/10.1007/978-3-030-05861-6_85.

[16] M. Stack, J. Rodling, M.T. Mathew, H. Jawan, W. Huang, G. Park, and C. Hodge., "*Micro-abrasion–corrosion of a Co–Cr/UHMWPE couple in Ringer's solution: An approach to construction of mechanism and synergism maps for application to bio-implants*". Wear. 269 (2010), 376-382. http://dx.doi.org/10.1016/j.wear.2010.04.022.

[17] D. Bahena, I. Rosales, O. Sarmiento, R. Guardian, C. Menchaca, and J. Uruchurtu., "*Electrochemical noise chaotic analysis of NiCoAg alloy in Hank solution*". International Journal of Corrosion, (2011), 1-11. http://dx.doi.org/10.1155/2011/491564.

CHAPTER III

STRUCTURAL

&

MECHANICAL CHARACTERIZATION

III. INTRODUCTION

In this chapter, we present the various experimental results and their interpretations obtained by the various techniques used during this thesis to study the effect of milling time on the structural and mechanical properties of nanostructured Ti_{50}-Ni_{50} alloys produced by using planetary high energy ball mill.

Several techniques were used to evaluate the structural and mechanical properties of the alloys, including scanning electron microscopy (SEM) analysis in conjunction with energy dispersive spectroscopy (EDS), which is used to determine the chemical composition of the powders while they are being ground, X-ray diffraction (XRD), nanoindentation test, and profilometer analysis.

III.1 STRUCTURAL CHARACTERIZATION

III.1.1 Morphology and microstructure of milled powders

The SEM images of the powders that were produced after milling show the effects of the ball milling technique, including the introduction of lattice defects and changes in particle size and shape (Fig. III.1). It is commonly known that the milling technique affects the shape and size of powders due to the repeated two processes of cold welding and fracturing. Additionally, particle sizes are larger when cold welding is the predominant mechanism and smaller when fracture is the primary process [1]. Figure III.1 (a-d) presents the SEM micrographs of the milled Ti_{50}-Ni_{50} powders captured after different grinding times (2, 6, 12, and 18 h). It is evident that after 2 hours of milling, there have been significant morphological changes.

At the beginning of the milling process (2 h) as observed in Figure III.1(a), certain particles have been flattened and crushed as a result of the powders colliding with the milling media (the balls and vials) during ball milling. Additionally, the particles have irregular shapes, and their sizes are relatively broad, due to the cold welding of the starting powders [2].

After 6 h of the ball-milling process, the particles (Fig. III.1.b) continued to increase with the existence of some smaller ones. Additionally, the particles at this stage have irregular shapes and a dispersed distribution.

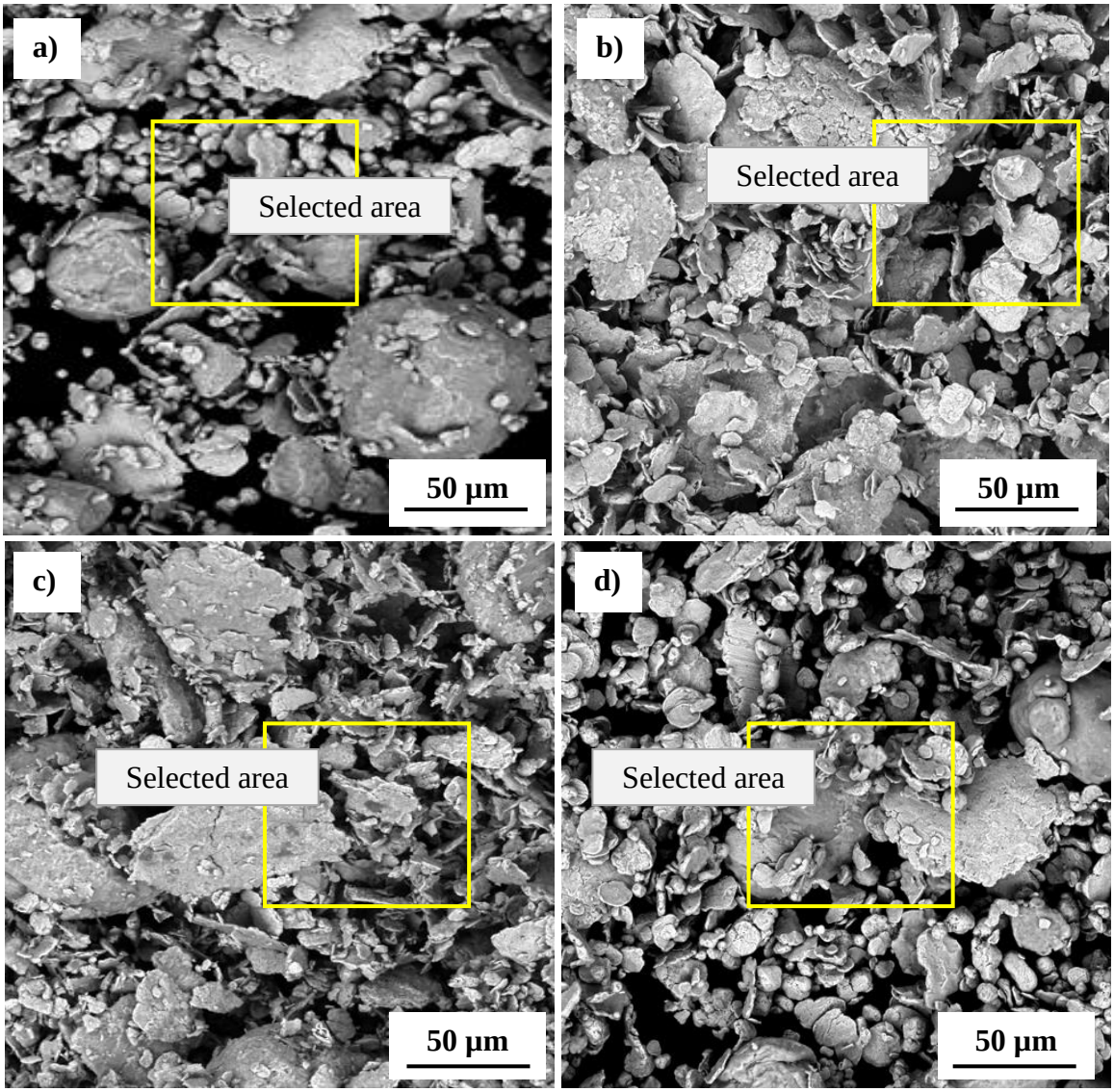

Figure III.1: SEM micrographs with selected area for EDS analysis for milled Ti-Ni powders fabricated with a ratio of 50%/50% at varying milling times: a) 2 h, b) 6 h, c) 12 h, and d) 18 h.

Nevertheless, as shown in Figure III.1(c) and (d), the particle size decreased (increasing in tiny particles) when the grinding times were extended (i.e., 12 and 18 hours) proving the effectiveness of the fracture mechanisms over the earlier cold-welding [3]. After that, at longer milling periods, a balance between cold welding and fracture is reached, bringing the particles closer to their stable condition [4, 5]. *Sakher et al.*, [6] reported similar morphological observations for Ti_{50}-Ni_{50} produced at different milling times.

In summary, the final shape and properties of the Ti-Ni alloy powders are significantly influenced by the milling period.

III.1.2 EDS analysis

According to the results of the EDS analysis (Table III.1), the tested material contained precursors of Ti and Ni, and their amounts matched the sample's nominal chemical composition. The amount of oxygen (O) in the milled powders is present through the ambient air during grinding since ball grinding is the initial phase of contamination [7]. Additionally, the presence of Silicon (Si) and carbon (C) element residues confirmed that the powders were contaminated by the grinding media, which included balls and vials.

Powder contamination from the grinding media (vial and balls) may be harmful to living organisms. For instance, metal ions introduced from grinding media may cause unfavorable cellular reactions when the final product is used in biomedical applications. However, our investigation showed that the amount of contamination from the grinding media was so low that it could be ignored. As noted by *Reid et al.*, [8] in their study, a low degree of contamination by zirconia milling media did not result in a loss of biocompatibility

Table III.1: The EDS analysis of powders milled with corresponding milling times.

Milling time (h)	**Atomic percentage (at. %)**				
	Ti	Ni	Si	C	O
2	47.45	47.40	1.92	0.63	2.6
6	48.50	47.45	1.70	1.20	1.15
12	51.40	44.07	2.11	1.41	1.01
18	51.66	45.39	1.25	/	1.70

III.1.3 X ray diffraction (XRD)

The average size of crystallites, lattice parameters, average rate of microstrain/lattice strain, and various phases can all be determined using the XRD spectrum. Figure III.2 (a) shows the XRD diffraction patterns of the Ti_{50}-Ni_{50} milled powders. From the figure, the peaks corresponding to Ti and Ni are detected at the early stages of grinding (2 h and 6 h).

The hexagonal closed pack (hcp) Ti is indicated by the peaks of the (100), (002), (101) and (110) planes at 2Θ = 35.21°, 38.5°, 40.18° and 61.68° (*ICDD PDF 4, card no 00-044-1294* [9]), respectively. Whereas, the face-centered cubic (fcc) Ni represented by the peaks of the (111) and (200) planes are situated at 2Θ = 44.71° and 53.03° (*ICDD PDF 4, card no 00-004-0850* [9]), respectively. The Ni and Ti diffraction peaks' intensity decreased and gradually weakened and broadened as the milling times rose. The broadening and weakening of the diffraction peaks are linked to a rise in microstrain and a reduction in crystallite size, demonstrating the effect of the milling process on the microstructure of the material, as mentioned by *Guittoum et al* [10]. Additionally, the peaks moved toward lower diffraction angles (Fig. III.2.b), indicating that the Ni lattice parameters increased and Ti atoms permeated the Ni matrix [11]. For 12 h of grinding, the body-centered cubic-structured Ti-Ni phase (B2) starts to appear, and its apparent increases during the grinding operation.

All of the peaks associated with Ti and Ni disappeared during the 18-hour grinding operation, leaving just the noticeable peaks of the Ti-Ni phase (B2). The planes (002) and (101) with angles of 38.5° and 40.18°, respectively, represent the two primary peaks of this phase (*ICDD PDF 4, card no 03-065-0917* [9]). Significant plastic deformation during milling produced this phase, facilitating atomic rearrangement and the creation of the ordered B2 structure [6]. Furthermore, the Ti-Ni peaks expanded due to the refining effect of crystallite size [12]. Similar performance was observed in previous work by *Sharma* [11] and *Neeraj et al* [13].

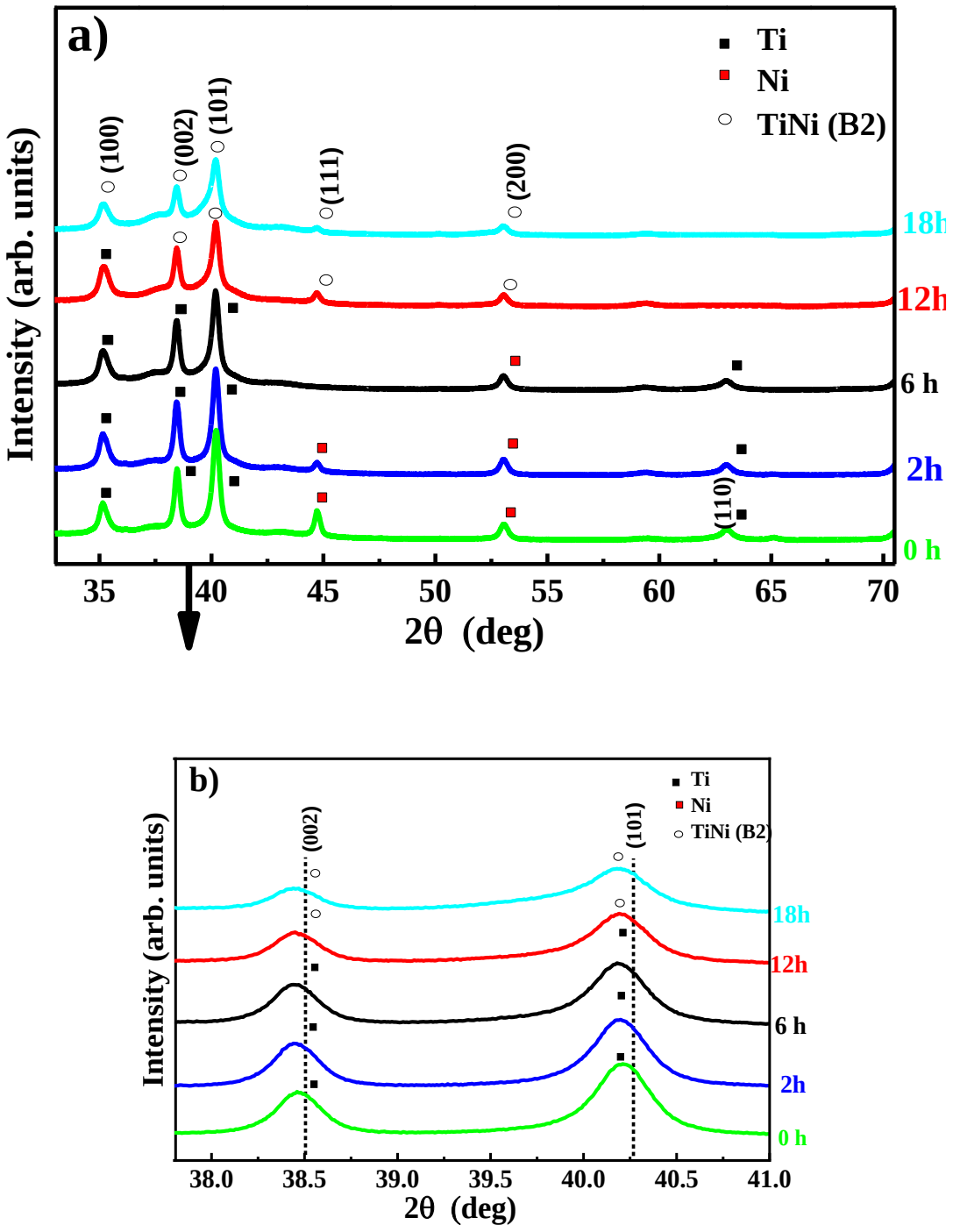

Figure III.2: a) XRD spectra of Ti_{50}-Ni_{50} particles following different periods of grinding, b) display the shift toward low angles.

III.1.4 Evolution of crystallite size {D}, microstrain {ε}, and lattice parameters {a}

Figure III.3 illustrates Williamson-Hall (W-H) plots of Ti_{50}-Ni_{50} powders at different grinding times, where the fitted data are displayed as solid lines, while the experimental data appear as symbols. Microstrain {ε} is determined by the slope of the linear fitted line. Furthermore, the intersection $\frac{K\lambda}{D}$ can be utilized to estimate the crystallite size {D}. From the figures, The Ti_{50}-Ni_{50} samples clearly show a positive slope, indicating that they are exhibiting tensile strain [14, 15].

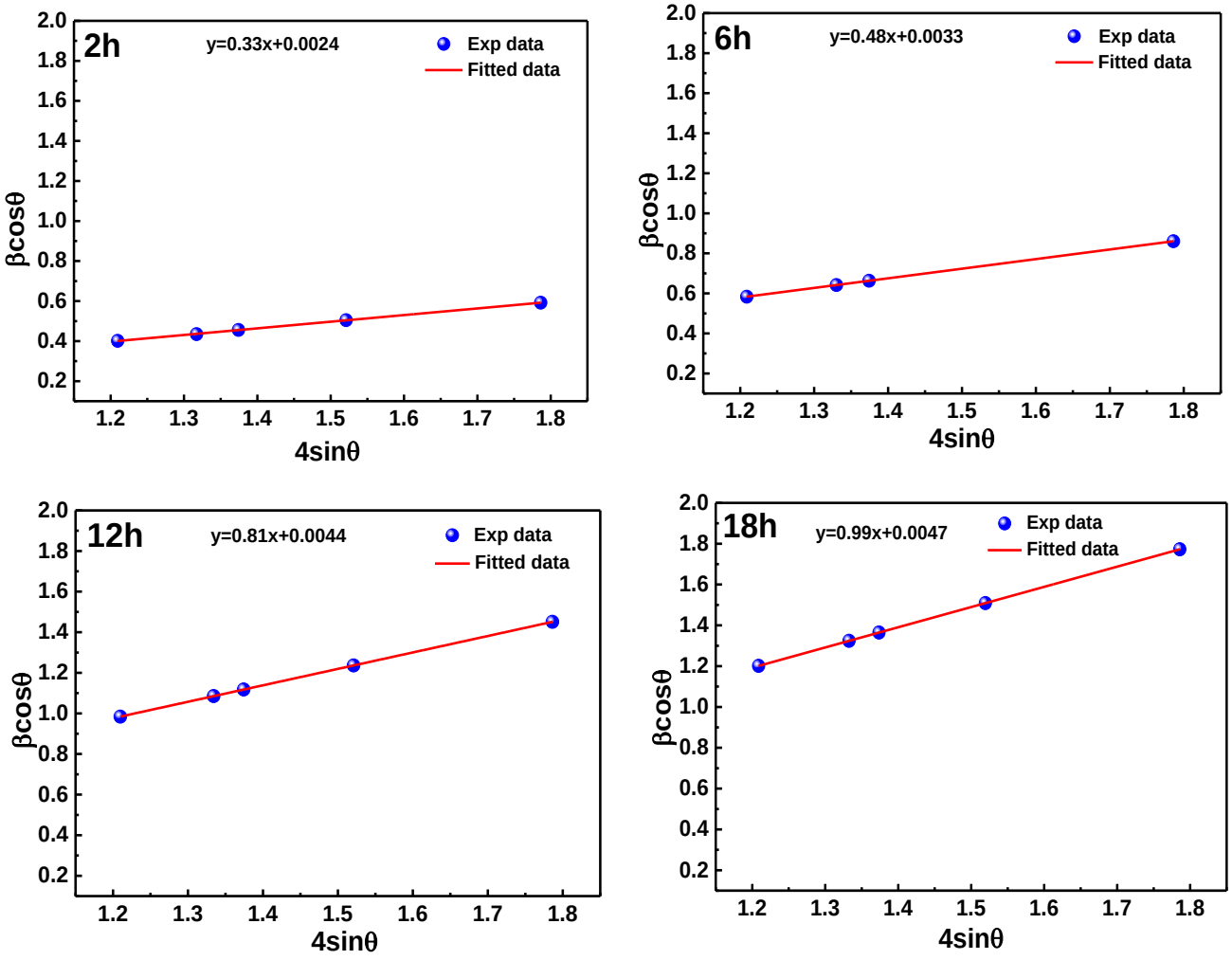

Figure III.3: Williamson-Hall plots of Ti_{50}-Ni_{50} alloy after different milling times.

Our research especially concentrated on determining the microstrain and crystallite size of powders that had been ground. We may assess how mechanical milling affects these properties using this method prior to submitting them to other processing steps (HIP and sintering). Ti_{50}-Ni_{50} samples' microstrain (ε) and crystallite size (D) are significantly impacted by the grinding time. The average microstrain and crystallite size of milled powders are shown to change with milling time in Figure III.4 (a). The graph indicates proportionality between microstrain and milling durations, but an inverse relationship with crystallite size.

It is evident that as the grinding duration rose from 2 to 18 hours, the crystallite size decreased first quickly and then gradually from 57 nm to 29 nm. This is mostly due to the significant deformation of the powders throughout the milling process. Another cause could be greater defect densities, which raise the potential for sites of nucleation during crystallization [16].

The microstrain values rose in tandem with this decrease in crystallite size, eventually reaching 0.99 % at the end of milling. This can be explained by the introduction of several kinds of lattice defects, such as dislocations and impurities, and the hardening of the alloy caused by mechanical milling [17].

The lattice parameter of milled Ti_{50}-Ni_{50} alloys is also significantly influenced by the milling time (see Fig. III.4.b); the figure shows that as milling times increased, the lattice parameter (a) increased as well, reaching a value of 3.22 Å. Extreme plastic deformations and the buildup of several structural problems, including as stacking faults, grain boundaries, and a rising dislocation density throughout the milling process, are to blame for this [18, 19]. Similar results were reported by *Huang et al.* [20]; the lattice parameters rose as the ball-milling process lasted longer.

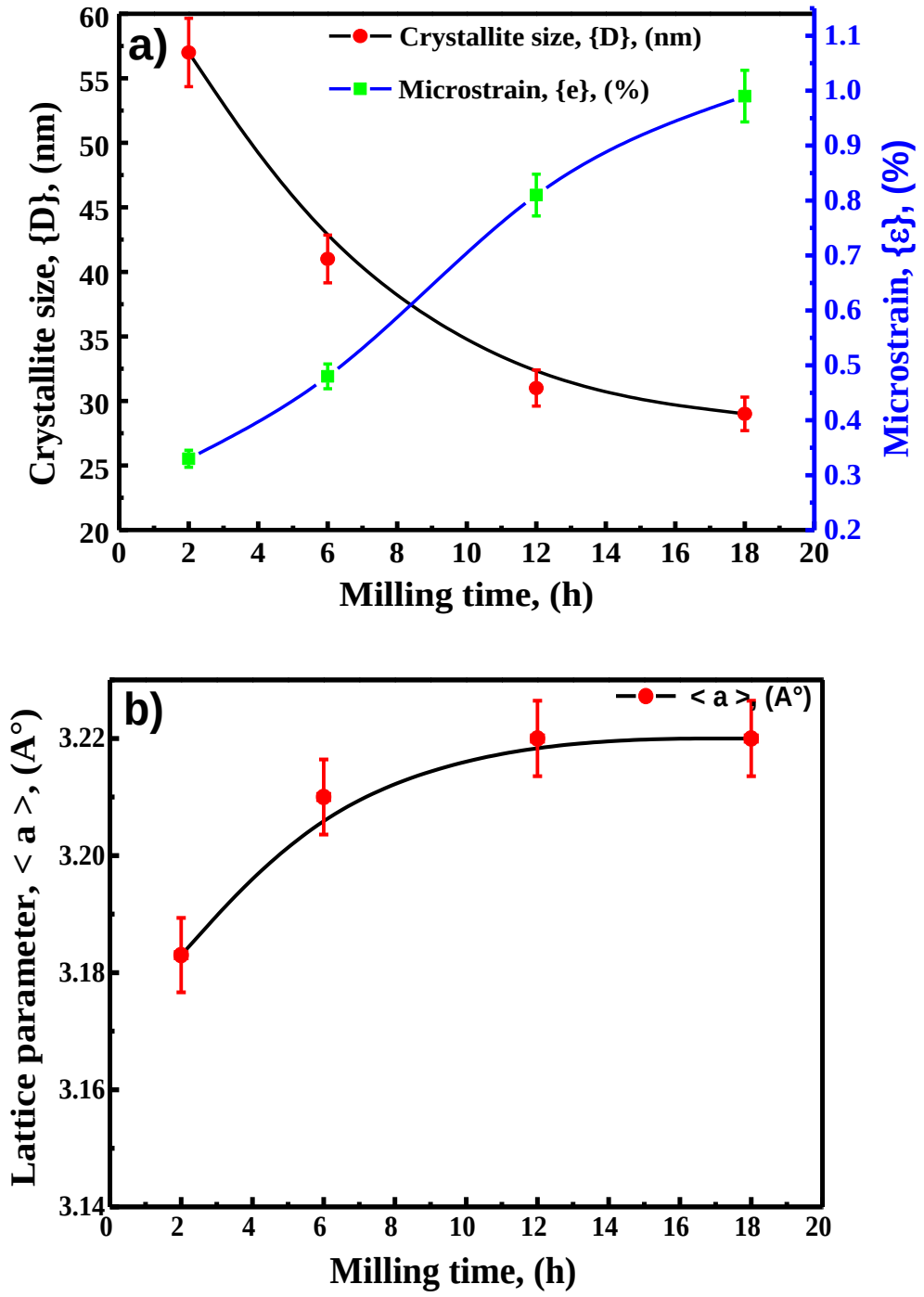

Figure III.4: Evolution of: a) crystallite sizes {D} and microstrain {ε}; b) lattice parameters {a} of Ti_{50}-Ni_{50}.

III.2 PHYSICAL AND MECHANICAL CHARACTERIZATIONS

III.2.1 Pore size distribution

The pore size of biomaterials is crucial for bone formation, according to both in vitro and in vivo research [21]. The Ti_{50}-Ni_{50} alloys' pore size distribution (PSD) changes after 2, 6, 12, and 18 hours of ball milling are shown in Figure III.5. It is evident that as the grinding time rose, the pore size decreased.

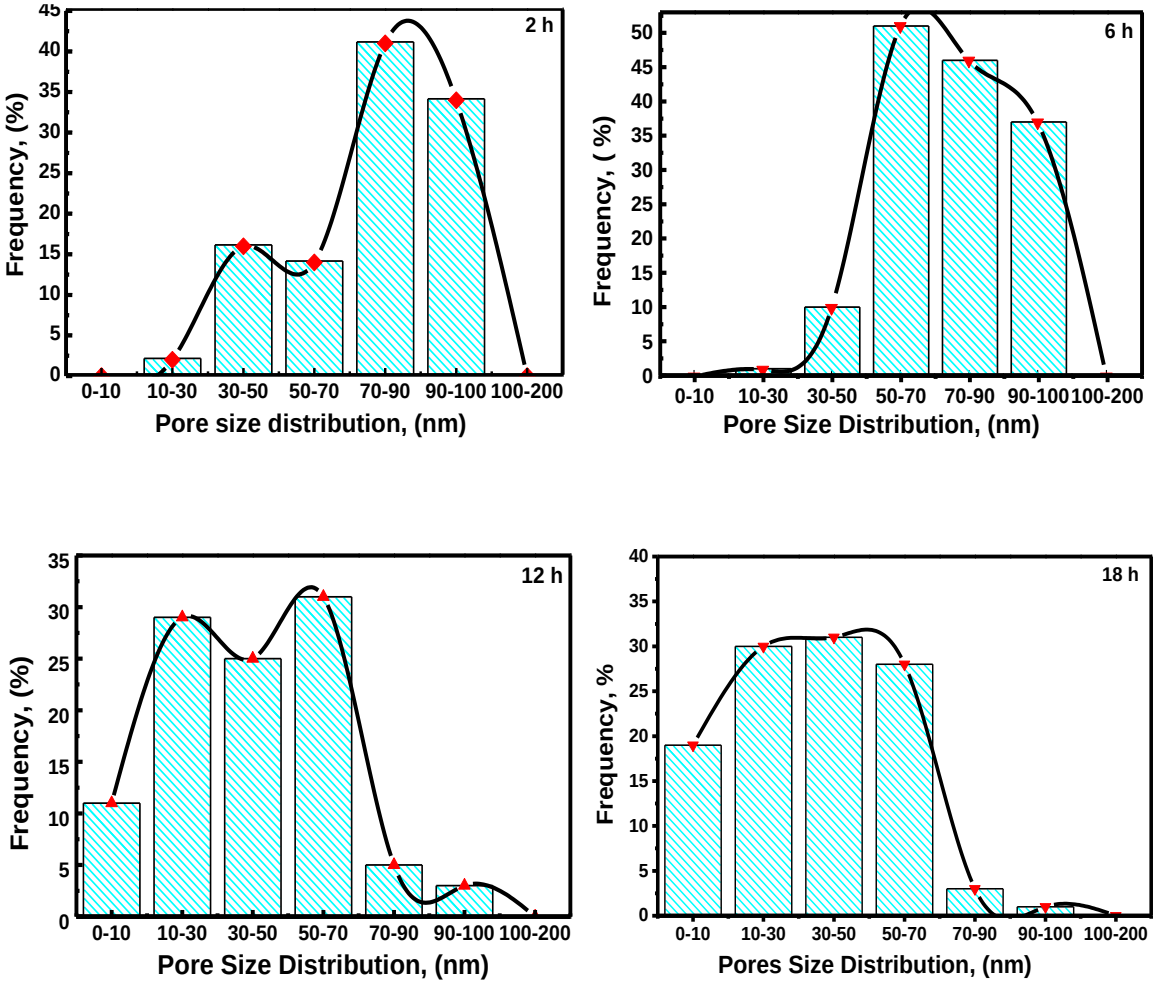

Figure III.5: Pore size distribution frequency of Ti_{50}-Ni_{50} alloys after different grinding durations.

The range of pore sizes as a function of milling duration is between 10 to 100 nm. The vast majority of pores were sized between 70 and 100 nm in the first phases of milling (2 h and 6 h). At the highest grinding times (12 h and 18 h), the specimen's pores were smaller, regular, and

decreased to 10 nm compared to the initial stages. A more extended milling period leads to the reduction of the powders' pore size. The same results were documented by *Kim et al*., [22] in their study about Ti-Nb-Zr biomaterials, which showed that the grinding time affects the size of the pore particles.

III.2.2 Relative porosity, relative density, and mean pore size measurements

The evolution of the mean pore size of the Ti_{50}-Ni_{50} alloys at various milling times is shown in Figure III.6 (a). It is clear that the mean pore size decreased as the grinding time was increased from 2 to 18 hours. At the end of milling, the final pore size was 42 nm due to grain size refinement generated by milling.

In Figure III.6 (b), the relative density and relative porosity evolution of HIPed and sintered Ti_{50}-Ni_{50} specimens produced under different grinding times are shown. The relationship between density and milling time is proportional. Density increases along with grinding time, however it inversely correlates with porosity.

The samples had the largest porosity (19 %) and the lowest density (81 %), following 2 hours of grinding. The relative porosity decreased till it was at least 11 % when the grinding period was extended to 18 hours. In contrast, the relative density reached the maximum of 89 % at the end of the milling. Reduced particle size and increased specific surface area from longer milling times accelerate the sintering shrinkage speed, which lowers the samples' porosity and raises their density [23].

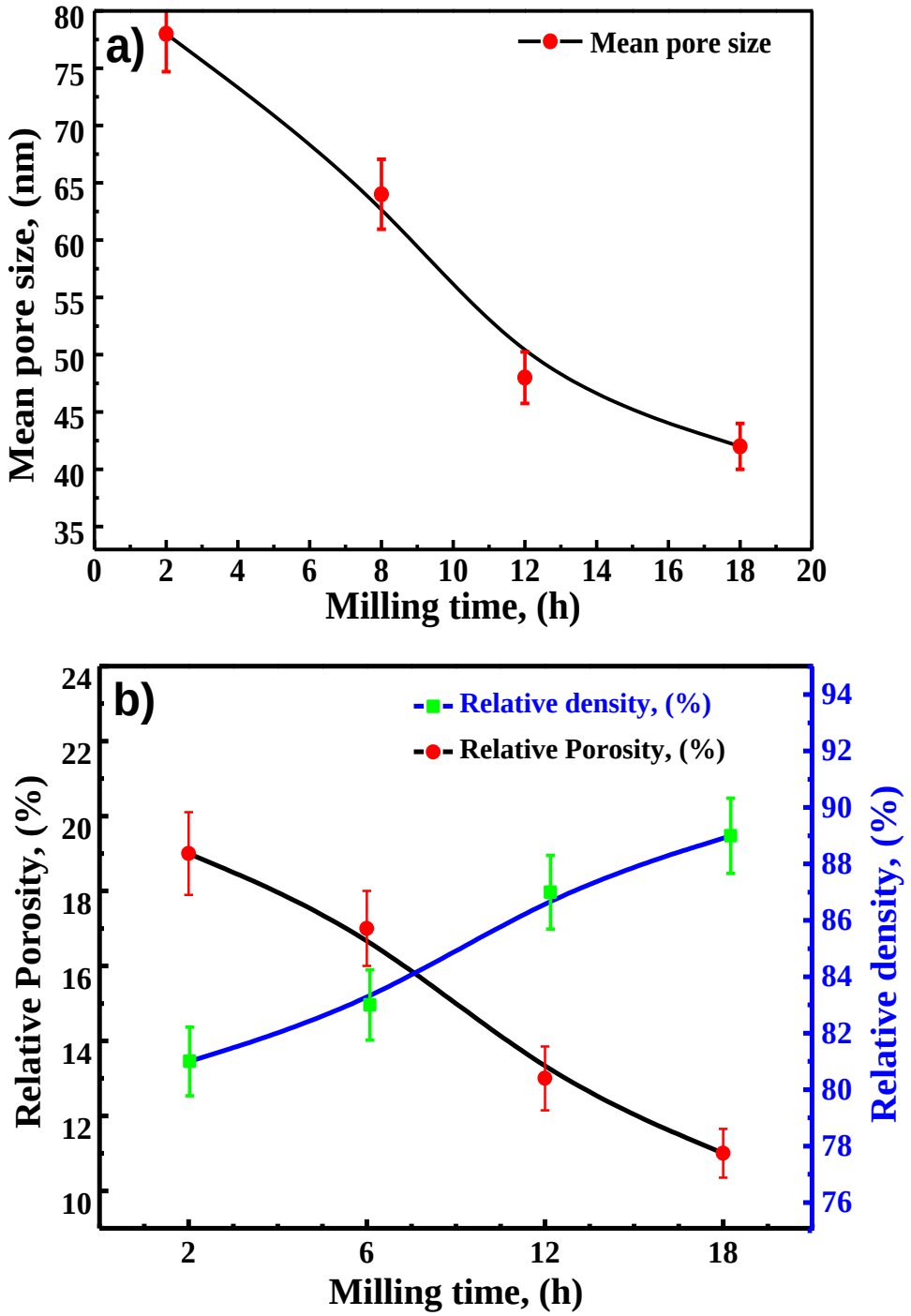

Figure III.6: Evolution of: a) mean pore size (nm); b) relative porosity and density (%) of Ti_{50}-Ni_{50} as a function of milling time.

III.2.3 Hardness and young's modulus characterization

One of the most important considerations in the field of orthopedic implant materials is Young's modulus, sometimes referred to as elastic modulus. The mechanical properties of materials, such as their hardness and Young's modulus, are greatly influenced by their microstructures. Grain refining has been found to be an effective way of improving the mechanical performance of materials. The elastic modulus of titanium alloy usually exceeds 80 GPa, whereas human bone can only reach 30 GPa [24]. Stress shielding offered by a high-modulus implant can result in bone deterioration and harm to the implant/bone interface [25]. For hard-tissue replacement, a small Young's modulus implant material is hence a preferred choice.

The effect of grinding time on the Ti_{50}-Ni_{50} samples' hardness and Young's modulus is shown in Figure III.7. According to the data, after 2 hours of grinding, the hardness value was 201 HV; nevertheless, it rose over the course of the milling period, reaching 341 HV after 18 hours. In this way, the accumulation of strain energy causes the hardness value increase as the milling time increases [26]. The results are in good agreement with a previous work on Ti-Cu-Ni ternary alloys by *Ghadiri and Saidi* [27] and a study on Ti-16Sn-4Nb by *Nouri et al.* [28], which found that hardness increases with grinding time.

Figure III.7 displays the binary Ti_{50}-Ni_{50} specimens' Young's modulus values under various grinding times. As can be seen, the modulus of the samples increased with increasing milling periods (2, 6, 12, and 18 hours), reaching values of 89 GPa, 94 GPa, 101 GPa, and 103 GPa, respectively.

By comparing the obtained results of elastic modulus of the Ti_{50}-Ni_{50} alloys with other Ti-based alloys, it can be seen that Ti_{50}-Ni_{50} alloys have smaller Young's modulus values than that of $Ti_{80}Ni_{20}$ (varied from 130.73 to 164.53 GPa) [29], Ti-6Al-4Fe (110 GPa) [30], Ti-6Al-4V (112 GPa) [31], and Ti-Al-7Nb (105 GPa) [1]. As mentioned before, in order to avoid stress shielding and implant failure or loosening, Young's modulus must be extremely near to the human bone.

According to the results obtained, the enhanced hardness and elastic modulus were attributed to the high relative density and refined grain size.

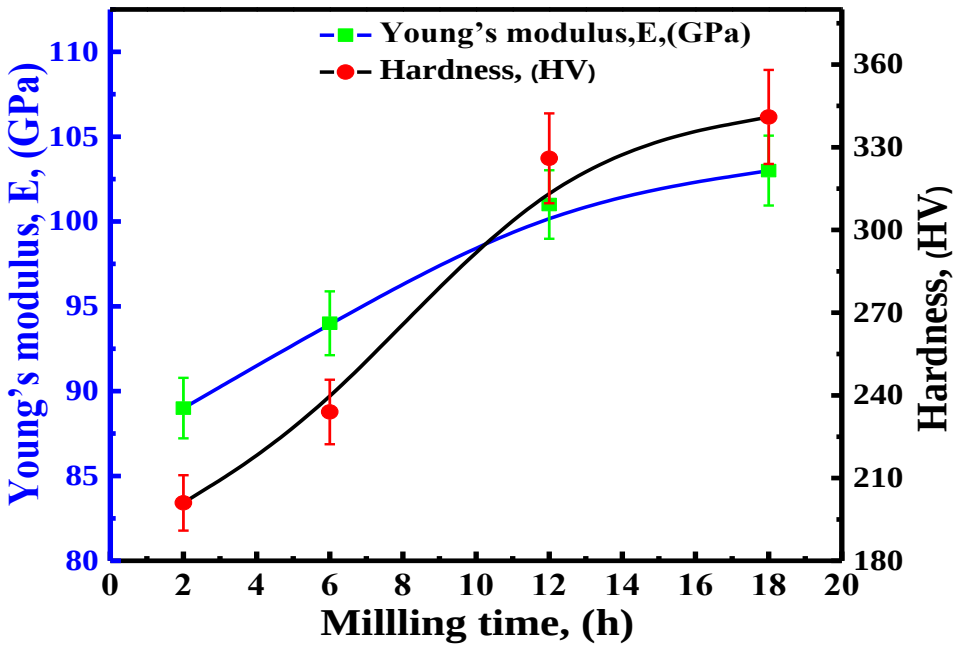

Figure III.7: Evolution of Young's modulus and Hardness of Ti_{50}-Ni_{50} alloys as a function of grinding time.

The ratio of hardness (H) to Young's modulus (E) can be used to characterize a material's capacity to resist elastic strain before failing in elastic-plastic behavior. Materials with greater H^3/E^2 and H/E typically show lower wear rates [32].

Figure III.8 displays the change in the H^3/E^2 and H/E ratios of the Ti_{50}-Ni_{50} alloys as a function of grinding time. As the milling duration rises, it has been observed that the H^3/E^2 and H/E ratios rise. The H/E values rise from 0.0221 to 0.0324 with increased grinding durations from 2 h to 18 h, respectively. Further, the H^3/E^2 values increased, going from 0.0009 GPa to 0.0035 GPa during 2 to 18 hours of milling, respectively.

The H^3/E^2 values of Ti_{50}-Ni_{50} alloys are higher at 12 and 18 hours than those of CP-Ti biomaterials (0.0014 GPa). Similarly, the Ti_{50}-Ni_{50} alloys' H/E values are higher than the CP-Ti alloy's (0.0238) after 6, 12, and 18 hours of grinding [33].

According to *Hezil et al.*, [1] the greatest values of H^3/E^2 and H/E (0.0035 GPa and 0.0324), respectively, suggest that the alloys on display have better wear resistance. Refinement of the grain size increases the mechanical qualities and yields the optimum wear resistance. Additionally, a lower friction coefficient and better tribological performance are the results of

decreased surface porosity [1].

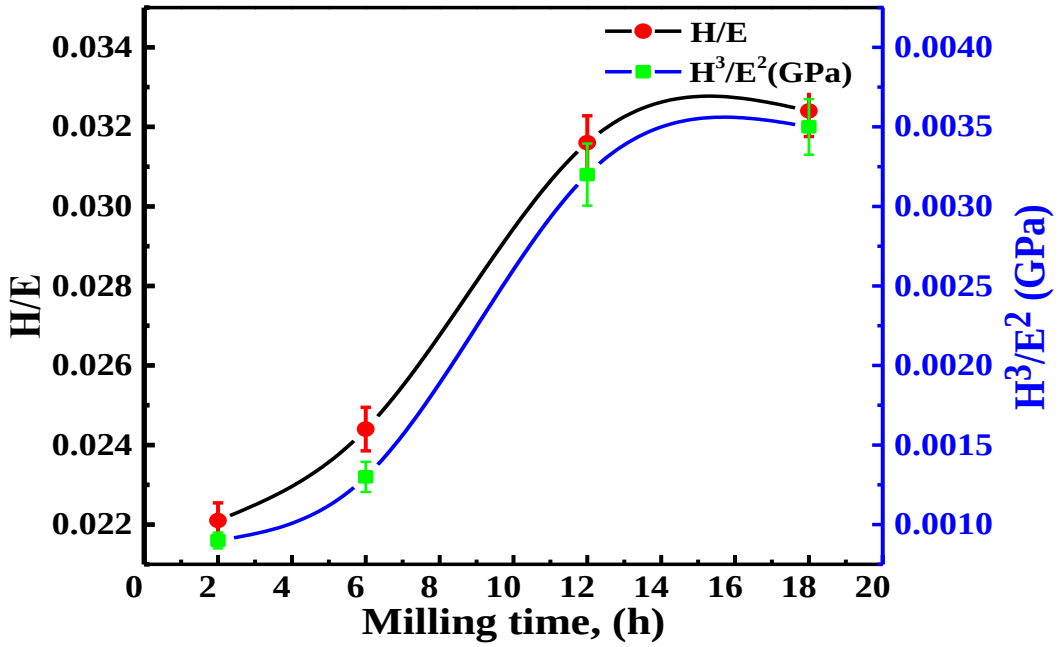

Figure III.8: Evolution of the H^3/E^2 and H/E ratios of Ti_{50}-Ni_{50} alloys as a function of grinding time.

III.2.4 Surface roughness analysis

Surface roughness (Ra) values of the Ti_{50}-Ni_{50} alloys as a function of grinding times are shown in Figure III.9. The results indicated that the roughness of the alloy sample surfaces reduced with increasing milling time, which could be connected to the higher hardness of the particles. The surface roughness was 8.4 nm after a brief 2-hour grinding time, which was higher than the final value of 7 nm during an 18-hour grinding period. The literature indicates that the nature and roughness of an implant's surface significantly affect how the surrounding tissues react to it. Because textured implant surfaces have a larger surface area than smooth surfaces, there is a higher chance of osseointegration. the development of healthy tissues [34].

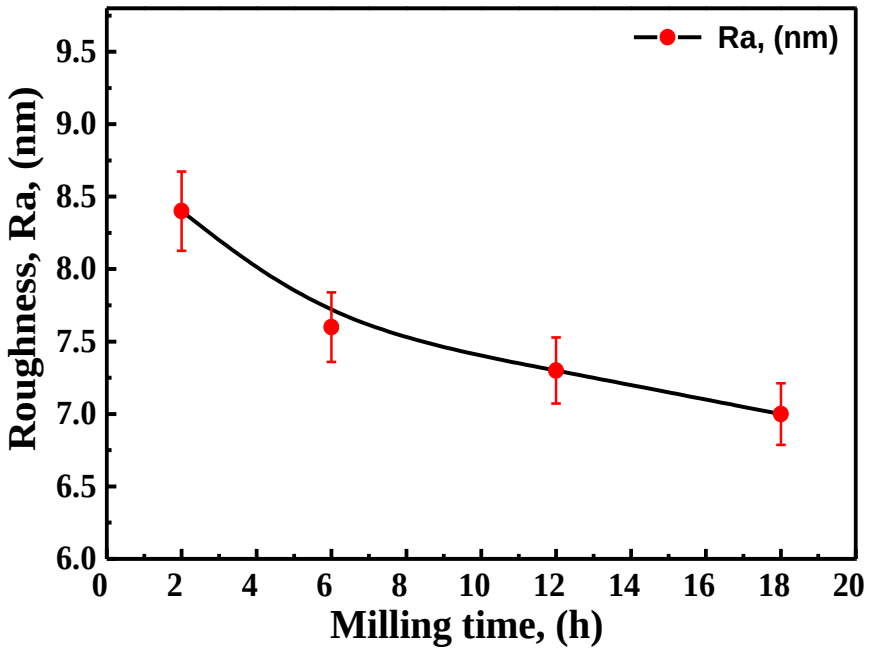

Figure III.9: Roughness (Ra) evolution of Ti_{50}-Ni_{50} alloys at different grinding time.

II.3 CONCLUSIONS

The mechanical and structural characteristics of nanostructured Ti_{50}-Ni_{50} alloys made by mechanical alloying at various grinding periods (2, 6, 12, and 18 hours), followed by pressing and sintering, were examined in this work. The following conclusions can be derived from the findings:

❖ ***Morphological and structural characterization of milled powders:***

- The powders' particle size and form are greatly influenced by the milling times.
- As the milling duration increased, the microstrain and lattice parameter increased, while the crystallite size of the powders was reduced.

❖ **Physical and mechanical Characterization of the HIPed and sintered samples:**

- The relative porosity of HIPed and sintered Ti_{50}-Ni_{50} alloys is significantly decreased with longer milling periods, which raises the alloys' density. Its wear rate and mechanical characteristics (hardness and Young's modulus) improved as a result of increased density

and decreased porosity.

- The HIPed and sintered Ti_{50}-Ni_{50} alloys' hardness and Young's modulus increased as the milling time increased, reaching 341 HV and 102 GPa, respectively, after 18 hours.
- One important biomaterials feature that influences how well they function and interact with cells and tissues is surface roughness, which decreased with milling time.

III.4 BIBLIOGRAPHIC REFERENCES

[1] N. Hezil, L. Aissani, M. Fellah, M. A. Samad, A. Obrosov, C. Timofei, and E. Marchenko., "*Structural, and tribological properties of nanostructured α + β type titanium alloys for* total hip". Journal of Materials Research and Technology, 19 (2022), 3568-3578. https://doi.org/10.1016/j.jmrt.2022.06.042.

[2] Z. Gao, H. Luo, Q. Li, and Y. Wan., "*Preparation and characterization of Ti-10Mo alloy by mechanical alloying*". Metallography, Microstructure, and Analysis, 1 (2012), 282-289. https://doi.org/10.1007/s13632-012-0045-5.

[3] I.R. Bertoli, L.M. Ferreira, B.X. de Freitas, C.A. Nunes, A.S. Ramos, M. Filgueira, C. dos Santos, and E.C.T. Ramos, "*Mechanical alloying and hot pressing of Ti-Zr-Si-B powder mixtures*". Metals, 8 (2018), 1-13. https://doi.org/10.3390/met8020082.

[4] R. Amini, F. Alijani, M. Ghaffari, M. Alizadeh, and A. K. Okyay., "*Formation of B19', B2, and amorphous phases during mechano-synthesis of nanocrystalline NiTi intermetallics*". Powder Technology, 253 (2014), 797-802. http://dx.doi.org/10.1016/j.powtec.2013.12.029.

[5] N. Yazdani, M.R. Toroghinejad, A. Shabani, and P. Cavaliere, "*Effects of Process Control Agent Amount, Milling Time, and Annealing Heat Treatment on the Microstructure of AlCrCuFeNi High-Entropy Alloy Synthesized through Mechanical Alloying*". Metals, 11 (2021), 1491. https://doi.org/10.3390/met11091493.

[6] E. Sakher, N. Loudjani, M. Benchiheub, S. Belkahla, and M. Bououdina, "*Microstructure Characterization of Nanocrystalline Ni50Ti50 Alloy Prepared Via Mechanical Alloying Method Using the Rietveld Refinement Method Applied to the X-Ray Diffraction*". Nanosistemi, Nanomateriali, Nanotehnologii, 15 (2017), 401-416. https://doi.org/10.15407/nnn.15.03.0401.

[7] M. Fellah, N. Hezil, M. Z. Touhami, M. AbdulSamad, A. Obrosov, D.O. Bokov, E. Marchenko, A. Montagne, I. Alain, and A. Alhussein, "*Structural, tribological and antibacterial properties of (α + β) based Ti-alloys for biomedical applications*". Journal of Materials Research and Technology, 9 (2020), 14061-14074. https://doi.org/10.1016/j.jmrt.2020.09.118.

[8] C.B. Reid, J.S. Forrester, H.J. Goodshaw, E.H. Kisi, and G.J. Suaning, "*A study in the mechanical milling of alumina powder*". Ceramics International, 34 (2008), 1551-1556. https://doi.org/10.1016/j.ceramint.2007.05.003.

[9] T. Goryczka, and P. Salwa, "*Influence of Batch Mass on Formation of NiTi Shape Memory Alloy Produced by High-Energy Ball Milling*". Metals. 11 (2021), 1-12. https://doi.org/10.3390/met11121908.

[10] A. Guittoum, A. Layadi, A. Bourzami, H. Tafat, N. Souami, S. Boutarfaia, and D. Lacour, "*X-ray diffraction, microstructure, Mössbauer and magnetization studies of nanostructured*

Fe50Ni50 alloy prepared by mechanical alloying". Journal of Magnetism and Magnetic Materials, 320 (2008), 1385-1392. https://doi.org/10.1016/j.jmmm.2007.11.021.

[11] P. Sharma, "*Ball milling for the formation of nanocrystalline intermetallic compounds from Ni-Ti elemental powders*". Journal of the Mechanical Behavior of Materials, 27 (2018), 1-5. https://doi.org/10.1515/jmbm-2018-2005.

[12] M. Ghadimi, A. Shokuhfar, H.R. Rostami, and M. Ghaffari, "*Effects of milling and annealing on formation and structural characterization of nanocrystalline intermetallic compounds from Ni–Ti elemental powders*". Materials Letters, 80 (2012), 181-183. http://dx.doi.org/10.1016/j.matlet.2012.04.098.

[13]S. Neeraj, T. Raj, and K.K. Jangra, "*Microstructural evaluation of NiTi-powder, Steatite, and Steel balls after different milling conditions*". Materials and Manufacturing Processes, 31 (2016), 628-632. http://dx.doi.org/10.1080/10426914.2015.1004710.

[14] M.I.A.Abdel Maksoud, G.S.El-Sayyad, A. Abokhadra, L.I.Soliman, H.H.El-Bahnasawy, and A.H.Ashour, "*Infuence of Mg^{2+} substitution on structural, optical, magnetic, and antimicrobial properties of Mn–Zn ferrite nanoparticles*". Journal of Materials Science: Materials in Electronic. 31 (2020), 2598–2616. https://doi.org/10.1007/s10854-019-02799-4.

[15] M. Fellah, N. Hezil, F. Hamadi, M. Abdul Samad, A.Alburaikan, H.A.E. Khalifa, A. Obrosov, *Effect of Fe content on physical, tribological and photocatalytical properties of Ti-6Al-xFe alloys for biomedical applications*, Tribology International,191(2024) 109146. https://doi.org/10.1016/j.triboint.2023.109146.

[16] M. Fellah, N. Hezil, M.A. Samad, M. Z. Touhami, A. Montagne, A. Iost, A. Mejias, and S. Kossman., "*The Effect of Milling Time on Structural, Friction and Wear Behavior of Hot Isostatically Pressed Ti–Ni Alloys for Orthopedic Applications*". The Minerals, Metals and Materials Society. (2019), 865-875. http://dx.doi.org/10.1007/978-3-030-05861-6_85.

[17] A. Abada, S. Bergheul, and A.Younes, "*Mechanical and structural behaviour of TiAlV nanocrystalline elaborated by mechanical milling technique*". Micro and Nano Letters. 15 (2020), 1023-1027. http://dx.doi.org/10.1049/mnl.2020.0336.

[18] K. C. Wai Jin, M. M. Anak Mathew Minggat, and R. Singh., "*Sintered Properties of Stainless Steel-doped YTZP Ceramics*". MATEC Web of Conferences. 152 (2018), 1-13. http://dx.doi.org/10.1051/matecconf/201815202006.

[19] N. Loudjani, M. Benchiheub, and M. Bououdina., "*Structural, Thermal and Magnetic Properties of Nanocrystalline $Co_{80}Ni_{20}$ Alloy Prepared by Mechanical Alloying*". Journal of Superconductivity and Novel Magnetism. 29 (2016), 2717-2726. https://link.springer.com/article/10.1007/s10948-016-3541-z.

[20] S.J. Huang, A. Munee, A. Abbas, and R. Sankar., "*The effect of Mg Content and Milling Time on the Solid Solubility and Microstructure of Ti-Mg Alloys Processed by Mechanical*

Milling". Journal of Materials Research and Technology. 11 (2021), 1424-1433. http://dx.doi.org/10.1016/j.jmrt.2021.01.097.

[21] X.-H.Wang, J.-S. Li, H.U. Rui, H.-C. Kou, and L. Zhou, "*Mechanical properties of porous titanium with different distributions of pore size*". Transactions of Nonferrous Metals Society of China. 23 (2013), 2317-2322. https://doi.org/10.1016/S1003-6326(13)62735-1.

[22]D. J. Kim, K. D. Woo, D. S. Kang, and T. Leo, "*Effect of milling time on pore size and distribution of Ti-Nb-Zr biomaterials with space holder consolidated by spark plasma sintering*". Korean Journal of Materials Research. 24 (2014), 1111-1115. http://dx.doi.org/10.3740/MRSK.2014.24.2.111.

[23] V.K. Balla, S. Bodhak, S. Bose, and A. Bandyopadhyay, "*Porous tantalum structures for bone implants: fabrication, mechanical and in vitro biological properties*" Acta Biomaterialia, 6 (2010), 3349-3359. https://doi.org/10.1016/j.actbio.2010.01.046.

[24] L. Shao, Y. Du, K. Dai, H. Wu, Q. Wang, J. Liu, Y. Tang, and L. Wang., "*β-Ti Alloys for Orthopedic and Dental Applications: A Review of Progress on Improvement of Properties through Surface Modification*". Coatings. 11 (2021), 1-19. https://doi.org/10.3390/coatings11121446.

[25] H. Ch. Hsu , S. Ch. Wu, S. K. Hsu, M. S. Tsai, T. Y. Chang, and W. F. Ho., "*Processing and mechanical properties of porous Ti–7.5Mo alloy*". Materials and Design. 47 (2013), 21-26. http://dx.doi.org/10.1016/j.matdes.2012.12.043.

[26] M. Fellah, N. Hezil, T. M. Zine, A. Obrosov, S. Weiß, E. B. Kashkarov, A. M. Lider, A. Montagne, and A. Iost., "*Enhanced structural and tribological performance of nanostructured Ti–15Nb alloy for biomedical applications*". Results in Physics, 15 (2019), 1-7. https://doi.org/10.1016/j.rinp.2019.102767.

[27] M. Ghadiri, and A. Saidi., "*Effect of Ni on Amorphization of Ti-Cu-Ni Ternary Alloys Prepared by Mechanical Alloying*". Journal of Advanced Materials and Processing. 2 (2014), 47-54.

[28] A. Nouri, P.D. Hodgson, and C. Wen., "*Effect of ball-milling time on the structural characteristics of biomedical porous Ti–Sn–Nb alloy*". Materials Science and Engineering: C. 31 (2011), 921-928. https://doi.org/10.1016/j.msec.2011.02.01.

[29] L. Dekhil, S. Louidi, M. Bououdina, and M. Fellah., "*Microstructural, Magnetic, and Nanoindentation Studies of the Ball-Milled Ti80Ni20 Alloy*". Journal of Superconductivity and Novel Magnetism. 32 (2019), 3623-3636. https://link.springer.com/article/10.1007/s10948-019-05145-1.

[30] F. Hammadi, M. Fellah, N. Hezil, L. Aissani, G. Mimanne, S. Mechachti, A. S. Mohammed, A. Montagne, A. Iost, S. Weiß, and A. Obrosov., "*The effect of milling time on the microstructure and mechanical properties of Ti-6Al-4Fe alloys*". Materials Today Communications. 27 (2021), 1-11. http://dx.doi.org/10.1016/j.mtcomm.2021.102428.

[31] E. Farber, A. Orlov, E. Borisov, A. Repnin, S. Kuzin, N. Golubkov, and A. Popovich. " *TiNi Alloy Lattice Structures with Negative Poisson's Ratio: Computer Simulation and Experimental Results*". Metals. 12 (2022), 1-14. https://doi.org/10.3390/met12091476.

[32] X. Zhang , Y. Ding, H. Ma, R. Zhao, L. Wang, and F. Zhang., "*Microstructure and Mechanical Properties of Co-Deposited Ti-Ni Films Prepared by Magnetron Sputtering*". Coatings. 13 (2023), 1-12. https://doi.org/10.3390/coatings13030524.

[33] P. Li, X. Ma, D. Wang, and H. Zhang., "*Microstructural and Mechanical Properties of β-Type Ti–Nb–Sn Biomedical Alloys with Low Elastic Modulus*". Metals. 9 (2019), 1-16. https://doi.org/10.1016/j.jallcom.2019.152412.

[34] R. K. Alla, K. Ginjupalli, N. Upadhya, M. Shammas, R. K. Ravi, and R. Sekhar., "*Surface Roughness of Implants: A Review*". Trends Biomater. Artif. Organs. 25 (2011), 112-118.

CHAPTER IV

TRIBOLOGICAL CHARACTERIZATION

IV. INTRODUCTION

The need for metal biomaterials will always be high because of the growing number of older people who need joint replacements. In general, biomaterials should have low friction coefficients and high wear resistance to minimize the creation of wear debris that could result in unfavorable cellular reactions and cause the implant to loosen.

This chapter will present the results of the tribological tests that were carried out in the physiological solution of a Ringer by using ball-on-plate tribometer performed under different applied loads of 2, 10, and 20 N. Additionally, the wear scars obtained during the tests examined by scanning electron microscopy (SEM) coupled with EDS.

IV.1 Friction coefficient evolution

Wear resistance is crucial in the majority of industrial domains, including biomedicine, nuclear power, aerospace, railroads, machining tools, bearings, and systems exposed to sliding motion, since the surfaces of these materials have to be subjected to friction [1]. Similarly, the wear resistance of bio-prosthetics and bio-sensors is important to their longevity [1-3].

The average friction coefficient (COF) of sintered and HIPed Ti_{50}-Ni_{50} samples under varying applied loads (2, 10, and 20 N) is shown in Figure IV.1. It is evident that the friction coefficient decreased as the milling time increased (i.e. friction resistance increased). Specifically, samples milled at 2 and 6 h had lower friction coefficients than samples milled at 12 and 18 h. This is explained by an improvement in mechanical features, especially hardness, as a result of closed porosity and grain refinement brought on by milling.

These results also showed that the COF value increases with increasing applied load from 2 N to 20 N, reaching a maximum value of 0.51 at 20 N. In contrast, when the applied load was reduced, the COF progressively dropped until it reached a minimum value of 0.31 at 2 N. This behavior can be explained by an increase in the normal load that causes the true contact area to increase, which increases the friction coefficient. Also, as the surface becomes harder with longer milling times (as discussed in the previous chapter), the actual area of contact reduces, which lowers the friction coefficient.

These findings highlight that the main factors influencing the material's frictional behavior are hardness, applied load, and longer grinding times. Similar performances were reported by *Fellah et al.*, [4] for the Ti-Ni, which was produced at various sintering temperatures.

It is also important to note that the sample synthesized after 18 h of milling had a low coefficient of friction value, which validates the estimation of the elasto-plastic ratios previously shown in Figure III.8. This indicates that the elasto-plastic resistance led to improved resistance to friction loads.

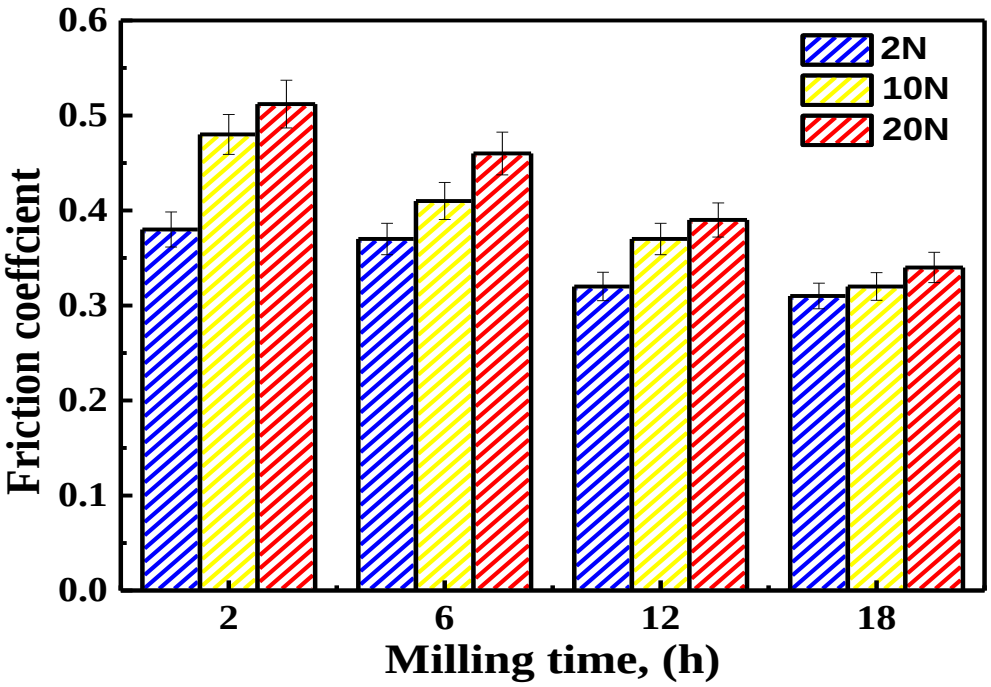

Figure IV.1: Changes in the average friction coefficient values of Ti_{50}-Ni_{50} samples produced at various milling periods.

IV.2 Evolution of wear volume and wear rate

It is important to note that wear resistance is inversely related to wear rate and volume; and that these two variables are directly proportional. Both the wear rate and the wear resistance are reduced when the wear volume is reduced.

The wear rate (W) can be expressed using Equation IV.1 [4] as the ratio of the wear volume to the applied normal load (F) along the sliding distance (L). Through the use of laser profilometry, the wear volume was directly calculated.

$$W=\frac{V}{F.L} \quad \text{(Eq. IV.1)}$$

Figure IV.2 shows how the wear rate and wear volume of the sintered Ti_{50}-Ni_{50} and HIPed samples changed with milling time. The findings demonstrated that when grinding times increased from 2 to 18 h, wear rate, and wear volume decreased.

The wear volume of the Ti_{50}-Ni_{50} specimens during the test (Fig. IV.2.a) varied between 28.37 and 61.34 × 10^7 for the samples that were milled for 2 h, and it significantly dropped to 11.87 to 34.33 × 10^7 µm³ for the samples that were milled for 18 h. Similarly, as shown in Figure IV.2 (b), the wear rate of Ti_{50}-Ni_{50} alloys reduced as the milling duration increased, which ranged from (38.64 to 56.22 × 10^{-3}), (36.35 to 51.54 × 10^{-3}), (31.92 to 47.76 × 10^{-3}) to (29.67 to 42.65 × 10^{-3}) $\mu m^3/N.\mu m$, for the samples milled at 2, 6, 12, and 18 h, respectively.

This trend suggests that longer milling times improve the Ti_{50}-Ni_{50} alloys' resistance to wear, as evidenced by decreased wear rate and volume as well as a lower friction coefficient. The observed enhancement was attributed to improved tribological performance and mechanical features brought about by grain refining. Additionally, both wear rate and wear volume increased with increasing applied loads (2, 10, and 20 N).

According to the data, the grinding time seems to have a significant impact on the alloys' wear volume and rate. The same effect of milling time on wear characteristics was confirmed by the study by *Mahran and Omran* [5]; they found that the volume loss decreased as the milling time increased for the Ti-35Nb-2.5Sn alloy, which had the least amount of wear (0.26 mm^3) following a 12-hour milling cycle (best wear resistance). In addition to milling time, the high temperature of HIPping and sintering has a significant impact on the tribological behavior of Ti_{50}-Ni_{50} alloys. According to earlier research, these high temperatures reduce porosity, creating a dense microstructure and increasing hardness, both of which are directly related to better wear resistance [6-8].

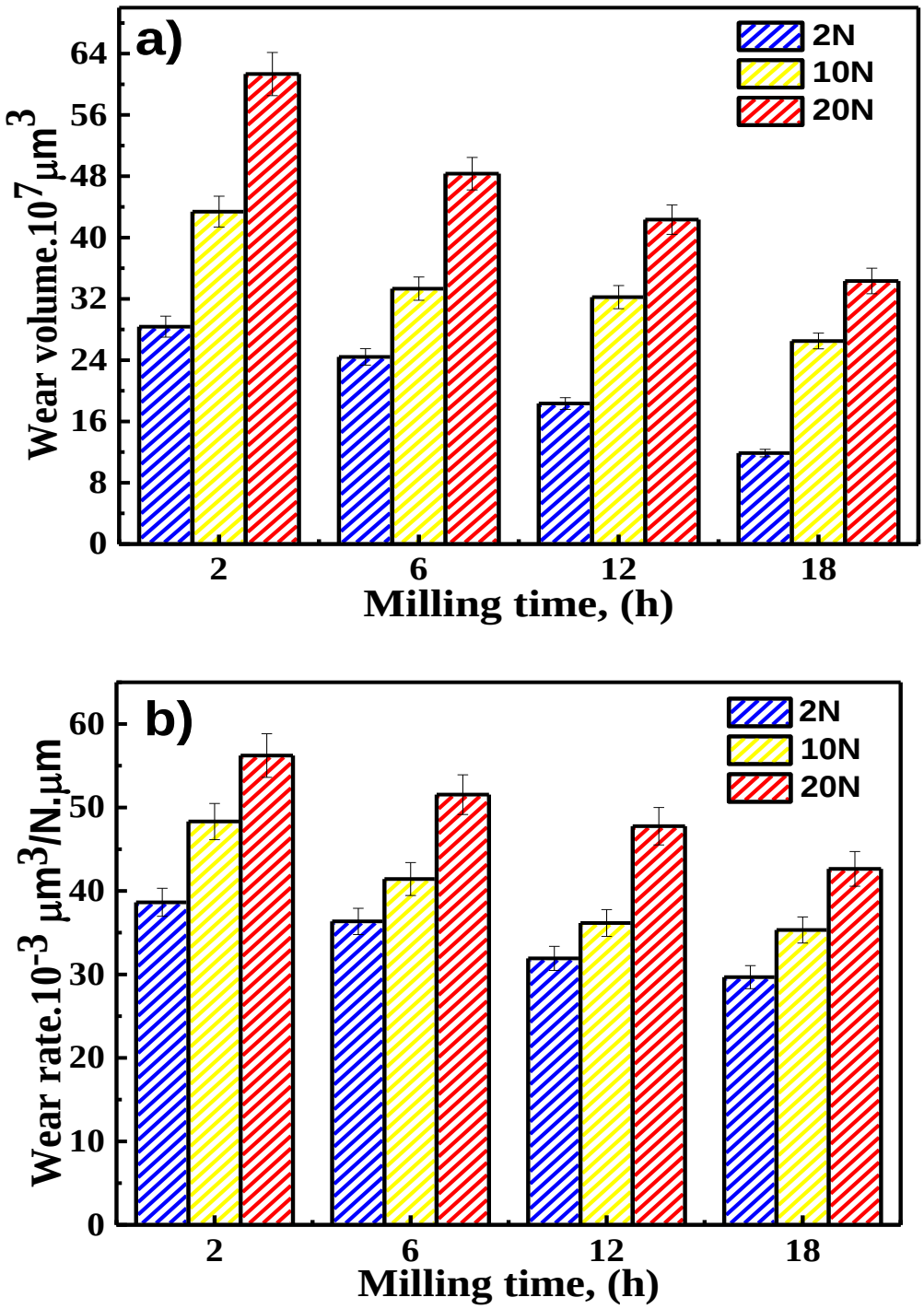

Figure IV.2: Evolution of: a) wear volume and b) wear rate of HIPed and sintered Ti_{50}-Ni_{50} synthesized at different milling time.

Numerous variables, such as the material composition, hardness, friction coefficient, and surface roughness, affect a material's wear characteristics [9-13]. A material's hardness is important

because a high hardness makes it far more resistant to abrasion and deformation, especially plastic deformation [9]. Ultimately, high resistance to plastic deformation will lower the likelihood of delamination, a type of wear that is frequently observed in metallic alloys with extremely low wear resistance and that is highly harmful to the material's lifespan [9].

Several investigations have demonstrated a significant correlation between hardness and wear resistance in materials based on titanium [14-17]; where the experimental findings show that as hardness increases, Ti-based alloys exhibit better wear resistance. In addition to that, *Li and Liu* [18] pointed out that the pseudo-elasticity of Ti-Ni alloys is the main cause of their improved wear behavior. Nonetheless, surface roughness significantly affects tribological performance since smoother surfaces improve material wear resistance and decrease friction.

In summary, the improved tribological features of Ti_{50}-Ni_{50} alloy (low COF and excellent wear resistance) are related to their high hardness and density.

The wear rate and friction coefficient of several titanium alloys under various test conditions were displayed in Table IV.1. In comparison to the other alloys, including CP-Ti, Ti-6Al-4V, Ti-17Nb-6Ta, titanium alloy grade 23, etc., it is evident that the Ti_{50}-Ni_{50} alloy has the lowest wear rate (29.67×10^{-3} $\mu m^3/N.\mu m$). This drop in wear rate suggests that Ti_{50}-Ni_{50} has a high level of wear resistance, which increases its durability in critical applications like implants. Furthermore, the low friction coefficient suggests that this alloy might lessen friction while in operation, which lowers surface wear and enhances material performance in human settings. This superior performance is due to its unique properties, including shape memory effect (SME), superelasticity (SE) and high mechanical features, giving it superiority over conventional alloys such as Ti-6Al-4V. These findings suggest that Ti_{50}-Ni_{50} performs better in medical applications in terms of wear resistance and decreased friction, extending the material life and lowering the need for regular maintenance or replacement.

Table IV.1: The wear rate and fiction coefficient of various types of titanium alloys.

Materials	Testing conditions	Wear rate	Friction coefficient	Refs
CP-Ti	Scratch tests Load of 1 N and 5 N at room temperature and dry sliding conditions, with a tangential scratch speed of 2.5 mm s^{-1}, a scratch length of 5 mm	Not specified	For 1 N load = 0.63±0.11 For 5 N load = 0.64 ± 0.06	[19]
Ti_{50}-Ni_{50}	Tribometer: Pin on plate Normal loads of 2, 10, and 20 N, at stroke length of 5 mm and a sliding speed of 25 mm.s^{-1}	29.67 × 10^{-3} μm^3/N.µm	0.31	In this work
Ti-6Al-4V	Tribometer: Pin on disk Normal load: 5N Sliding speed was varied from 0.2 to 0.8 m/s	10^{-3} mm^3/N.m	0.40-0.50	[20]
Titanium alloy grade 23	Tribometer: Pin on disk Load (30-50 N), sliding speed (1-2 m/s) and sliding distance [1000-2000 m]	Not specified	0.3308	[21]
Ti-17Nb-6Ta	Tribometer: Pin on disk Varied loads of 10, 15, and 20 N, the	0.016 mm^3/N.m	0.22	[22]

	track length was 10 mm, and the frequency was 2 Hz.			
Ti-25Nb-xZr	Tribometer: Ball on plate Varied loads of 2, 10, and 20 N, sliding at a speed of 15 mm/s.	6.23×10^3 $\mu m^3/N.\mu m$ (For 2 N load and Zr content 30 at. %)	Ranged from 0.3 to 0.5 (For 2 N load and Zr content 30 at. %)	[23]
$Ti_{13}Nb_{13}Zr$	Tribometer: Ball on plate The normal load of 29.4 N, the stroke length was fixed at 6 mm, and the frequency was 1 Hz.	1.36×10^{-4} $mm^3/N.m$	≈ 0.15	[24]
Ti-20Mo	Tribometer: Ball on disk Applied loads of 2, 8, and 16 N at a sliding velocity of 10 mm/s	4.21×10^3 $\mu m^3/N.\mu m$ (For 2 N load)	0.20 (For 2 N load)	[25]

IV.3 Wear scars morphology

Figure IV.3 (a-d) displays the SEM images of the worn surfaces and wear tracks of the Ti_{50}-Ni_{50} alloys that were milled at various milling times. The surface degradation of Ti_{50}-Ni_{50} alloys is caused by abrasive and adhesive wear mechanisms. Moreover, the debris becomes finer, the grooves get smaller, and the wear volume, which is shown by the size of the wear strips, reduces as the grinding time increases. It has been shown that significant damage appeared in the milled samples, particularly in those that were ground for 2 and 6 h. In addition, the formation of small-

sized wear debris brought on by the alloy's plastic deformation and fragmentation decreases with increasing milling time.

Plastic deformation is crucial to many wear processes, yet it is not regarded as a wear mechanism [9]. It is typically caused by the surface fatigue wear mechanism and is distinguished by numerous abrasive grooves oriented in the sliding direction on top of smooth, compacted layers. For biomaterials, plastic deformation—which is typically accompanied by delamination—indicates significant wear and is therefore undesirable [9].

According to the images, the main wear mechanism for the specimens that were milled for 2 and 6 h was abrasion (see Fig. IV.3.a and b). During the test, portions broke off from the sample surfaces, causing scratches on their surfaces, which led to the development of this wear mechanism. In addition, there were deep grooves in the wear tracks. On the other hand, delamination and adhesion were found to be the two main wear mechanisms for the samples ground at 12 and 18 h (refer to Fig. IV.3.c and d). In these cases, the debris and worn strips were reduced.

The wear rate values of the sintered samples produced after 12 and 18 h were much lower than those produced after 2 and 6 h of milling. Furthermore, the low coefficient of friction of these samples is compatible with the smooth appearance of the worn surface [26]. Hardness and wear rate also correlate. As alloy hardness increases, the wear rate reduces [27]. *Archard's law* states that the hardness of a material and wear loss is inversely related [28].

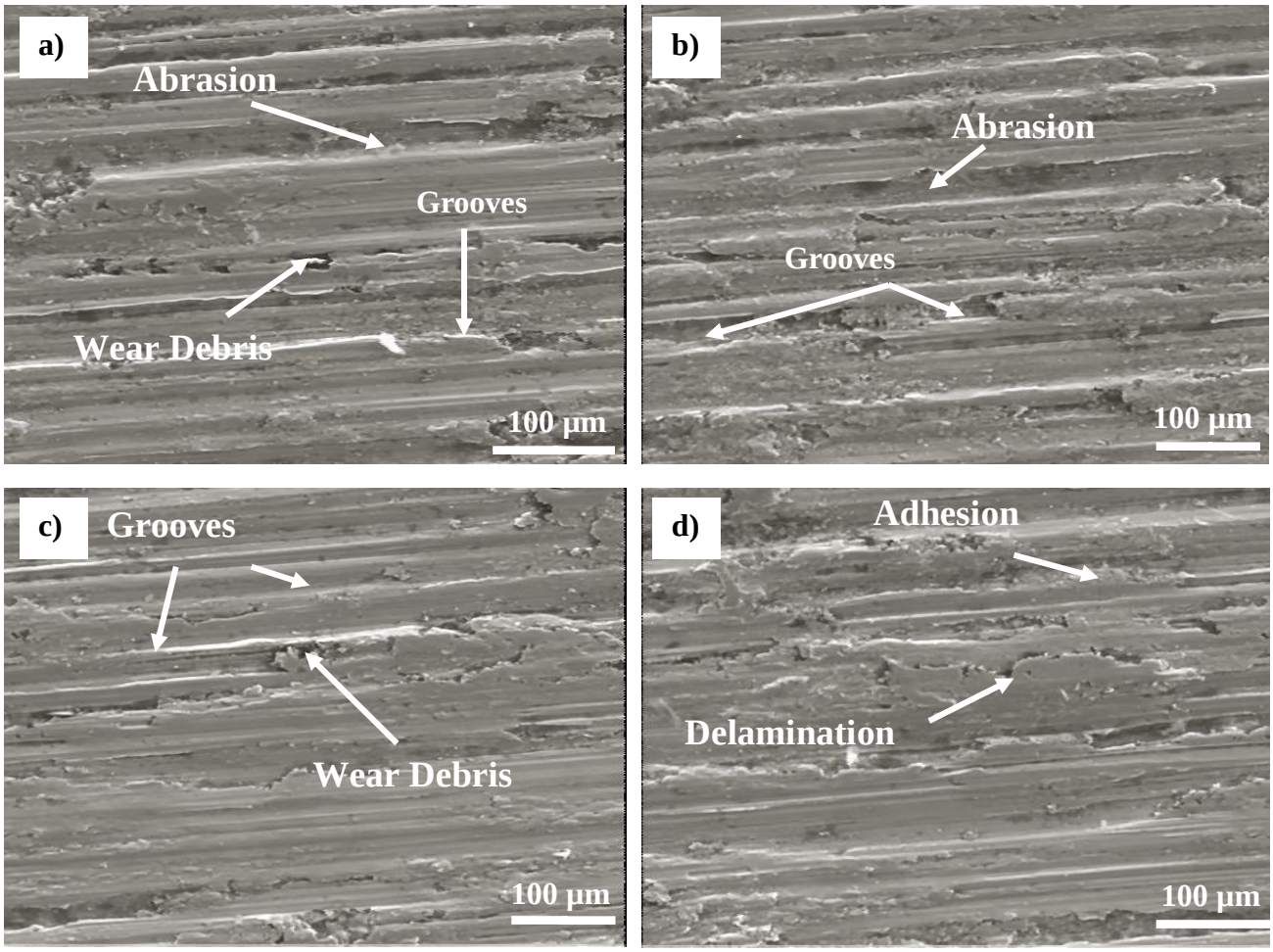

Figure IV.3: SEM micrographs showing the surface condition after wear test of Ti_{50}-Ni_{50} alloys with different milling times.

In the biomedical applications, material wear is an undesired phenomenon since it impacts the functionality and longevity of medical devices, such as implants and prosthetics. Additionally, wear is a major cause of component failure and a source of wear debris. In any tribological system, wear debris is generally undesirable since it pollutes the environment and affects the wear process in a variety of ways (third body effect). The primary cause of patients' long-term problems in biomedical applications, including total joint replacement, is the wear debris that is created [29].

Figure IV.4 shows the wear debris that was produced as a result of the alloy surfaces' oxidized and work-hardened layers deteriorating and surface asperities being destroyed. These processes

invariably result in a third body that contributes to surface deterioration, fostering the wear mechanism seen in Figure IV.3, which includes delamination, adhesion, and abrasion.

For biomaterials, minimizing wear volume, wear rate, and friction coefficient is essential because wear debris released from the implant as a result of poor tribological properties causes detrimental and negative reactions in the human body, which directly affect biocompatibility and result in unfavorable biological reactions.

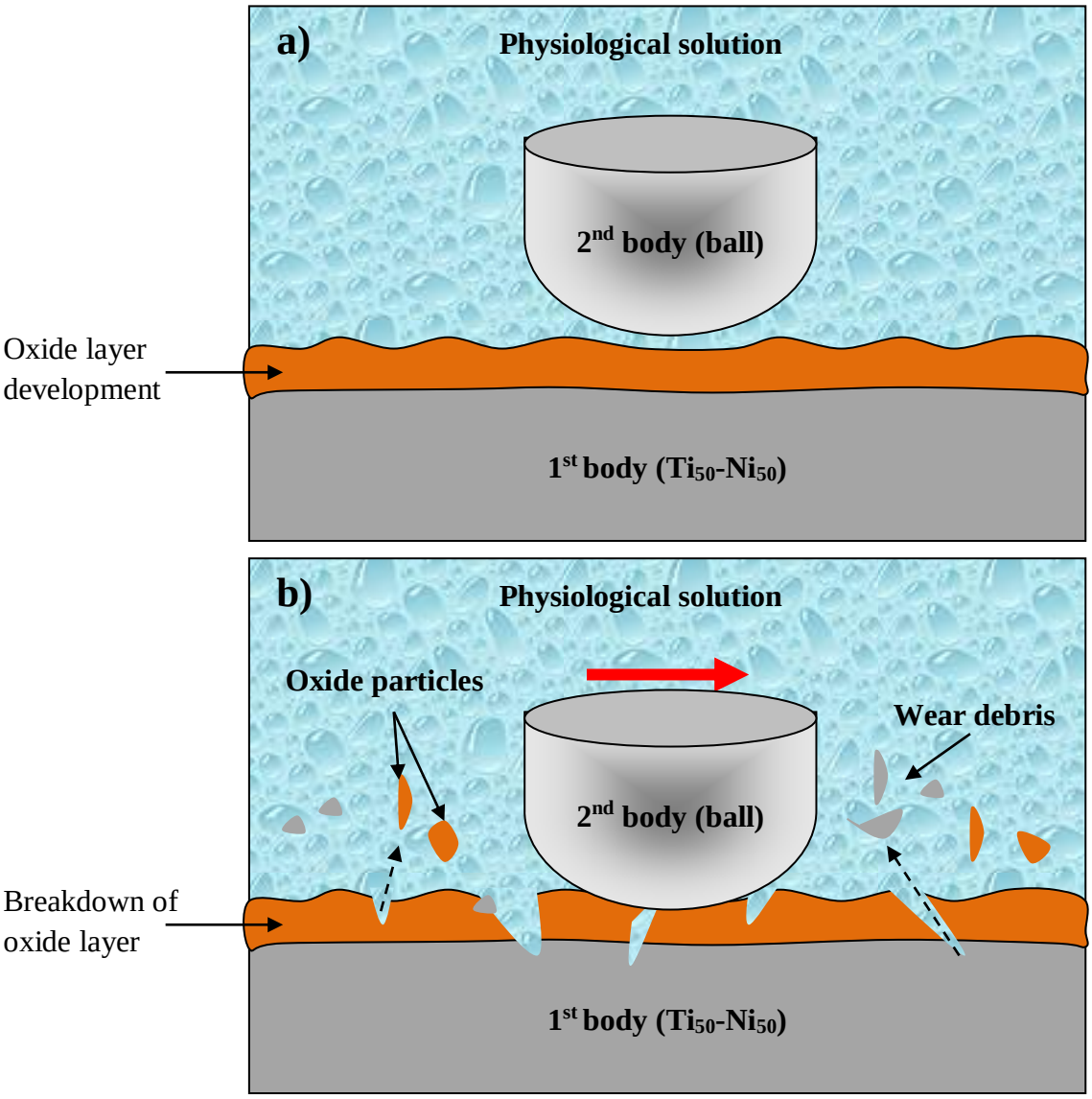

Figure IV.4: Schematic showing the tribological interaction results between Ti_{50}-Ni_{50} and a ball surface: a) before the sliding; b) after the sliding.

Table IV.2 shows the EDS examination of the wear tracks formed on the surfaces of Ti_{50}-Ni_{50} alloys following different grinding times. The depth of the scratch during the tribological test and the mechanical properties of the materials both affect the ratios. The elemental concentrations of Ti and Ni in most samples ground over longer times (12 and 18 hours) have been found to be slightly lower than those in samples ground at shorter times (2 and 6 hours). Apart from these essential components, the study also detects the existence of impurities, such as oxygen (O) came from the atmosphere. However, the oxygen found in the worn regions indicates that oxidation occurred due to the ability of alloys to oxidize. On the other hand, the milling media—interactions with agate balls and vials throughout the milling process—are what explained the existence of silicon (Si) and carbon (C).

Table IV.2: EDS Analysis of the wear tracks produced on the surfaces of Ti_{50}-Ni_{50} alloys tested at 20 N.

Milling time (h)	**Atomic percentage (at. %)**				
	Ti	**Ni**	**Si**	**C**	**O**
2	52.76	45.61	0.69	0.63	1.31
6	52.12	43.53	2.01	1.01	1.33
12	52.1	43.02	2.37	1.40	1.11
18	52.5	45.32	1.12	/	1.06

IV.4 CONCLUSIONS

The tribological behavior of Ti_{50}-Ni_{50} alloys has been studied through the determination of the coefficient of friction, the wear rate and the analysis of surface morphology. The main results of this section are summarized as follows:

- At higher milling time (18 h), the friction coefficient and wear rate significantly decreased, reaching 0.31 and 29.67 × 10^{-3} mm^3/N.mm, respectively.
- Because of the closed porosity and improved grain size refinement, the samples that were milled for 18 h had a lower friction coefficient and a stronger resistance to wear.
- Low coefficient of friction, high density, and hardness are the most parameters that lead to high wear resistance.

- The two primary wear mechanisms for samples that were ground for a longer time were adhesion and delamination. However, for samples that were ground for a short time, abrasion was the main wear mechanism.
- Finally, it can be suggested that the main way to increase the material's resistance to wear is to improve its surface mechanical properties and roughness.

IV.5 BIBLIOGRAPHIC REFERENCES

[1] A. Sayilan., "*Tribological behaviour of Ti-Based thin films: A small scale in situ investigation*". PhD Thesis, University of Lyon, (2023).

[2] K. Toualbia, M. Fellah, N. Hezil, H. Milles, and Z. Djafia., "*Effect of milling time on structural, mechanical and tribological properties of nanostructured HIPed near type Ti-15Mo alloys*". Tribology International, 197 (2024) 109731. https://doi.org/10.1016/j.triboint.2024.109731.

[3] M. Fellah, N. Hezil, F. Hamadi, M. Abdul Samad, A.Alburaikan, H.A.E. Khalifa, and A. Obrosov., "*Effect of Fe content on physical, tribological and photocatalytical properties of Ti-6Al-xFe alloys for biomedical applications*". Tribology International,191 (2024), 109146. https://doi.org/10.1016/j.triboint.2023.109146.

[4] M. Fellah, N. Hezil, M.Z Touhami, M.A. Hussien, A. Montagne, A. Mejias, A. Iost, S. Kossman, T. Chekalkin, A. Obrosov, S. Weiss., "*Effect of Sintering Temperature on Mechanical and Tribological Behavior of Ti-Ni Alloy for Biomedical Applications*". In: The Minerals, Metals and Materials Society (eds) TMS 2020 149th Annual Meeting and Exhibition Supplemental Proceedings. The Minerals, Metals and Materials Series. Springer, Cham (2020), 1701-1710. https://doi.org/10.1007/978-3-030-36296-6_157.

[5] G.M.A. Mahran, and A.M. Omran., "*Fabrication of a Ti–30Nb–4Sn Biomedical Alloy Using Mechanical Alloying*". Science of Advanced Materials, 10 (2018), 1509-1518.

[6] S.R. Oke, O.O. Ige, O.E. Falodun, B.A. Obadele, M.R.. Mphalele, and P.A. Olubambi., "*Influence of Sintering Temperature on Hardness and Wear Properties of TiN Nano Reinforced SAF*". IOP Conference Series: Materials Science and Engineering, 272 (2017), 012030. http://dx.doi.org/10.1088/1757-899X/272/1/012030.

[7] M. Fellah, N. Hezil, K. Abderrahim, M. Abdul Samad, A. Montagne, A. Mejias, A. Iost, S. Kossman, T. Chekalkin, A. Obrosov, and S. Weiss., "*Investigating the Effect of Sintering Temperature on Structural and Tribological Properties of a Nanostructured Ti-20Nb-13Zr Alloy for Biomedical Applications*". In: Li J. et al. (eds) Characterization of Minerals, Metals, and Materials 2020. The Minerals, Metals and Materials Series. Springer, Cham, (2020), 619-629. https://doi.org/10.1007/978-3-030-36628-5_61.

[8] M. Fellah, N. Hezil, D. Leila, M. Abdul Samad, R. Djellabi, S. Kosman, A. Montagne, A. Iost, A. Obrosov, and S. Weiss., "*Effect of sintering temperature on structure and tribological properties of nanostructured Ti-15Mo alloy for biomedical applications*". Transactions of Nonferrous Metals Society of China, 29 (2019), 2310-2320. https://doi.org/10.1016/S1003-6326(19)65137-X.

[9] N.R. Rundora, D.E.P. Klenam, S. Polat, N.M. Mathabathe, J. van der Merwe, and M.O. Bodunrin"., Dry sliding wear behavior of experimental low-cost titanium alloys". Tribology Transactions, 67 (2024), 560-572. https://doi.org/10.1080/10402004.2024.2357288.

[10] N. Ranganathan, F.Anto Lawrence, S. Rajkumar, R.J. Bensingh, M.A. Kader, and S.K. Nayak., "*Influence of surface roughness on tribological and mechanical properties of micro-milled and laser ablated poly (methyl methacrylate) PMMA organic glass*". Polymer Testing, 81 (2020), 106184. https://doi.org/10.1016/j.polymertesting.2019.106184.

[11] R.A. Al-Samarai, Haftirman, K.R. Ahmad, and Y. Al-Douri., "*Evaluate the effects of various surface roughness on the tribological characteristics under dry and lubricated conditions for Al-Si alloy*". Journal of Surface Engineered Materials and Advanced Technology, (2012), 167-173. http://dx.doi.org/10.4236/jsemat.2012.23027.

[12] T. Leśniewski, and S. Krawiec., "*The effect of ball hardness on four-ball wear test results*". Wear, 264 (2008), 662-670. http://dx.doi.org/10.1016/j.wear.2007.06.001.

[13] B. Leszczyńska-Madej, M. Madej, and J. Hrabia-Wiśnios., "*Effect of chemical composition on the microstructure and tribological properties of Sn-based alloys*". Journal of Materials Engineering and Performance, 28 (2019), 4065-4073. http://dx.doi.org/10.1007/s11665-019-04154-4.

[14] J. Cheng, S. Zhu, Y. Yu, J. Yang, and W. Liu., "*Microstructure, mechanical and tribological properties of TiAl-based composites reinforced with high volume fraction of nearly networkTi$_2$AlC particulates*". Journal of Materials Science and Technology, 34 (2018), 670-678. https://doi.org/10.1016/j.jmst.2017.09.007.

[15] G. Li, S.G. Qu, Y.X. Pan, and X.Q. Li., "*Effects of the different frequencies and loads of ultrasonic surface rolling on surface mechanical properties and fretting wear resistance of HIP Ti-6Al-4V alloy*". Applied Surface Science, 389 (2016), 324-334. https://doi.org/10.1016/j.apsusc.2016.07.120.

[16] K.S. Chan, M. Koike, and T. Okabe. "*Modeling wear of cast Ti alloys*". Acta Biomaterialia, 3 (2007), 383-389. https://doi.org/10.1016/j.actbio.2006.10.007.

[17] M. Fellah, N. Hezil, D. Bouras, N. Bouchareb, A. P. Larios, A. Obrosov, G. A. El-Hiti, and S. Weiß, "*Effect of Zr content on electrochemical and tribological properties of newly developed near β-type Ti-Alloys (Ti-25Nb-xZr) for biomedical Applications*". Journal of Science: Advanced Materials and Devices, 9 (2024), 100695. https://doi.org/10.1016/j.jsamd.2024.100695.

[18] D.Y. Li, and R. Liu., "*The mechanism responsible for high wear resistance of Pseudo-elastic TiNi alloy—a novel tribo-material*". Wear, 225-229 (1999), 777–783. https://doi.org/10.1016/S0043-1648(98)00388-3.

[19] D. Silva, C. Arcos, C. Montero, C. Guerra, C. Martínez, X. Li, A. Ringuedé, M. Cassir, K. Ogle, D. Guzmán, C. Aguilar, M. Páez, and M. Sancy"., *A Tribological and Ion Released*

Research of Ti-Materials for Medical Devices Daniela Silva". Materials, 15 (2021), 131. https://doi.org/10.3390/ma15010131.

[20] A. Mishra., "*Analysis of friction and wear of titanium alloys*". International Journal of Mechanical Engineering and Robotics Research, 3 (2014), 570-573.

[21] P. Sivaprakasam, T. Hailu, and G. Elias., "*Experimental investigation on wear behavior of titanium alloy (Grade 23) by pin on disc tribometer*". Results in Materials, 19 (2023), 100422. https://doi.org/10.1016/j.rinma.2023.100422.

[22]R. Soni, S. Pande, S. Kumar, S. Salunkhe, H. Natu, and H.M. Abdel Moneam Hussein., "*Wear characterization of laser cladded Ti-Nb-Ta alloy for biomedical applications*". Crystals, 12 (2022), 1716. https://doi.org/10.3390/cryst12121716.

[23] M. Fellah, N. Hezil, D. Bouras, N. Bouchareb, A. Perez Larios, A. Obrosov, G.A. El-Hiti, and S. Weiß., "*Investigating the effect of Zr content on electrochemical and tribological properties of newly developed near β-type Ti-alloys (Ti–25Nb-xZr) for biomedical applications*". Journal of Science Advanced Materials and Devices 9 (2024), 100695. https://doi.org/10.1016/j.jsamd.2024.100695.

[24] S. Xiaolei, L. Yong, W. Junyang, W. Qingliang, Q. Jianghao, B. Andrew, B. Michael, and J. Zhongmin., "*Structure, tribological properties, and the growth mechanism of in-situ generated TiC in titanium cermet*". Friction, 10 (2022), 706-716. https://doi.org/10.1007/s40544-020-0484-y.

[25] M. Fellah, N. Hezil, M. Abdul Samad, R. Jellabi, A. Montagne, A. Mejias, S. Kossman, A. Iost, A. Purnama, A. Obrosov, and S. Weiss., "*Effect of Molybdenum Content on Structural, Mechanical, and Tribological Properties of Hot Isostatically Pressed β-Type Titanium Alloys for Orthopedic Applications*". Journal of Materials Engineering and Performance, 28 (2019), 5988-5999. https://doi.org/10.1007/s11665-019-04348-w.

[26] M. Fellah, N. Hezil, M.Z. Touhami, M.A. Samad, A. Obrosov, D.O. Bokov, E. Marchenko, A. Montagne, A. IOST, and A. Alhussein., "*Structural, tribological and antibacterial properties of (α+β) based ti-alloys for biomedical applications*". Journal of Materials Research and Technology, 9 (2020), 14061-14074. https://doi.org/10.1016/j.jmrt.2020.09.118.

[27] Ş. Karadeniza, and E. Arslan., "*Microstructural Characterization and Wear Behavior of Porous Equimolar TiNbZr Medium-Entropy Alloys Scaffolds Produced by Mechanical Alloying*". Materials Research, 25 (2022), 1-7. https://doi.org/10.1590/1980-5373-MR-2022-0238.

[28] J. Archard., "*Contact and rubbing of flat surfaces*". Journal of Applied Physics. 24 (1953), 981-988.

[29] A. Abdelbary, and L. Chang., Practical applications of tribology. In book: Principles of Engineering Tribology, (2023). http://dx.doi.org/10.1016/B978-0-323-99115-5.00005-0.

CHAPTER IV

ELECTROCHEMICAL CHARACTERIZATION

V. INTRODUCTION

Titanium and its alloys are widely used in the medical field because of their mechanical properties and corrosion resistance, especially for implants that must fit harmoniously into the human body. These implants come into contact with potentially corrosive bodily fluids in the biological environment. One important phenomenon that can cause material deterioration, metal ion release, and inflammatory responses in nearby tissues is electrochemical corrosion. Understanding the electrochemical behavior of titanium alloys used in orthopedic implants is essential to ensuring their safety and efficacy, reducing the risk of corrosion and enhancing patient health in a complex environment based on their durability and biocompatibility.

This chapter will present the results of the electrochemical tests (OCP, PD, and EIS) that were carried out in the physiological solution of Hank.

V.1 Open circuit potential (OCP) measurements

A common method for assessing the chemical stability of specimens and the corrosion process is open-circuit potential (OCP) [1]. Figure V.1 illustrates the changes in the open-circuit potential (OCP) of the Ti_{50}-Ni_{50} samples produced at various milling times after they were submerged for 2500 seconds in Hank's solution. OCP changes are related to the structure, composition and development of the passive film [2]. In all cases, the OCP values rose with increasing immersion time until stabilizing; this suggests that a passive film is forming on the sample's surface [3]; this can strengthen its resistance to corrosion by preventing the discharge of metal ions [4]. In titanium and its alloys, especially Ti-Ni alloys, the passive layer that formed on their surface is mostly composed of TiO_2 [5].

The OCP curves move toward the higher values, particularly for those produced with a longer milling time (18 hours). By passivation the sample surfaces when the OCP moves to the nobler levels, the alloys are shielded from corrosion and become more resistant [6]. The OCP values stabilized at -0.20275, -0.17408, -0.13031, and -0.074 $V/_{SCE}$ for specimens milled at 2, 6, 12, and 18 hours, respectively; the constant OCP value showed that the alloys' protective oxide layer had fully developed. Similar findings were made by *Martina et al.,* [7] who discovered that Ti-based alloys typically had greater electropositive OCP values than pure Ti. Over time, these values rise

to nobler levels, indicating improved corrosion resistance and passive state. The open circuit potential of the Ti_{50}-Ni_{50} specimens is impacted by grinding time. The powders' crystallite size usually decreases as the milling time increases from 2 to 18 hours because of mechanical deformation and fracture processes. The surface reactivity of finer grains is increased by their higher grain boundary density and greater number of lattice defects [8, 9]. The OCP values are positively impacted by the increased surface reactivity. *Grosjean et al.,* [9] corroborated the favorable effect of ball milling by showing that that OCP values increase as the milling duration increases. The larger OCP for samples that underwent 18 hours of milling would indicate a greater reactivity with the electrolyte to create a dense and protective passive layer [9].

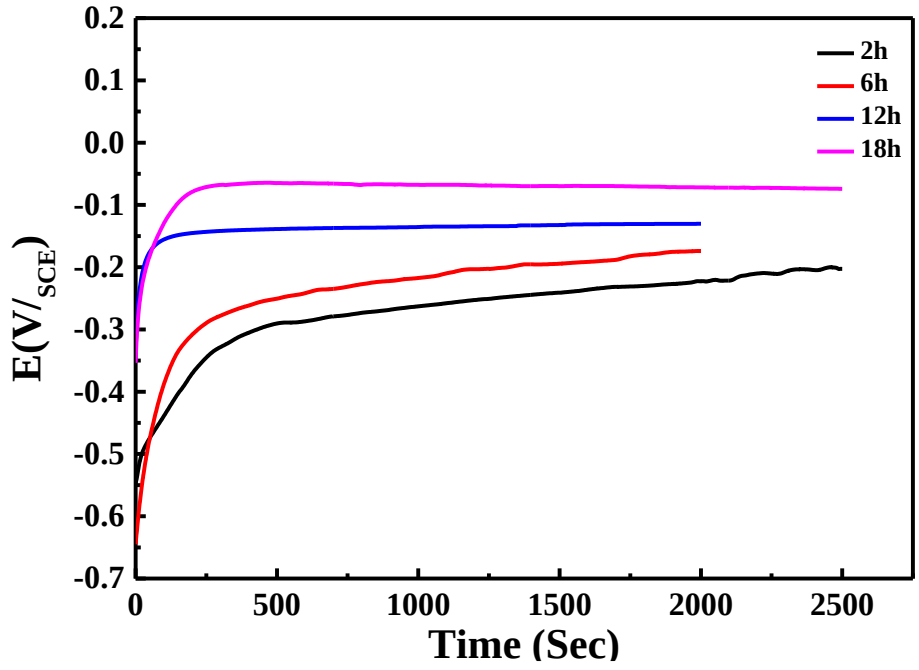

Figure V.1: OCP evolution for Ti_{50}-Ni_{50} samples in Hank's solution during a period of 2500 seconds.

Moreover, high-temperature pressing and sintering after milling have a significant impact on the OCP by reducing porosity and raising density due to grain refinement. *Danny et al.'s* investigation [10] verified this effect, showing that Ti-Si alloy electrodes that underwent mechanical alloying (MA) and subsequent heat treatment had marginally higher positive OCP values than samples that were not heat treated or pure Ti.

V.2 Potentiodynamic polarization measurements (PD)

The polarization test is a method used to evaluate the corrosion resistance of metallic materials by examining the relationship between the current density per unit surface area and the artificially scanned potential [11]. Figure V.2 illustrates how grinding time affects the potentiodynamic polarization curves of the Ti_{50}-Ni_{50} alloys immersed in Hank's solution. We find that all Ti_{50}-Ni_{50} alloys exhibit a passivation region. The passivation region in polarization curves indicates that a passive coating has formed on the material's surface, reducing its susceptibility to corrosion [12]. Therefore, the existence of the polarization curve's passivation region is one of the most important factors in determining a material's resistance to corrosion.

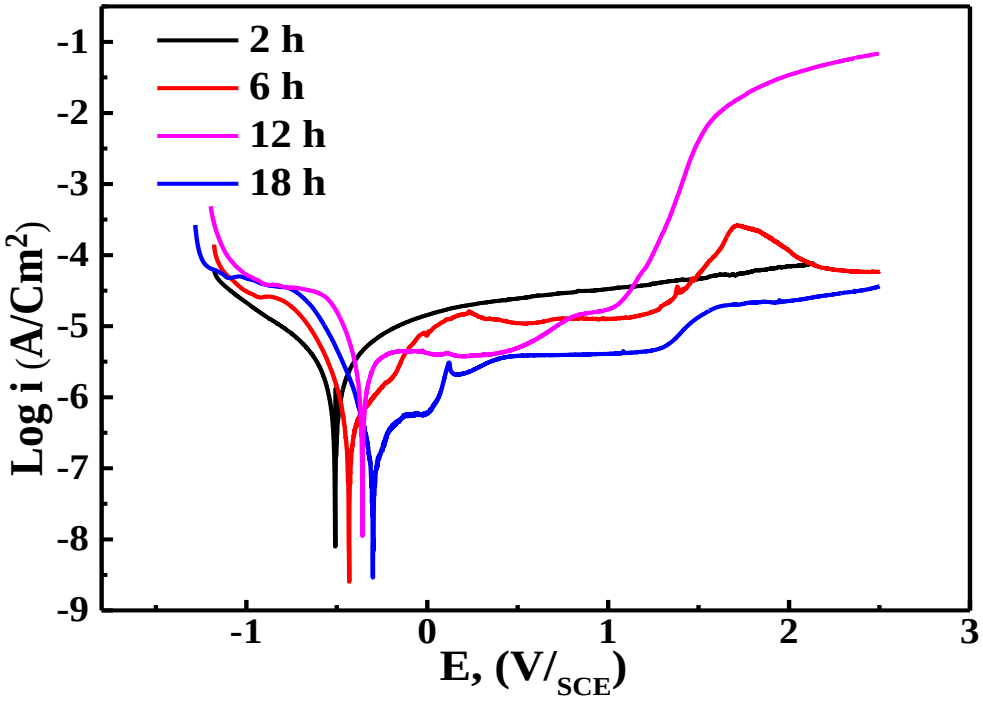

Figure V.2: Potentiodynamic polarization curves for Ti_{50}-Ni_{50} samples manufactured at different milling periods (2, 6, 12, and 18 hours).

In order to assess the materials' resistance to corrosion and comprehend the behavior of corrosion, the Tafel method was utilized to compute the corrosion potential (E_{corr}), corrosion current (i_{corr}), and corrosion rate (CR). To extract the E_{corr} and i_{corr} from the polarization data, the

Tafel fit method was applied using C $_{View}$ software. Table V.1 provides an illustration of these parameters' values.

Table V.1: Corrosion parameters for Ti_{50}-Ni_{50} in Hank's solution derived from potentiodynamic polarization curves Log i = f (E).

Milling Times	Potentiodynamic parameters						
	E_{corr} (V/SCE)	i_{corr} (A/cm^2)	i_{pass} (A/cm^2)	β_c (mV)	β_a (mV)	CR (mm/year)	R_P (Ω/cm^2)
2 h	-0.51255	1.0179×10^{-6}	3.1893×10^{-5}	191.49	2449	0.014902	427136.86
6 h	-0.43214	5.1039×10^{-7}	1.3248×10^{-5}	194.48	5367.3	0.013088	851863.497
12 h	-0.35817	4.6603×10^{-7}	4.1750×10^{-6}	231.54	269.44	0.011215	932949.832
18 h	-0.29997	3.6945×10^{-7}	4.0083×10^{-6}	537.45	581.21	0.0074722	1176837.49

Table V.1 demonstrates that as milling times increase from 2 to 18 hours, the corrosion current (i_{corr}) and corrosion rate (CR) decrease, reaching values of 3.6945×10^{-7} A/cm^2 and 0.0074722 mm/year, respectively. This further suggests that a passive protective layer has developed on its surface [6]. Thus, the specimen made at the longer milling time (18 hours) shows lower icorr values, indicating that the material has developed a more stable passive layer that reduces the corrosion rate (CR), improving corrosion resistance [5].

Because the biomaterial releases metallic ions into the human body, a low CR lowers the likelihood of allergic reactions and other unwanted occurrences brought on by ionic pollution [13]. However, the corrosion potential (E_{corr}) values moved in a more noble direction as the milling time rose due to the increasing grain refinement that occurred during the ball-milling operation [14].

Variations in the corrosion potential (E_{corr}) and corrosion current density (i_{corr}) values for specimens exhibiting passive behavior are caused by two significant factors that can significantly affect the material's electrochemical properties: density and grain refinement (fine grain size). According to *Ihsan-ul-Haq's* research [15]; specimens with refined microstructures, higher densities, and smaller porosities typically exhibit better passivation behavior by having lower icorr values and higher E_{corr}. Along with the grinding duration, high temperatures also affect the corrosion parameters (E_{corr} and i_{corr}). *Guo et al.'s* study [16] on Ti-24Nb-4Zr-7.9Sn alloys found that lower densities (sintered at low temperatures) had lower E_{corr} and greater i_{corr}, which indicated worse corrosion resistance, and vice versa. The structure became more porous and less dense when sintered at low temperatures, which decreased its resistance to corrosion. Increased density results in less interconnected porosity, which enhances corrosion resistance because there is a decreased possibility of electrolyte entering these interconnected pores [16]. Another study on the impact of sintering temperature on density and corrosion characteristics is published by *Bautista et al* [17]. At a higher sintering temperature, they found that the alloy with the best corrosion resistance was the one with the maximum sintering density.

Similarly, the passive current density (i_{pass}) is an important parameter for comparing and assessing passive metals' resistance to corrosion. Similar to i_{corr}, the i_{pass} results showed a decline with higher milling. The samples that were milled for 18 hours had the lowest result, 4.0083×10^{-6} A/cm^2, which suggests that their passive film is more stable and protective [18]. As a result, extended milling creates a passive film that is more resilient and protective.

The values of R_p were obtained using the following equation [19].

$$R_p = \frac{1}{icorr}\left(\frac{\beta_c \beta_a}{2.3(\beta_c \beta_a)}\right) \quad \text{(Eq. V.1)}$$

Where: i_{corr} is the corrosion current density, R_p is the polarization resistance, and β_a and β_c are the anodic and cathodic Tafel slope values, respectively.

Table V.1 shows that as the milling time increases, the polarization resistance (R_p) of the Ti_{50}-Ni_{50} samples increases from 427136.86 Ω/cm^2 to 1176837.49 Ω/cm^2. This is due to variations in

the microstructure and surface characteristics of the alloys [1]. Numerous factors, including the environment, microstructure, composition of the alloy, manufacturing procedures, intermetallic formation, etc., influence the corrosion resistance of titanium alloys, according to the literature [3, 20]. The presence of a passive layer on the specimens' surface was also suggested by the higher R_p values [21]. Better corrosion resistance of materials is thus suggested by improved polarization resistance.

V.3 Electrochemical impedance spectroscopy (EIS) and equivalent circuit analysis

The impact of milling times on the corrosion resistance of Ti_{50}-Ni_{50} samples has been investigated using the impedance approach. The kinetic characteristics of electron transport reactions at the metal/environment interface are described by EIS [19]. Figure V.3 displays the Nyquist and Bode curves for the EIS measurements of the Ti_{50}-Ni_{50} samples in Hank's solution.

The Nyquist plots of Fig. V.3.a shows the variation of the imaginary impedance component (Z″) with a real impedance component (Z′). Every sample that was analyzed had semicircle impedance spectra that were not complete. Higher corrosion resistance is indicated by a larger arc diameter, and lesser corrosion resistance is indicated by a smaller arc diameter [22, 23]. The semicircle diameter increases with increasing milling times (Fig. V.3.a), reaching its greatest value for the alloy produced at a greater milling period (18 h); this suggests that the particles milled for 18 h have increased the stability of the passive film [24, 25].

The surface of titanium alloy spontaneously passivates, forming a protective layer that prevents the metal from oxidizing further [13]. Because titanium has a strong affinity for oxygen, it and its alloys form oxide layers on their surfaces, improving corrosion resistance and osseointegration [13, 26].

The Bode plots in Figure V.3 (b) show that the impedance increased as the grinding times increased. The impedance of the interface |Z| was higher in the sample that was obtained at longer grinding durations (12 and 18 hours), suggesting that it was more resistant to corrosion. According to *Seikh et al.*, [27] the alloy's high impedance value indicates that it has good corrosion resistance.

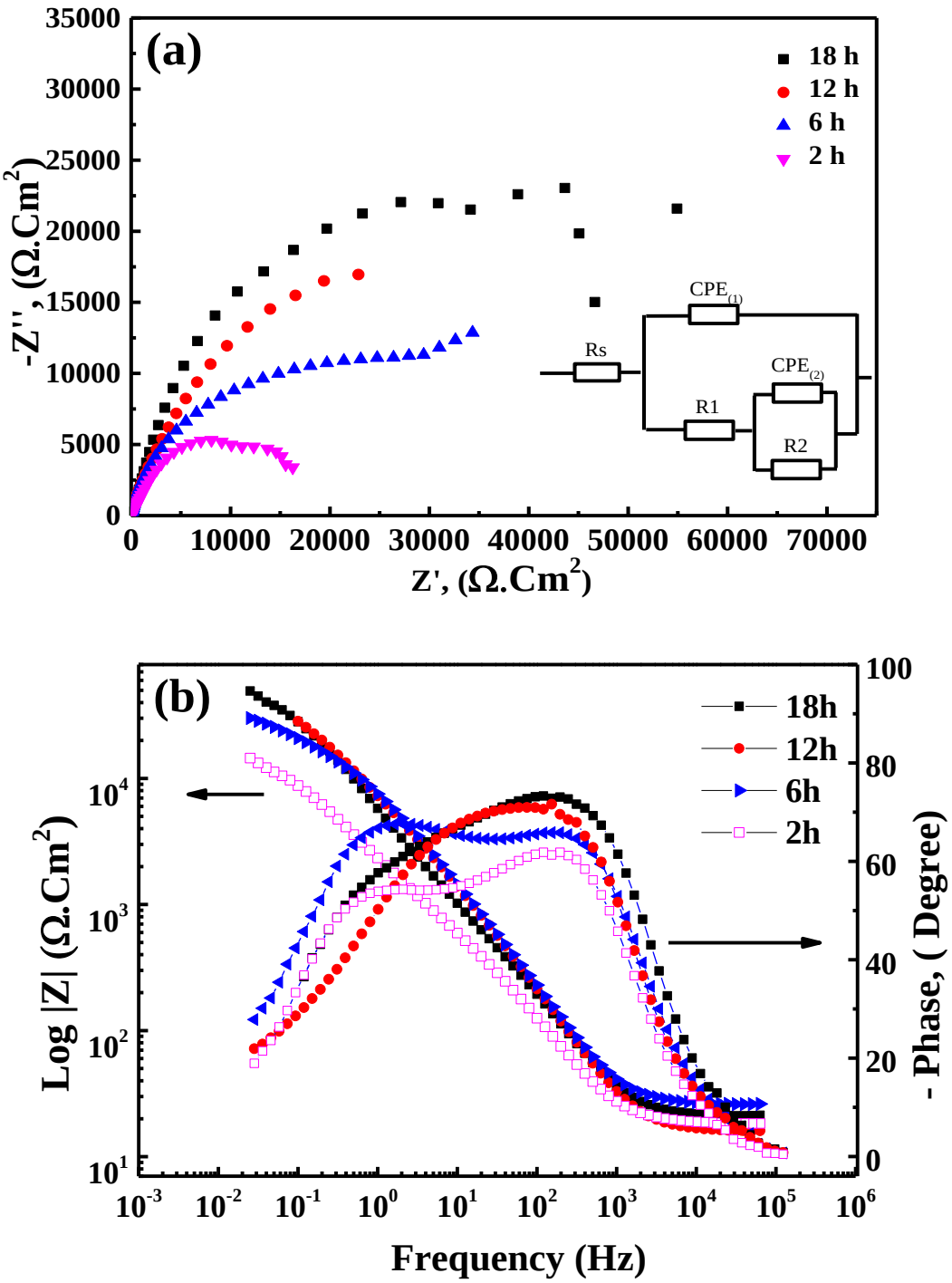

Figure V.3: Electrochemical impedance spectra of the Ti_{50}-Ni_{50} produced at various milling times: a) Nyquist plots and b) Bode plots.

Additionally, at the middle frequencies range, the phase angle (φ) of all Ti_{50}-Ni_{50} samples was stable, with values of 61.43°, 65.97°, 71.43°, and 74.44° for 2, 6, 12, and 18 hours, respectively.

This suggests that the alloy has a compact passive oxide film [28]. It should be mentioned that powders that are ground for 12 and 18 hours exhibit a maximum phase angle when compared to powders that are ground for 2 and 6 hours. Higher phase angle values signify a layer that is highly resistant and insulating, while lower phase angle values indicate a layer that is less resistant and porous, allowing for melting and incorporation processes with the surrounding environment [18]. According to earlier research, the high phase angle and high impedance (Z) suggest a capacitive behavior associated with corrosion-resistant material [29]. Furthermore, the suggested model "equivalent circuit" (Fig. V.4) confirms that the film on titanium alloys is bi-layered, with an inner barrier layer and an outer porous layer [30].

Table V.2: Equivalent circuit parameters for Ti_{50}-Ni_{50} alloys following their submersion in Hank's solution.

Alloys	**Rs (Ω/cm^2)**	**C 1 (F/cm^2)**	**n 1**	**R1 (Ω/cm^2) 10^3 porous**	**C 2 (F/cm^2)**	**n 2**	**R2 (Ω/cm^2) 10^6 barrier**	**X^2 (10^{-4})**
2 h	134	32 (±0.3)	0.99	11.5	41 (±0.31)	0.99	2.01	2.3
6 h	124	29 (±0.9)	0.99	15.2	29 (±1.1)	0.97	3.33	2.1
12 h	113	25(±1.3)	0.99	23.0	27 (±0.9)	0.99	3.87	1.8
18 h	101	19 (±1.8)	0.98	39.2	23 (±0.9)	0.98	4.02	1.9

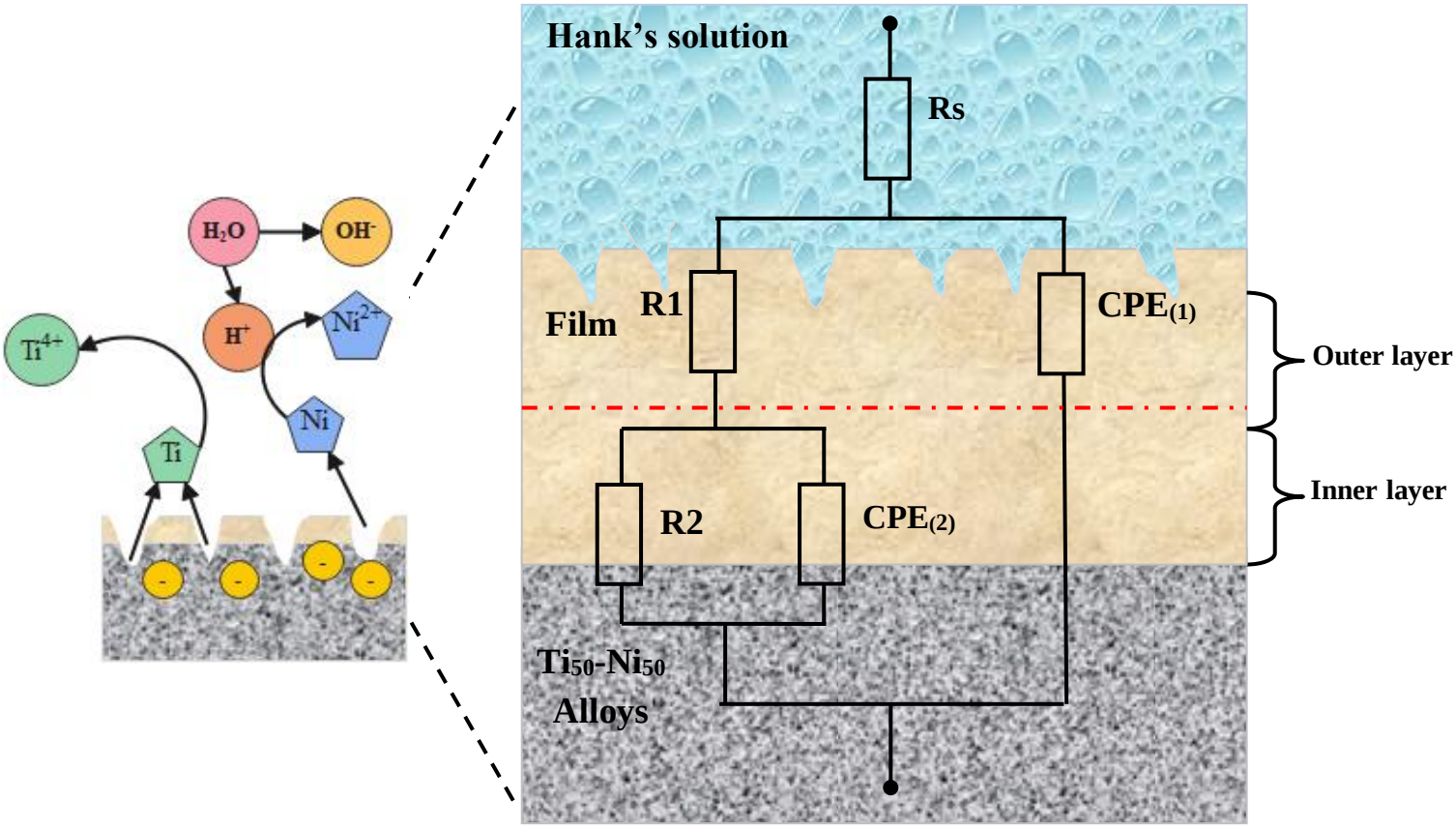

Figure V.4: Equivalent circuit utilized for fitting data obtained for Ti_{50}-Ni_{50}.

The EIS data obtained from binary Ti_{50}-Ni_{50} alloys was simulated using an equivalent circuit (Fig. V.4).The fitted parameters of the model are shown in Table V.2, where Rs is the resistance of the solution. The resistance of the porous layer is denoted by R1, while the charge transfer resistance of the barrier layer is denoted by R2. Capacitances C1 and C2 of porous and barrier layers, respectively, make up a constant phase element denoted by CPE (1) and CPE (2).

$Z_{CPE} = [Y_0 (j\omega)^n]^{-1}$ is the definition of the impedance of the phase element, where Y_0 is the CPE admittance, $j = -1$, $\omega = 2\pi f$ is the angular frequency, and n ranges from -1 to 1 [28]. There is a correlation between the value of n and the non-uniform current distribution caused by surface imperfections and roughness [31]. The fitting quality of equivalent circuits was assessed using the values of χ^2 (order of 10^{-4}).

The results presented in Table V.2 show that the inner barrier layers (R2) are much larger than the outer porous layer (R1), indicating that the barrier layer plays a major role in the protection

provided by the passive layer [30]. Furthermore, the values of these resistances (i.e., R1 and R2) rose as milling times increased, indicating that higher passivation improved the alloys' corrosion resistance [32]. Longer milling times enhance passivation by microstructural refinement [33]; where longer ball milling times increase the Ti_{50}-Ni_{50}'s corrosion resistance by reducing both i_{corr} and i_{pass} and increasing R_p, as shown by polarization tests (Table V.1). A higher protective oxide layer and increased electrochemical resistances at the alloy-environment interface lead to improved corrosion resistance.

The charge transfer resistance is directly related to the rate of corrosion. Because the alloy particles aggregate and there are fewer voids between them, the Ti_{50}-Ni_{50} alloy that has been milled for 18 hours has the highest value of charge transfer of any sample [34]. Its nobler electrochemical behavior is demonstrated by the greater charge transfer resistance value, which shows that the formation of a stable passive coating on its surface has been effective in thwarting the corrosive attack [35]. Consequently, the Ti_{50}-Ni_{50} alloy's low passive current densities and strong charge transfer resistance, which were obtained after 18 hours of milling in Hank's solution, show that it has good corrosion resistance in the human body's environment.

The following formula (Eq. V.2) was used to compute the C1 and C2 [36, 37]:

$$C = (CPE \times R^{1-n})^{1/n} \quad \text{(Eq. V.2)}$$

Where: R represents charge transfer resistance.

The comparatively high capacitance values imply strong corrosion activity on the material surface [38]. According to Table V.2, the capacitance values (C1 and C2) decrease sharply as milling times increase, going from 32 F/cm^2 and 41 F/cm^2 to 19 F/cm^2 and 23 F/cm^2, respectively. This suggests the formation of a protective layer that lessens surface corrosion sites and, as a result, lowers capacitance [38].

In conclusion, the data reveal that the development of a persistent passive layer that functions as a barrier on the surface of the Ti_{50}-Ni_{50} alloys improves their resistance to corrosion. Additionally, the formation of this stable layer that lowers the corrosion rate is demonstrated by the increase in charge transfer resistance and decrease in capacitance with increasing milling

time. Furthermore, because of the refinement of the grain, samples ground at longer milling times are more resistant to corrosion; when there are more grain boundaries, which act as passive film nucleation sites, the finer grains promote the formation of a more noble and compact passive film [39].

The findings of this study indicate a correlation between the porosity, density, mechanical characteristics, particularly hardness, and corrosion resistance of Ti_{50}-Ni_{50} alloys that were generated after 2, 6, 12, and 18 hours of milling. Grain refinement increased the density during the ball grinding process, led to the reduction of the porosity which affected the alloy's corrosion behavior. Metal materials' mechanical and corrosion characteristics are significantly impacted by their porosity [31]. With longer milling durations, this alloy's mechanical characteristics (such as hardness and elastic modulus) improved due to its low porosity and refined grain. According to Fellah et al., this improvement in mechanical qualities (high hardness) can result in better corrosion behavior of a material [12].

Finally, these alloys are a coveted class of metallic biomaterials suitable for a range of biomedical uses, such as total hip replacement, due to their improved mechanical and physical properties, exceptional corrosion resistance in biological conditions, and unique microstructure.

V.4 CONCLUSIONS

In this study, we employed a number of electrochemical methods to examine the corrosion of the Ti_{50}-Ni_{50} alloys in the presence of Hank’s solution, such as electrochemical impedance spectroscopy (SIE), potentiodynamic polarization curves (PD), and open circuit potential (OCP). The following conclusions are drawn from the study's findings:

- The development of a stable passive layer on the sample surface is indicated by the OCP curves, which rise as immersion time increase up to 2500 seconds.
- The corrosion current and rate decreased with increasing milling times, reaching 3.6945×10^{-7} A/cm^2 and 0.0074722 mm/year, respectively. However, the values of the corrosion potential (E_{corr}) shifted in a nobler direction.
- The passive current density value was lowest in samples that were milled for 18 hours, suggesting a more stable and protective passive film.

- The EIS results demonstrate that Ti_{50}-Ni_{50} exhibits capacitive behavior by forming a two-layer film on the alloy's surfaces and by improving passive film resistance to corrosion through longer grinding durations.
- The formation of a stable protective layer on the metal surface is indicated by a decrease in capacitance and an increase in charge transfer resistance.
- Grain refinement is the cause of metals' improved corrosion behavior.
- The results reveal that the Ti_{50}-Ni_{50} material's corrosion characteristics improve with extended milling durations.

V.5 BIBLIOGRAPHIC REFERENCES

[1] I. Şimşek and D. Özyürek, "*Investigation of wear and corrosion behaviors of Ti15Mo alloy produced by mechanical alloying method in SBF environment*". Powder Metallurgy and Metal Ceramics, 58 (2019), 446-454. http://dx.doi.org/10.1007/s11106-019-00094-9.

[2] H. Liu, Z. Wang, J. Cheng, N. Li, S.-Xing Liang, L. Zhang, F. Shang, D. Oleksandr, and L.-Yu Chen, "*Nb content dependent passivation behavior of Ti-Nb alloys for biomedical application*". Journal of Materials Research and Technology, 27 (2023), 7882-7894. https://doi.org/10.1016/j.jmrt.2023.11.203.

[3] C. Li, J. Chen, W. Li, Y. Ren, and J. He, "*Investigation on the preparation and mechanical properties of porous Cu35Ni15Cr alloy for a molten carbonate fuel cell*". Materials Science-Poland, 33 (2015), 887-893. http://dx.doi.org/10.1515/msp-2015-0113.

[4] M. Liu, J.N. Zhu, V.A. Popovich, E. Borisov, J.M.C. Mol, and Y. Gonzalez-Garcia, "*Corrosion and passive film characteristics of 3D-printed NiTi shape memory alloys in artificial saliva*". Rare Metals, 42 (2023), 3114-3129. https://doi.org/10.1007/s12598-023-02329-6.

[5] S.G. Anikeev, M.I. Kaftaranova, V.N. Hodorenko, S.D. Ivanov, N.V. Artyukhova, A.V. Shabalina, S.A. Kulinich, G.V. Slizovsky, A.V. Mokshin, and V.E. Gunther., "*TiNi-based material with shape-memory effect for surgical treatment of diseases of small intestine in newborn and young children*". Journal of Functional Biomaterials, 14 (2023), 1-20. https://doi.org/10.3390/jfb14030155.

[6] B. Sefer, I. Dobryden, N. Almqvist, R. Pederson, and M.L. Antti, "*Chemical Milling of Cast Ti-6Al-4V and Ti-6Al-2Sn-4Zr-2Mo Alloys in Hydrofluoric-Nitric Acid Solutions*". Corrosion Science Section, 73 (2017), 394-407. http://dx.doi.org/10.5006/2277.

[7] L. Martina, E. Pellicer, J. Sort, M.D. Baró, J. Kovač, S. Novak, and S. Kobe, "*Improvement to the Corrosion Resistance of Ti-Based Implants Using Hydrothermally Synthesized Nanostructured Anatase Coatings*". Materials, 7 (2014) 180-194. https://doi.org/10.3390/ma7010180.

[8] D. Song, A. Ma, J. Jiang, P. Lin, D. Yang, and J. Fan, "*Corrosion behavior of equal-channel-angular-pressed pure magnesium in NaCl aqueous solution*". Corrosion Science, 52(2010), 481-490. https://doi.org/10.1016/j.corsci.2009.10.004.

[9] M.H. Grosjean, M. Zidoune, L. Roué, J. Huot, and R. Schulz, "*Effect of ball milling on the corrosion resistance of magnesium in aqueous media*". Electrochimica Acta, 49 (2004), 2461-2470. https://doi.org/10.1016/j.electacta.2004.02.001.

[10] G. Danny, C. García, Á. Soliz, R. Sepúlveda, C. Aguilar, P. Rojas, I. Iturriza, and C. Luno-Bilbao, "*Article Synthesis and Electrochemical Properties of Ti-Si Alloys Prepared by Mechanical Alloying and Heat Treatment*". Metals, 8 (2018), 417. http://dx.doi.org/10.3390/met8060417.

[11] S. Tamilselvi, R. Murugaraj and N. Rajendran, "*Electrochemical impedance spectroscopic studies of titanium and its alloys in saline medium*". Materials and Corrosion, 58 (2007), 113-120. http://dx.doi.org/10.1002/maco.200603979.

[12] M. Fellah, N. Hezil, D. Bouras, N. Bouchareb, A. P. Larios, A. Obrosov, G. A. El-Hiti, and S. Weiß, "*Effect of Zr content on electrochemical and tribological properties of newly developed near β-type Ti-Alloys (Ti-25Nb-xZr) for biomedical Applications*". Journal of Science: Advanced Materials and Devices, 9 (2024), 100695. https://doi.org/10.1016/j.jsamd.2024.100695.

[13] R. Soni, S. Pande, S. Salunkhe, H. Natu, E.A. Nasr, R. Shanmugam, and H.M.A.M. Hussein, "*In Vitro and Electrochemical Characterization of Laser-Cladded Ti-Nb-Ta Alloy for Biomedical Applications*". Crystals, 12 (2022), 954. https://doi.org/10.3390/cryst12070954.

[14] L. Xue, Y. Ding, K.G. Pradeep, R. Case, H. Castaneda, and M. Paredes, "*The grain size effect on corrosion property of Al2Cr5Cu5Fe53Ni35 high-entropy alloy in marine environment*". Corrosion Science, 208 (2022); 110625. http://dx.doi.org/10.1016/j.corsci.2022.110625.

[15] T. Ihsan-ul-Haq, "*Effect of Sintering Holding Time on the Corrosion Properties of Nano-Structured Fe-18Cr-2Si Alloy Prepared by SPS*". International Journal of Electrochemical Science, 11 (2016), 2897-2908. https://doi.org/10.1016/S1452-3981(23)16149-9.

[16] S. Guo, A. Chu, H. Wu, C. Cai, and X. Qu, "*Effect of sintering processing on microstructure, mechanical properties and corrosion resistance of Ti–24Nb–4Zr–7.9Sn alloy for biomedical applications*". Journal of Alloys and Compounds, 597 (2014), 211-216. https://doi.org/10.1016/j.jallcom.2014.01.087.

[17] A. Bautista, A. Gonzalez-Centeno, G. Blanco, and S. Guzman, "*Application of EIS to the study of corrosion behaviour of sintered ferritic stainless steels before and after high-temperature exposure*". Materials Characterization, 59 (2008), 32-39. https://doi.org/10.1016/j.matchar.2006.10.008.

[18] M.F. Ijaz, C. Vasilescu, S.I. Drob, P. Osiceanu, M. Marcu, H.Y. Kim, S. Miyazaki, D.M. Gordin, and T. Gloriant, "*Electrochemical characterization of the superelastic (Ti-Zr)-Mo-Sn biomedical alloy displaying a large recovery strain*". Materials and corrosion, 68 (2017), 1220-1227. https://doi.org/10.1002/maco.201709484.

[19] E. M. Sherif, J.A. Mohammed, H.S. Abdo, and A.A. Almajid, "*Corrosion behavior in highly concentrated sodium chloride solutions of nanocrystalline aluminum processed by*

high energy ball mill". International Journal of Electrochemical Science, 11 (2016), 1355-1369. http://dx.doi.org/10.1016/S1452-3981(23)15927-X.

[20] M.A. Rahman, R. Karunanithi, and N. Sirajudeen, "*Effect of milling time on the density, hardness and corrosion behavior of Al 7150 alloy produced by high energy ball milling*". Materials Research Express, 6 (2019). http://dx.doi.org/10.1088/2053-1591/ab1749.

[21] R. Sundaram, R. Nachimuthu, A.K. Sivanandam, and J. Natarajan, "*Electrochemical and hot corrosion behaviour of steel reinforced with AlSiBeTiV high entropy alloy using friction stir processing*". Science and Technology of Advanced Materials, 25 (2024), 2320083. https://doi.org/10.1080%2F14686996.2024.2320083.

[22] I. Cvijović-Alagić, Z. Cvijović, J. Bajat, and M. Rakin, "*Composition and processing effects on the electrochemical characteristics of biomedical titanium alloys*". Corrosion Science, 83 (2014), 245-254. https://doi.org/10.1016/j.corsci.2014.02.017.

[23] H. Zhao, L. Xie, C. Xin, N. Li, B. Zhao, and L. Li, "*Effect of molybdenum content on corrosion resistance and corrosion behavior of Ti-Mo titanium alloy in hydrochloric acid*", Materials Today Communications, 34 (2023); 105032. https://doi.org/10.1016/j.mtcomm.2022.105032.

[24] G. Yang, Y. Du, S. Chen, Y. Ren, and Y. Ma, "*Effect of secondary passivation on corrosion behavior and semiconducting properties of passive film of 2205 duplex stainless steel*". Journal of Materials Research and Technology, 15 (2021), 6828-6840. https://doi.org/10.1016/j.jmrt.2021.11.118.

[25] J. Lu, W. Zhang, W. Huo, Y. Zhao, W. Cui, and Y. Zhang. "*Electrochemical Corrosion Behavior and Mechanical Properties of Nanocrystalline Ti–6Al–4V Alloy Induced by Sliding Friction Treatment*". Materials, 12 (2019), 760. https://doi.org/10.3390%2Fma12050760.

[26] N. Eliaz, "*Corrosion of Metallic Biomaterials: A Review*". Materials, 12 (2019), 407. https://doi.org/10.3390%2Fma12030407.

[27] A.H. Seikh, M. Baig, H.R. Ammar, and M.A. Alam, "*The Influence of Transition Metals Addition on the Corrosion Resistance of Nanocrystalline Al Alloys Produced by Mechanical* Alloying". Metals, 6 (2016), 140. https://doi.org/10.3390/met6060140.

[28] I. Çahaa, A.C. Alvesa, P. A.B. Kurodab, C.R. Grandinib, A.M.P. Pintoa, L.A. Rochab, and F. Toptana. "*Degradation behavior of Ti-Nb alloys: Corrosion behavior through 21 days of immersion and tribocorrosion behavior against alumina*". Corrosion Science, 167 (2020), 108488. http://dx.doi.org/10.1016/j.corsci.2020.108488.

[30] S. Luiz de Assis, S. Wolynec, and I. Costa. "*Corrosion characterization of titanium alloys by electrochemical techniques*". Electrochimica Acta, 51 (2006), 1815-1819. http://dx.doi.org/10.1016/j.electacta.2005.02.121.

[31] X.T. Sun, Z.X. Kang , X.L. Zhang, H.J. Jiang, R.F. Guan, and X.P. Zhang. "*A comparative study on the corrosion behavior of porous and dense NiTi shape memory alloys in NaCl solution*". Electrochimica Acta, 56 (2011), 6389-6396. http://dx.doi.org/10.1016/j.electacta.2011.05.019.

[32] E.M. Sherif, Y.A. Bahri, H.F. Alharbi, and M.F. Ijaz, "*Corrosion Passivation in Simulated Body Fluid of Ti-Zr-Ta-xSn Alloys as Biomedical Materials*". Materials, 16 (2023), 4603. https://doi.org/10.3390/ma16134603.

[33] S.M. Almotairy, M.E Sherif, N.H. Alharthi, H.S. Abdo, H.F. Alharbi, and M. Luqman "*Influence of Milling Route on the Corrosion Passivation of Al-2%SiC Nanocomposites in Chloride Solutions*". Crystals, 11 (2021), 1231. https://doi.org/10.3390/cryst11101231.

[34]J. Lv Q. Wang, P. Chen, H. Liu, Z. Su, J. Zhao, W. Liu, J. Hou, and S. Gao, "*Effect of ball-milling time and Pd addition on electrochemical hydrogen storage performance of Co_2B alloy*". Solid State Sciences, 103 (2020), 106184. http://dx.doi.org/10.1016/j.solidstatesciences.2020.106184.

[35] Q. Kong, X. Lai, X. An, W. Feng, C. Lu, J. Wu, C. Wu, L. Wu, and Q. Wang, "*Characterization and corrosion behaviour of Ti-13Nb-13Zr alloy prepared by mechanical alloying and spark plasma sintering*". Materials Today Communications, 23 (2020), 101130. https://doi.org/10.1016/j.mtcomm.2020.101130.

[36] L. Zhang, D. Ren, H. Ji, A. Ma, E. Felix Daniel, S. Li, W. Jin, and Y. Zheng, "*Study on the corrosion behavior of NiTi shape memory alloys fabricated by electron beam melting*". Materials Degradation, (2022), 79. https://doi.org/10.1038/s41529-022-00289-3.

[37] M.B. Radovanovic, Ž.Z. Tasic, A.T. Simonovic, M.B.P. Mihajlovic, and M.M. Antonijević, "*Corrosion Behavior of Titanium in Simulated Body Solutions with the Addition of Biomolecules*". ACS Omega, 5 (2020), 12768–12776. http://dx.doi.org/10.1021/acsomega.0c00390.

[38] A.A. Hussain Al-Amiery, N.A. Betti, L.M. Shaker, "*Exploring the effectiveness of 3-chloro-4-morpholin-4-yl-1,2,5-thiadiazole as an eco-friendly corrosion inhibitor for mild steel in HCl solution: Experimental and DFT analysis*". Results in Engineering, 24 (2024), 103014. http://dx.doi.org/10.1016/j.rineng.2024.103014.

[39] W. Xu, X. Lu, B. Zhang, C. Liu, L. Shaomin, S. Yang, and X. Qu, "*Effects of Porosity on Mechanical Properties and Corrosion Resistances of PM-Fabricated Porous Ti-10Mo Alloy*". Metals, 8 (2018), 188. https://doi.org/10.3390/met8030188.

GENERAL CONCLUSION & PERSPECTIVES

GENERAL CONCLUSION

This work mainly aims to synthesize Ti_{50}-Ni_{50} alloys and improve their mechanical, tribological, and electrochemical performance for use in total hip prostheses.

By employing high-energy ball milling at different milling times (2, 6, 12, and 18 hours), followed by pressing and sintering, nanostructured Ti_{50}-Ni_{50} alloys were successfully developed. The investigation into the influence of milling time on the structural, mechanical, tribological, and electrochemical behavior of the Ti_{50}-Ni_{50} system enables the following conclusions:

- The milling process affects the size and shape of powders; as milling times increase from 2 to 18 hours, the proportion of fine particles rises because of significant fracturing and deformation. This refinement is essential because it can increase the hardness of the Ti_{50}-Ni_{50} alloy, which will increase its resistance to corrosion and wear, making it more appropriate for use in biomedical applications.
- As the grinding duration increased, the crystallite size decreased to 29 nm, but the microstrain and lattice parameters increased to 0.99 % and 3.22 A°, respectively.
- With longer milling durations, the Ti_{50}-Ni_{50} alloys' relative porosity dramatically drops to 11 %, increasing the alloys' density to 89 %. Increases in porosity and density improve the material's mechanical properties (hardness and elastic modulus), resistance to wear, and corrosion behavior.
- The specimens' pore size was reduced to 10 nm at the maximum grinding times (12 and 18 hours) in comparison to the early milling phases.
- The maximum hardness and Young's modulus values of the sintered Ti_{50}-Ni_{50} alloys were 341 HV and 103 GPa, respectively, following 18 hours of milling.
- One important biomaterials feature that influences how well they function and interact with cells and tissues is surface roughness, which decreased with milling time.
- With prolonged milling times (18 h), the wear rate and COF were significantly decreased, reaching values of 29.67×10^{-3} $\mu m^3/N.\mu m$ and 0.31, respectively.
- The refined grain size and closed porosity of powders milled for 18 hours are responsible for their improved tribological features, which include a reduced friction coefficient and higher wear resistance.

- The development of a stable passive layer on the sample surface is indicated by the OCP curves, which rise as immersion times increase up to 2500 seconds.
- All Ti_{50}-Ni_{50} alloys have a passivation region, which indicates the development of a passive film on their surface.
- The current and the corrosion rate decreased with longer milling times, reaching 3.6945×10^{-7} A/cm^2 and 0.0074722 mm/year, respectively. However, the values of the corrosion potential shifted in the nobler direction.
- As the milling time increases, the Ti_{50}-Ni_{50} specimens' polarization resistance rises from 427136.86 Ω/cm^2 to 1176837.49 Ω/cm^2, indicating improved material corrosion resistance.
- The EIS findings support the capacitive behavior of Ti_{50}-Ni_{50} by showing that the alloy's surfaces form a two-layer film and that longer grinding durations enhance the passive film's ability to resist corrosion.
- Finally, the Ti_{50}-Ni_{50} alloys may be ideal to be utilized as orthopedic implants.

PERSPECTIVES

In order to better understand the passivation phenomenon and the nature of oxide film formed on the surface of the Ti_{50}-Ni_{50} alloy, other appropriate and efficient surface characterization techniques must be considered, especially XPS and Raman spectroscopy.

A second perspective concerns the development of new biomaterials (based on titanium) and their comparison with Ti_{50}-Ni_{50}.

A third perspective concerns the application of surface coatings by plasma or other processes.

Finally, a tribocorrosion study could be considered to assess the synergy between wear and corrosion phenomena and their combined action

RESEARCH PROFILE

PAPERS

PAPER 1

Materials Today Communications xxx (xxxx) 108201

Contents lists available at ScienceDirect

Materials Today Communications

journal homepage: www.elsevier.com/locate/mtcomm

Effect of milling time on structural, mechanical and tribological behavior of a newly developed Ti-Ni alloy for biomedical applications

Nabila Bouchareb [a, b, *], Naouel Hezil [b], Fouzia Hamadi [b], Mamoun Fellah [c, **]

[a] Laboratory of Engineering and sciences of Advanced Materials (ISMA), ABBES Laghrour –University, Khenchela P.O 1252, 40004, Algeria
[b] Matter Sciences Department, ABBES Laghrour – University, P.O 1252, Khenchela 40004, Algeria
[c] Mechanical Engineering Department, ABBES Laghrour-University, P.O 1252, Khenchela 40004, Algeria

ARTICLE INFO

Keywords:
Ti-Ni
Mechanical alloying
Milling time
Structural evaluation
Mechanical properties
Tribological behavior
Biomedical implant

ABSTRACT

Ti-Ni alloy is the most attractive material in the medical field for orthopedic implants like total hip replacement due to its special properties. The purpose of this study was to examine the impact of grinding/milling times on the characteristics of the nanostructured Ti_{50}-Ni_{50} alloys produced via the mechanical alloying process (MA), utilizing a planetary high-energy ball mill at different grinding times (2, 6, 12, and 18 h). The grinding time causes grain refinement and a decrease in the porosity of materials, which allows for the improvement of a material's mechanical properties and wears resistance. The structural, physical and tribological behavior of Ti_{50}-Ni_{50} alloy was characterized using X-ray diffraction (XRD), scanning electron microscopy (SEM), nanoindentation test, and ball-on-disk tribometer operated under varying applied loads of 2, 10, and 20 N. The findings demonstrated that the crystallite size was reduced and the microstrain increased reaching values of 29 nm, and 0.99%, respectively, at higher grinding times. The percentage of porosity in the Ti_{50}-Ni_{50} alloy was 11%, while the density attained was 89% after 18 h of grinding. Moreover, as the grinding duration increased up to 18 h, the hardness increased (341 HV) owing to the refinement of the grains. It was also noted that the Ti_{50}-Ni_{50} alloy that was milled at 2 h exhibited the lowest elastic modulus (89 GPa). In addition, it was found that wear rates and the coefficient of friction were decreased reaching the values of 29.67 $\mu m^3/N.\mu m$, and 0.31, respectively, for the samples milled at 18 h and examined under 2 N. Enhanced structural and mechanical qualities are responsible for this improvement in tribological properties. These properties make Ti_{50}-Ni_{50} alloys clinically relevant for human biomedical implantation.

1. Introduction

Research in the field of biomedical materials has expanded as a result of the necessity for replacing or repairing damaged parts of the human body to regain the missing shape or functionality of biological tissue such as in total hip replacements [1,2]. It is estimated that the annual number of hip replacement surgeries will surpass 300,000 by the end of 2030 as a result of degenerative diseases like musculoskeletal issues and arthritis [2,3]. Before identifying any clinically relevant implantable material, it is essential to ensure that it does not have any negative effects; in other words, it must be biocompatible with the human body [4], and possess mechanical properties that are appropriate for bone structure [5].

Currently, around 70–80% of prostheses are produced from metallic materials [6–8]. Specifically, titanium (Ti) and its alloys are considered the best biomaterials used to replace hard tissues that incur heavy loads [9] due to its remarkable mixture of mechanical, corrosion resistance, and biocompatibility characteristics [10–14]. In addition, Ti alloys more closely match the demands of effective materials used for implantation than other substances, such as chromium-cobalt (Cr-Co) alloys and stainless steels [7,15].

Shape memory alloys (SMAs) are a significant group of smart or functional materials that have drawn increasing interest in the last few years and which are extensively used in various fields, such as civil engineering, aviation, and biomedicine [16]. Therefore, employing shape memory alloys as implant materials affects their mechanical properties including stiffness which enhances bone healing ability and decreases the rate of transplantation failures [17].

Among the most well-known SMAs is nickel-titanium alloy (Ni-Ti), also known as nitinol [18]. This alloy exhibits two structural compo-

* Corresponding author at: Matter Sciences Department, ABBES Laghrour – University, P.O 1252, Khenchela 40004, Algeria.
** Mechanical Engineering Department, ABBES Laghrour-University, P.O 1252, Khenchela 40004, Algeria
E-mail addresses: nabila.boucharb@univ-khenchela.dz (N. Bouchareb), mamoune.fellah@univ-khenchela.dz (M. Fellah).

https://doi.org/10.1016/j.mtcomm.2024.108201
Received 9 November 2023; Received in revised form 27 December 2023; Accepted 22 January 2024
2352-4928/

PAPER 2

The International Journal of Advanced Manufacturing Technology (2024) 131:3539–3553
https://doi.org/10.1007/s00170-024-13207-5

ORIGINAL ARTICLE

Effect of milling time on structural, physical and photocatalytical properties of Ti-Ni alloy for biomedical applications

Nabila Bouchareb[1,2] · Mamoun Fellah[3,4] · Naouel Hezil[1,4] · Fouzia Hamadi[1,4] · Alex Montagne[5] · Obrosov Aleksei[6] · Krishna Kumar Yadav[7,8] · Gamal A. El-Hiti[9]

Received: 9 November 2023 / Accepted: 2 February 2024 / Published online: 16 February 2024

Abstract

Ti-Ni shape memory alloys (SMA) are used extensively in the field of orthopedics owing to their unique physical and mechanical features, excellent corrosion resistance, and good biocompatibility in the human body environment. This study aims to investigate how milling time affects the characteristics of Ti-Ni alloys which were synthesized with equal atomic percentages by using a high-energy ball milling type (Planetary Micro Mill Pulverisette P7, Fritsch GmbH, Germany) under varying milling periods (2, 6, 12, and 18 h). The duration of the grinding process refines the grain and diminishes the material's porosity, improving the material's physical and structural characteristics as well as its photocatalytic activity. The milled powders of Ti_{50}-Ni_{50} alloys underwent characterization employing scanning electron microscopy (SEM) associated with an energy dispersive spectrometer (EDS), X-ray diffraction (XRD), and spectrophotometery of visible and ultraviolet light (UV–VIS) to measure the solution absorbance of methylene blue (MB). The results revealed that the milling process influences the particle size and shape of powders, where the proportion of fine particles increased with increasing grinding times from 2 to 18 h due to severe deformation and fracturing. The crystallite size was reduced, and the microstrain increased, attaining values of 29 nm and 0.99%, respectively. In addition, the pores of samples were decreased to 10 nm at higher milling times. Furthermore, solutions of MB containing powders of Ti_{50}-Ni_{50} milled at 18 h exhibited good photocatalytic activity with a degradation rate value of 93.23% after 60 min of irradiation time because of a greater surface area. The improved properties of Ti_{50}-Ni_{50} alloys make them clinically useful for biomedical implantation in humans. Plus, they are considered to be effective materials for photocatalytic applications.

Keywords Ti-Ni shape memory alloys · Milling time · Structural evaluation · Nanostructure · Biomedical implant · Photocatalytic activity

✉ Nabila Bouchareb
nabila.boucharb@univ-khenchela.dz

✉ Mamoun Fellah
mamoun.fellah@yahoo.fr

1 Matter Sciences Department, ABBES Laghrour –University, P.O 1252, 40004 Khenchela, Algeria

2 Laboratory of Engineering and Sciences of Advanced Materials (ISMA), ABBES Laghrour –University, P.O 1252, 40004 Khenchela, Algeria

3 Mechanical Engineering Department, ABBES Laghrour-University, P.O 1252, 40004 Khenchela, Algeria

4 Biomaterial, Synthesis and Tribology Research Team, ABBES Laghrour-University, P.O 1252, 40004 Khenchela, Algeria

5 LAMIH UMR, Université Polytechnique Hauts-de-France, 8201 -F-59313 Valenciennes, France

6 Department of Physical Metallurgy and Materials Technology, Brandenburg Technical University, 03046 Cottbus, Germany

7 Faculty of Science and Technology, Madhyanchal Professional University, Ratibad, Bhopal 462044, India

8 Environmental and Atmospheric Sciences Research Group, Scientific Research Center, Al-Ayen University, Thi-Qar, Nasiriyah 64001, Iraq

9 Department of Optometry, College of Applied Medical Sciences, King Saud University, 11433 Riyadh, Saudi Arabia

PAPER 3

Journal of Alloys and Compounds 1010 (2025) 178046

Contents lists available at ScienceDirect

Journal of Alloys and Compounds

journal homepage: www.elsevier.com/locate/jalcom

Electrochemical analysis of mechanically alloyed $Ti_{50\%}$-$Ni_{50\%}$ alloy for bone implants use

Mamoun Fellah [a,*], Nabila Bouchareb [b,*], Naouel Hezil [b], Neçar Merah [c,d], Yasser Alashkar [e], Mohd Imran [f], Obrosov Aleksei [g], Sabine Weiss [g]

[a] Mechanical Engineering Department, ABBES Laghrour-University, P.O 1252, Khenchela 40004, Algeria
[b] Matter Sciences Department, ABBES Laghrour –University, P.O 1252, Khenchela 40004, Algeria
[c] Mechanical Engineering Department, King Fahd University of Petroleum and Minerals, Box 1180, Dhahran 31261, Saudi Arabia
[d] Interdisciplinary Research Center for Advanced Materials, King Fahd University of Petroleum and Minerals, Dhahran 31261, Saudi Arabia
[e] Department of Civil Engineering, College of engineering, King Khalid Univrsity, Abha 61411, saudi arabia
[f] Department of Chemical Enginering, College of Engieering and Computrer sciences, Jazan University, PO. Box 706, Jazan 45142, Saudi arabia
[g] Department of Physical Metallurgy and Materials Technology, Brandenburg Technical University, Cottbus 03046, Germany

ARTICLE INFO

Keywords:
Ti-Ni alloys
Biomaterials
Mechanical alloying
Nanomaterial
Corrosion behavior
Electrochemical impedance spectroscopy

ABSTRACT

The corrosion resistance of an implant material is an essential element of its biocompatibility. This research focuses on studying the effect of grinding/milling time on the corrosion behavior of the mechanically alloyed $Ti_{50\ \%}$-$Ni_{50\ \%}$ (at%) alloy, for bone implant use, at varying milling times of 2, 6, 12, and 18 h. The powder particles' size, shape, and homogeneous chemical content were examined employing scanning electron microscopy (SEM) and energy dispersive spectroscopy (EDS). The alloyed particles' structural characteristics were determined by X-ray diffraction (XRD). Moreover, the characterization of the electrochemical properties was performed utilizing open-circuit potential (OCP) measurement, the Potentiodynamic Polarization (PD), and the Electrochemical Impedance Spectroscopy (EIS) technique. Electrochemical tests were conducted in physiological mediums simulating the human body: Hank's solution. The results revealed that; as the grinding time increased the crystallite size reduced from 57 nm to 29 nm, whereas the lattice parameters increased slightly from 3.18 to 3.22 Å, while the microstrain increased from 0.32 % to 0.99 %. Moreover, the hardness and Young's Modulus increased by about 70 and 16 %, respectively with milling period going from 2 to 18 h. The findings of the electrochemical test demonstrated that as milling progressed, corrosion resistance increased. The evolution of OCP curves as a function of the duration of immersions indicated that OCP increased with the duration of immersion up to 2500 s; this is due to a stable passive layer that has formed on the samples' surface. The results of potentiodynamic polarization curves revealed that both corrosion current density (i_{corr}) and corrosion rate (CR) decreased reaching a value of 3.6945E-07 A/cm^2 and 0.0074722 mm/year, respectively, at longer milling time (18 h). While, corrosion potential (E_{corr}) increased from −0.51255 $V_{/SCE}$ to −0.29997 $V_{/SCE}$ with increasing grinding time. Additionally, the EIS data indicated that the resistance of the passive film increased with increasing milling times. The samples of Ti_{50}-Ni_{50} produced at longer milling time exhibited excellent corrosion resistance due to the formation of a stable passive film which makes them useful for bone implants.

1. Introduction

One of the significant challenges in orthopedics is replacing biological tissue that has deteriorated or damaged with artificial organs, particularly in the case of the knee and hip joints [1]. In the United States (US), it is estimated that over 1 million knee and hip replacements are carried out annually [2]. Owing to aging populations everywhere and rising demands for a higher standard of living, this number is predicted to double [3,4].

The biomaterials field has expanded rapidly in recent years to treat age-related deterioration of the bones and joints as well as unfortunate bone fractures [5]. However, in order to accomplish these aims and qualify biomaterials for usage in body implant applications, certain requirements should be met. Specifically, human tissues must be

* Corresponding authors.
E-mail addresses: mamoune.fellah@univ-khenchela.dz (M. Fellah), nabila.bouchareb@univ-khenchela.dz (N. Bouchareb).

https://doi.org/10.1016/j.jallcom.2024.178046
Received 8 September 2024; Received in revised form 14 November 2024; Accepted 10 December 2024
Available online 16 December 2024

PAPER 4

Kuwait Journal of Science 51 (2024) 100276

Contents lists available at ScienceDirect

Kuwait Journal of Science

journal homepage: www.sciencedirect.com/journal/kuwait-journal-of-science

Full Length Article

Microstructural and photocatalytic properties of nanostructured near-β Ti-Nb-Zr alloy for total hip prosthesis use

Mamoun Fellah [a,*], Naouel Hezil [b], Dikra Bouras [c], Majeed Ali Habeeb [d], Fouzia Hamadi [b], Nabila Bouchareb [b], Salah Eddine Laouini [e], Alejandro Perez Larios [f], Obrosov Aleksei [g], Gamal A. El-Hiti [h]

[a] Mechanical Engineering Department, Abbes Laghrour University -Khenchela, 40004, Algeria
[b] Matter Sciences Department, Abbes Laghrour University -Khenchela, 40004, Algeria
[c] Faculty of Science and Technology, University of Souk-Ahras, Algeria
[d] Department of Physics, College of Education for Pure Sciences, University of Babylon Babil, Iraq
[e] Laboratory of Biotechnology Biomaterials and Condensed Matter, Faculty of Technology, University of El Oued, El Oued, 39000, Algeria
[f] Nanocatalysis Research Laboratory, Department of Engineering, Centro Universitario de Los Altos, University of Guadalajara, Tepatitlán de Morelos, Jalisco, Mexico
[g] Department of Physical Metallurgy and Materials Technology Brandenburg Technical University, Cottbus, 03046, Germany
[h] Department of Optometry, College of Applied Medical Sciences, King Saud University, Riyadh, 11433, Saudi Arabia

ARTICLE INFO

Keywords:
Ti-25Nb-25Zr alloy
Biomaterial alloys
Total hip replacement
Photocatalytic
Biocompatibility
Artificial bone
Orthopedic implants

ABSTRACT

With its unique corrosion resistance, light weight, mechanical strength, and biocompatibility, TNZ is a versatile metal alloy that is used in the aerospace and medical industries. The current study aims to investigate the effect of milling time (2, 12, 24, and 36 h) on the nanostructured ternary alloy Ti-25Nb-25Zr (TNZ) prepared by high energy ball milling, a process involving the use of a high-energy ball mill to mix and grind the alloy powders, on its structural, physical, and photocatalytic characterizations. The alloys' characteristics, such as morphology, structural properties, relative density/porosity, surface roughness, hardness, and Young's modulus, were evaluated using SEM, XRD, surface profilometer, and microdurometer, respectively. The photocatalytic characterization was conducted by measuring their absorbance as a function of time using a spectrophotometer of visible and ultraviolet light in the wavelength range of 250–650 nm. Results showed that the crystallite and mean pore size reduced with increasing milling time, with the smallest values of 25 nm and 34 μm, respectively, after 36 h. This indicates that longer milling times result in a more compact and uniform structure, which could enhance the mechanical properties of the alloy. Structural characterization shows that the amount of the β-Ti phase increased with increasing milling time, resulting in the spherical morphology and texturing of the synthesized alloys. The milled alloys' structural evolution and morphological changes were sensitive to their milling times. Also, the relative density, Young's modulus, and hardness increased, reaching values of 89 %, 105 GPa, and 352 HV, respectively, due to grain size decreasing with increasing milling time. This suggests that longer milling times lead to a denser and harder alloy, which could be beneficial for its use in total hip prostheses. The photocatalytical characterization demonstrated that the degradation of orange II (OII) increased with increasing milling time. The Ti-25Nb-25Zr catalyst gave the best degree of degradation, which meant that the decolorization process could be operated rapidly and at a relatively low cost without UV irradiation.

1. Introduction

The degenerative conditions of osteoporosis (bone weakening) and osteoarthritis (bone joint inflammation), along with trauma, cause the mechanical characteristics of bone to deteriorate because of excessive loading or a lack of normal biological self-healing processes (Mazigi et al., 2017). Therefore, the need for artificial biomaterials is increasing because they are the best solution to these issues. Metals and their alloys have been widely used in the fields of organ repair and human implants due to their extraordinary strength, great corrosion resistance, and remarkable biocompatibility (Karadeniza and Arslan, 2022). Among the metal biomedical materials used in orthopedic devices and surgical

* Corresponding author.
E-mail address: mamoune.fellah@univ-khenchela.dz (M. Fellah).

https://doi.org/10.1016/j.kjs.2024.100276
Received 12 September 2023; Received in revised form 29 May 2024; Accepted 20 June 2024
Available online 21 June 2024

PAPER 5

Journal of Science: Advanced Materials and Devices 9 (2024) 100695

Contents lists available at ScienceDirect

Journal of Science: Advanced Materials and Devices

journal homepage: www.elsevier.com/locate/jsamd

Investigating the effect of Zr content on electrochemical and tribological properties of newly developed near β-type Ti-alloys (Ti–25Nb-xZr) for biomedical applications

Mamoun Fellah [a,**], Naouel Hezil [b], Dikra Bouras [c], Nabila Bouchareb [b], Alejandro Perez Larios [d], Aleksei Obrosov [e,*], Gamal A. El-Hiti [f], Sabine Weiß [e]

[a] Mechanical Engineering Department, Khenchela University, 40004, Algeria
[b] Matter Sciences Department, Khenchela University, 40004, Algeria
[c] Faculty of Science and Technology, University of Souk-Ahras, Algeria
[d] Nanocatalysis Research Laboratory, Department of Engineering, Centro Universitario de Los Altos, University of Guadalajara, Tepatitlán de Morelos, Jalisco, Mexico
[e] Brandenburg University of Technology Cottbus-Senftenberg, Konrad-Wachsmann-Allee 17, Cottbus, 03046, Germany
[f] Department of Optometry, College of Applied Medical Sciences, King Saud University, Riyadh, 11433, Saudi Arabia

ARTICLE INFO

Keywords:
Ti-Nb-Zr alloys
Nanobiomaterials
Tribological behavior
Corrosion
Ringer's solution
Biomedical applications

ABSTRACT

In order to create alloys with exceptional properties for orthopedic uses, this study focuses on the impact of zirconium (Zr) content on the structural, electrochemical, and tribological qualities of nanostructured Ti–25Nb-xZr [x = 5, 10, 15, 20, 25, and 30 atomic (at.) %] alloys. The structural evolution was investigated using XRD and SEM techniques. The mechanical characteristics of the produced alloys, including Vickers hardness and Young's modulus, were measured. In addition, the corrosion tests were performed using the OCP, EIS, and PD methods in Ringer's solution within the independent pH range at 37 °C. A ball-on-disc tribometer was used to investigate the tribological behavior of the alloys under various loads and wet conditions using the Ringer solution. It has been verified that Zr content (at. %) in the alloys had an impact on their morphologies, structural evolution, and mechanical characteristics. According to the morphological analysis, the particle and crystallite size decreases with increasing Zr content. Young's modulus and Vickers hardness show the same tendency. The EIS data demonstrated that a single passive film formed on the alloy surfaces, and the addition of Zr enhanced the corrosion resistance of the passive films. The polarization curves demonstrate that the alloys had low corrosion current densities and large passive areas without the passive films disintegrating. Likewise, the inclusion of Zr resulted in a reduction in the corrosion and passive current density values. All of these results suggested that the titanium alloys exhibit a more noble electrochemical activity caused by Zr. From the tribological perspective, it was found that the friction coefficient of the alloys reduced with increasing Zr content.

1. Introduction

The mechanical properties of bones can deteriorate due to abnormal endogenous self-healing mechanisms or excessive stress, osteoarthritis, degenerative diseases, and trauma [1–5]. The creation of artificial biomaterials that can be surgically implanted in the proper morphology to enable the restoration of damaged systems is one of the solutions to these problems [1–5]. The biocompatibility of these materials is a significant problem, as tissue neoformation with posterior characteristics develops on the implanted devices [6]. Therefore, these basic characteristics of the implanted materials, such as their microstructure, morphology, content, and organic properties, dictate their efficiency [2].

Therefore, the materials produced must be biocompatible, have high corrosion resistance, and exhibit the correct mechanical properties to be considered excellent candidates for biomedical applications [7,8]. Numerous biomaterial alloys with significantly improved characteristics have been created in the last few decades. However, most of these newly

Peer review under responsibility of Vietnam National University, Hanoi.
* Corresponding author.
** Corresponding author.
E-mail addresses: mamoune.fellah@univ-khenchela.dz (M. Fellah), aleksei.obrosov@b-tu.de (A. Obrosov).

https://doi.org/10.1016/j.jsamd.2024.100695
Received 20 January 2024; Received in revised form 23 February 2024; Accepted 29 February 2024
Available online 7 March 2024

CHAPTERS: In TMS

CHAPTER 1: In book: Characterization of Minerals, Metals, and Materials 2025
Publisher: Springer

Investigating the Tribological Behavior of Nitinol Alloys Manufactured via Mechanical Alloying for Hip Implant Applications

Bouchareb Nabila, Hezil Naouel, Fellah Mamoun, Bouras Dikra, Majeed Ali Habeeb, Rim Imen, Merah Neçar, Alejandro Perez Larios, A. El-Hiti Gamal, Obrosov Aleksei, and Montagne Alex

Abstract The equiatomic titanium-nickel alloy, known as nitinol, is a highly sought-after titanium-based alloy used in biomedical applications, particularly in orthopedic implants. Its outstanding properties, such as low density, shape memory effect, high wear and corrosion resistance, good biocompatibility, and low Young's modulus

B. Nabila · H. Naouel · R. Imen
Matter Science Department, Abbes Laghrour-University, P.O 1252, 40004 Khenchela, Algeria
e-mail: nabila.bouchareb@univ-khenchela.dz

H. Naouel
e-mail: hezil.nawel@univ-khenchela.dz

R. Imen
e-mail: imen.rim@univ-khenchela.dz

F. Mamoun (✉)
Mechanical Engineering Department, Abbes Laghrour-University, PO 1252 40004 Khenchela, Algeria
e-mail: mamoune.fellah@univ-khenchela.dz

H. Naouel · F. Mamoun
Biomaterial, Synthesis and Tribology Research Team, Abbes Laghrour University, PO 1252 40004 Khenchela, Algeria

B. Dikra
Department of Science of Matter, Faculty of Science and Technology, University of Souk-Ahras, Souk Ahras, Algeria

M. A. Habeeb
Department of Physics, College of Education for Pure Sciences, University of Babylon Babil, Babylon Babil, Iraq
e-mail: pure.majeed.ali@uobabylon.edu.iq

M. Neçar
Mechanical Engineering Department, King Fahd University of Petroleum and Minerals, Dhahran PO 1180, 31261, Saudi Arabia

Interdisciplinary Research Center for Advanced Materials, King Fahd University of Petroleum and Minerals, Dhahran 31261, Saudi Arabia

Z. Peng et al. (eds.), *Characterization of Minerals, Metals, and Materials 2025*, The Minerals, Metals & Materials Series,
https://doi.org/10.1007/978-3-031-80680-3_38

CHAPTER 2: In book: Characterization of Minerals, Metals, and Materials 2025
Publisher: Springer

Synthesis and Characterization of Surfactant-Modified Clays for Adsorption Applications

Imen Rim, Mamoun Fellah, Naouel Hezil, Nabila Bouchareb, Gamal A. El-Hiti, Neçar Merah, Obrosov Aleksei, and Montagne Alex

Abstract Clay is commonly used to remove pollutants like heavy metals from water. It has excellent properties, such as high cation exchange capacity and a large specific surface area. Various techniques can be used to improve these materials, including organic modification using polymers, calcination, acid activation, and modification through surfactant adsorption. This research aims to discuss recent findings on

I. Rim (✉) · N. Hezil · N. Bouchareb
Matter Science Department, Abbes Laghrour-University, Khenchela, P.O. 1252, 40004 Khenchela, Algeria
e-mail: imen.rim@univ-khenchela.dz

N. Hezil
e-mail: hezil.nawel@univ-khenchela.dz

N. Bouchareb
e-mail: nabila.bouchareb@univ-khenchela.dz

M. Fellah (✉) · N. Hezil
Biomaterial, Synthesis and Tribology Research Team, Abbes Laghrour-University, Khenchela, P.O. 1252, 40004 Khenchela, Algeria
e-mail: mamoune.fellah@univ-khenchela.dz; mamoun.fellah@yahoo.fr

M. Fellah
Mechanical Engineering Department, Abbes Laghrour-University, Khenchela, P.O. 1252, 40004 Khenchela, Algeria

G. A. El-Hiti
Department of Optometry, College of Applied Medical Sciences, King Saud University, Riyadh 11433, Saudi Arabia
e-mail: gelhiti@ksu.edu.sa

N. Merah
Mechanical Engineering Department, King Fahd University of Petroleum and Minerals, P.O. 1180, Dhahran 31261, Saudi Arabia

Interdisciplinary Research Center for Advanced Materials, King Fahd University of Petroleum and Minerals, Dhahran 31261, Saudi Arabia

N. Merah
e-mail: nesar@kfupm.edu.sa

Z. Peng et al. (eds.), *Characterization of Minerals, Metals, and Materials 2025*, The Minerals, Metals & Materials Series,
https://doi.org/10.1007/978-3-031-80680-3_46

CHAPTER 3: In: Supplemental UE: TMS 2025 Conference Proceedings

Publisher: Springer

Tribocorrosion Behavior of Near-Beta Alloys for Biomedical Applications

Khaled Toualbia, Fellah Mamoun, Hezil Naouel, Majeed Ali Habeeb, Nabila Bouchareb, Dihkra Bouras, Rim Imen, Alex Montagne, Alejandro Perez Larios, and Gamal A. El-Hiti

Abstract In order to combat inflammation and allergic reactions brought on by biomaterial implants into the human body, corrosion prevention in biomaterials has become essential. Most of these metal implants developed strong antagonistic relationships with one another when they came into touch with fluidic environments like the bloodstream and bodily tissue, which in turn encouraged corrosion. Due to its combined benefits of a high strength-to-weight ratio, excellent corrosion resistance, and favorable biocompatibility, titanium (Ti) and its alloys have emerged as the most appealing metallic materials used in medical applications, particularly

K. Toualbia (✉) · H. Naouel · N. Bouchareb · R. Imen
Matter Science Department, ABBES Laghrour-University, P.O 1252, 40004 Khenchela, Algeria
e-mail: khaled.toualbia@univ-khenchela.dz

F. Mamoun (✉)
Mechanical Engineering Department, ABBES Laghrour-University, P.O 1252, 40004 Khenchela, Algeria
e-mail: mamoune.fellah@univ-khenchela.dz

F. Mamoun · H. Naouel
Biomaterial, Synthesis and Tribology Research Team, ABBES Laghrour University, P.O 1252, 40004 Khenchela, Algeria

M. A. Habeeb
Department of Physics, College of Education for Pure Sciences, University of Babylon Babil, Hillah, Iraq

D. Bouras
Faculty of Science and Technology, University of Souk-Ahras, Souk-Ahras, Algeria

A. Montagne
Laboratory of Mechanics Surfaces and Materials Processing, ARTS ET METIERS ParisTech, Boulevard Louis XIV, 59046 Lille Cedex, France

A. P. Larios
Nanocatalysis Research Laboratory, Department of Engineering, Centro Universitario de los Altos, University of Guadalajara, Tepatitlán de Morelos, Jalisco, Mexico

G. A. El-Hiti
Department of Optometry, College of Applied Medical Sciences, King Saud University, Riyadh 11433, Saudi Arabia

TMS 2025 154th Annual Meeting & Exhibition Supplemental Proceedings, The Minerals, Metals & Materials Series, https://doi.org/10.1007/978-3-031-80748-0_47